The Web and the Tree
On the interplay between ecological processes and evolutionary histories

A thesis submitted in partial fulfilment of the requirements for the Degree of
Doctor of Philosophy in Mathematics
in the University of Canterbury
by

Giulio Valentino Dalla Riva

Supervisors:
Prof. Mike Steel (Mathematics and Statistics)
Prof. Daniel Stouffer (Biology)
Prof. Charles Semple (Mathematics and Statistics)

Biomathematics Research Centre
University of Canterbury

· 2016 ·

Contents

Verschiedenheit der
Anschauungen, die man etwa
von einem Apfel haben kann: die
Anschauung des kleinen Jungen,
der den Hals strecken muß, um
noch knapp den Apfel auf der
Tischplatte zu sehn, und die
Anschauung des Hausherrn, der
den Apfel nimmt und frei dem
Tischgenossen reicht.[1]

Die Zürauer Aphorismen
Aphorismus 11/12
Franz Kafka

[1]The variety of views that one may have, say, of an apple: the view of the small boy who has to crane his neck for a glimpse of the apple on the table, and the view of the master of the house who picks up the apple and hands it to his guest.
Translation by Hofmann, M. (2006). *The Zurau Aphorisms*. Schocken.

Preface

In this thesis, we introduce and explore a mathematical framework in which to study the evolution of and within ecological networks. Hence, we focus on a peculiar interpretation of the "biodiversity" concept, namely one that includes the complex pattern of interactions among species, along with the species abundancy and evolutionary distinctiveness.

Our objects of inquiry are species communities as complex wholes. Classically, communities have been approached from two distinct points of view: on one hand, we can consider the graph describing the energy flows among species in an ecosystem (i.e., an ecosystem's *food web*); on the other hand, we can consider the species' *phylogeny*, the tree graph describing the evolutionary relatedness of those species. The structure of an ecosystem (its biological diversity and the topology of its interactions) is the product of fast ecological processes within food webs and of the long-term evolutionary processes that give shape to the tree of life. In particular, early ecological literature recognized that the evolutionary history of a species (or its taxonomical classification, in the pre-Darwin era) helps to determine the species' role as part of an ecological network of interacting species. Conversely, the "ghost of past competition" and arms races are famous examples of the fact that a species' interactions with its resources and consumers helps to determine the evolutionary trajectory of that species.

As the empirical research presents strong evidence that the ecology-evolution (eco-evo) feedback loop is, indeed, significant, the ecological and evolutionary points of view are laboriously being connected more and more strongly. A theoretical framework has been developed for some important scenario (e.g., the co-evolution of hosts and parasites, butterfly and flowers, or plants and pollinators).

The case of complex food webs, where is not possible to distinguish two neatly separated trophic layers, has resisted such a treatment. We argue that this can be partially addressed by moving from a rigidly binary view of food webs to the representation of species interactions in a continuous metric space, where species evolution can be gradual. In **Chapter 3** we show how this metric space representation of a food web can be estimated efficiently and gather insights about the evolutionary signature of food webs. Species' ecological interdependency, arising from their role as part of complex food webs, is something that the classic model of trait evolution has avoided. One reason is that it is hard to give a model determining the presence (and strength) of species interactions throughout their history. In **Chapter 3 Appendix** we show how the metric space representation of food webs may constitute a suitable environment in which to define such a model.

Assessing species' contribution to biodiversity is an important task that scientifically informs conservation efforts. In **Chapter 4** we define a family of measures

assessing the relative ecological importance of a species in a food web. These measures are defined directly on the food web's metric space representation we propose in the first chapter. We explore the relationship between evolutionary and ecological uniqueness.

In **Chapter 5** we tackle the "mode" of food web evolution more directly exploiting, once again, the functional trait representation of food webs. In particular, we formulate two contrasting hypotheses on the evolution of frugivore birds' functional ecological niches and test it on a dataset of frugivore birds in the Andes.

Finally, in **Chapter 6** we make a little detour from food webs and consider a different kind of ecological network: geographically grounded population networks composed of patches and corridors among patches. Population networks play a crucial role in evolution (e.g., determining the dynamics of genes' flows). The insight we gained throughout the previous work (especially in the second chapter) supports the notion that the relevance of a species in a network is not always perfectly captured by the species' local properties (such as its number of connections). In this spirit, we assess the importance of a patch in a geographic network by the global effect that removing that patch has on the whole network.

All the code and data used in this thesis will be available on a public Github repository (see gvdr.github.io).

Acknowledgements

Many thanks to the Marsden Foundation and the Allan Wilson Centre for Molecular Ecology and Evolution for the financial support.

Many thanks to Megan Foster (leafittome.co.nz) for the much needed proofreading. If any typo, mistake or grammatical orror still persist, it is only my fault.

I would express my gratitude to thank Devin De Zwaan, Kendra Munn, Jenna Hutchen, and Arne Ø. Mooers for the wonderful dated phylogenetic tree of species in the Serengeti food web and their kind hospitality at their lab in the Simon Fraser University.

I began to consider some of the ideas in this thesis after a (somewhat unrelated) talk that my coauthor Carey E. Priebe gave at the University of Canterbury while he was visiting as an Erskine Programme Fellow.

Paul Brouwers, Steve Gourdie and Allen Witt endured my repeated attempts to crash the Department servers, provided an efficient working environment and enlightened me in the way of the Nice.

No man is an island, not even when he is in a remote island. I am extremely grateful to so many friends and colleagues. Nick J. Baker, Malyon Bimler, Melissa Broussard, Fernando Cagua, Camille Coux, Carla Gomez-Creutzberg, Guilhem Doulcier, Andrew Francis, Marilia Gaiarsa, Olivier Gascuel, Stinus Lindgreen, Audrey Lustig, AJ Misra, Timothée Poisot, Marco Reale, Raazesh Sainudiin, Jason Tylianakis, Kate Wootton, Ana-Johanna Voinopol-Sassu: thank you for for your helpful comments and suggestions. A special thanks to my coauthors Alyssa R. Cirtwill, Arne Ø. Mooers, Carey E. Priebe, Bernat Bramon Mora, Matthias Dehling, Matthew Hutchinson for shaping my Pindaric flights into sound science.

My supervisors, Mike Steel, Daniel B. Stouffer, and Charles Semple have proven to be excellent scientific advisors and wonderful human beings. Thank you.

Many thanks to my family, who tolerated an extremely sparse communication rate. I will skype more, I promise.

This thesis was possible only thanks to the loving care and strength of Francesca.

Chapter 1

List of research manuscripts authored

- First Author:
  - *Exploring the evolutionary signature of food webs' backbones using functional traits.* GVDR and Daniel B. Stouffer.
    published in *Oikos* (2015). doi: 10.1111/oik.02305
  - *Important, Unique and Central: Species' Relevance in Food Webs.* GVDR, and Carey E. Priebe.
    submitted to *Royal Society Open Science*
  - *Coexistence in a megadiverse foraging guild is explained by short-term resource-use modification and long-term niche shifts.* GVDR, Matthew C. Hutchinson, Daniel B. Stouffer and D. Matthias Dehling.
    submitted to *Proceedings of the National Academy of Sciences*
  - *Assessing network connectivity through random walks.* GVDR, Mike Steel and Arne Ø. Mooers.
    To be submitted.
- Co-author:
  - *Conservation of interaction partners between related plants varies widely across communities and between plant families.* Alyssa R. Cirtwill, GVDR, Nick J. Baker, Joshua Thia, Christie Webber and Daniel B. Stouffer.
    submitted to *New Phytologist*
  - *A phylogenetic aware null model for food webs.* Bernat Bramon Morat, GVDR, Daniel B. Stouffer.
    To be submitted.

Chapter 2

Introduction

2.1 Tangled evolution

2.1.1 The abiotic environment

Charles Darwin shed light on the relationship between the environment and evolution by studying how earthworms [Darwin, 1892] and corals [Darwin, 1889] affect the landscape they live in. Both animals are adapted to an environment that would not exist if it was not for the animals' activity. Clearly, disentangling the evolutionary and environmental processes is problematic.

The interdependence of the two processes is commonly considered as being substantially asymmetric: on one hand, long-term changes in the environment alter the evolutionary path of a species; on the other hand, the environmental modification induced by a species' activity is of minor or negligible importance [Eldredge, 2003; Lieberman, 2012]. George E. Hutchinson elegantly summarised this asymmetric conceptualisation in the title of one of his books "The Ecological Theater and the Evolutionary Play" [Hutchinson, 1965]: ecology sets the scene where species evolution take place but—as the actors of a play do not manipulate the scenography of the theatre—the environmental changes unfold independently from the species' evolutionary processes. Apart from some rare exception, species do not build the environment; rather, they adapt to it.

An interesting counterexample is given by beavers. These rodents, building impressive dams, turning the environment they live in into a suitable habitat: a process known as *niche construction* [Odling-Smee et al., 2003, 2013]. In fact, like earthworms and corals, beavers are adapted to a par-

ticular ecological niche that would not exist but for their ability to modify the environment. Richard Lewontin expressed the difference between the "beaver" and the "theatre/play" models of evolution in mathematical terms [Lewontin, 2001].

Let E be a variable expressing the environmental factors affecting the life of a certain species and let O be a variable describing the phenotype of that species. The evolution of the environment and the species across time are captured by the variables' time derivatives, $\frac{\mathrm{d}E}{\mathrm{d}t}$ and $\frac{\mathrm{d}O}{\mathrm{d}t}$, respectively.

Under the "theatre/play" model of evolution, the species' time derivative can be written as a function of O and E, whereas the environment's time derivative can be written as a function of only E (and not of the species O). As a formula:

$$\begin{cases} \frac{\mathrm{d}O}{\mathrm{d}t} &= g\left(O, E\right) \\ \frac{\mathrm{d}E}{\mathrm{d}t} &= f\left(E\right) . \end{cases} \tag{2.1}$$

On the other hand, under the "beaver" model of evolution, the species and environment are coupled—although the strength of the interaction can be asymmetrical. As a formula:

$$\begin{cases} \frac{\mathrm{d}O}{\mathrm{d}t} &= g\left(O, E\right) \\ \frac{\mathrm{d}E}{\mathrm{d}t} &= f\left(E, O\right) . \end{cases} \tag{2.2}$$

This line of enquiry has been pushed further by John F. Odling-Smee, Kevin N. Laland and Marcus Feldman, with a particular attention given to the human species [Odling-Smee et al., 2003].

Establishing the relative importance of biotic and abiotic factors in the evolution of the species, or the frequency of the "beaver" and "theatre/play" models of evolution is beyond the scope of this thesis. See [Benton, 2009; Voje et al., 2015] for two reviews of the evidence so far from two different perspectives.

2.1.2 The biotic environment

Bipartite networks

Darwin's work on earthworms and on corals, and the "Niche construction theory" introduced by Odling-Smee et al. [2003] focus especially on an abiotic characterisation of the environment. Thus they are particularly concerned

with the abiotic factors (climatic, geological, topographical, etc.) that affect organisms' development and can be affected by organisms' activity. In doing so, they can limit their analysis to one or a small number of species at a time.

In this thesis, we adopt a "food web" description of an organism's environment: we identify a species' habitat with its set of interactions with other species; in other words, with the biotic component of the environment.

Again, we find that this ground was covered early on by Charles Darwin: he studied the evolutionary relationship between orchids and their insect pollinators [Darwin, 1888] and ventured to predict the existence of a pollinator with a really long proboscis that was responsible for the pollination of *Angraecum sesquipedale*—a bet which he posthumously won [Arditti et al., 2012] when *Xanthopan morganii praedicta* was discovered.

Following Lewontin's notation, letting O_1 and O_2 denote two interacting species, we can represent their evolutionary dependence by two coupled differential equations. As a formula:

$$\begin{cases} \frac{\mathrm{d}O_1}{\mathrm{d}t} &= g\left(O_1, O_2\right) \\ \frac{\mathrm{d}O_2}{\mathrm{d}t} &= f\left(O_1, O_2\right) . \end{cases} \tag{2.3}$$

Since Paul R. Herlich's and Peter H. Raven's work on the entwined evolutionary histories of butterflies and flowering plants [Ehrlich and Raven, 1964], the study of coevolutionary processes—whereby the diversification of two clades of species are tightly linked—has become established as a classic topic in evolutionary ecology [Futuyma and Slatkin, 1983; Thompson, 1994, 2005, 2013]. Mathematicians, particularly phylogeneticists, have contributed significantly to the understanding of coevolution, developing statistical methods to detect the presence of significant correlations between two clades' phylogenies, [Page, 2003]. However, not all conceptual and algorithmic problems are resolved (for example, disentangling coevolution and cospeciation is not trivial [Poisot, 2015]). The topic has been widely studied as a variety of natural systems show evidence of coevolution, including mutualistic and antagonistic interactions: hosts and parasites in plants [Refrégier et al., 2008] and animals [Hafner and Page, 1995], plants and their pollinators [Kawakita et al., 2004], plants and their herbivores [Agrawal et al., 2012] (but see [Futuyma and Agrawal, 2009] for a review of the evidences) in both natural and

experimental conditions [Brockhurst et al., 2007; Berenos et al., 2009].

Beyond bipartite networks

Only recently, community ecologists and evolutionary biologists have begun to approach the coevolutionary processes of species embedded in large ecological networks with rigour [Fussmann et al., 2007; Post and Palkovacs, 2009; Hand et al., 2015]. In the bipartite case, a food web is made of two discrete non-overlapping sets of interacting species, such as hosts and plants: the interactions happen between the two sets, and not within. In food webs, this neat separation is not, in general, possible: species' evolution is affected, in a non-additive way, by a complex web of interactions. Theoretical models for the evolution of species in complex food webs are just now beginning to be proposed [Itô et al., 2009; Takahashi et al., 2013; Allhoff et al., 2015]. The empirical evidence collected so far has been promising [Crawford et al., 2015], yet rare.

Nevertheless, how to test the presence of coevolution in food webs remains an open problem.

2.2 Relevant Literature

Here, we review a limited selection of works of general interest that touch on the theme of this thesis. Additional and more specific literature is covered in the main chapters.

2.2.1 The Trees

A *phylogeny* is a connected, acyclic, directed graph describing the evolutionary relationships of a set of species. A phylogeny is said to be a *tree* if it does not contain reticulation events; in other words, each node has, at most, one inward branch. A rigorous review of the mathematical results concerning phylogenetic trees is offered in [Semple and Steel, 2003]. More recent mathematical and computational developments can be found in [Gascuel and Steel, 2007]. Not all evolutionary histories are tree-like: horizontal transfer of genes, recombination, gene duplication and hybridisation all produce reticulation events. A phylogeny containing reticulation events is called a *phylogenetic network*. A introduction to phylogenetic networks is presented in [Huson

et al., 2010].

Evolution of traits

A recurrent theme in this thesis is the evolution of species' *traits*. By this, we mean any measurable inherited property of a species or its individuals. In Chapters 3 and 4, we introduce and make use of "abstract traits": traits inferred from the species' interaction networks rather than measured directly. This extension of traits beyond empirical observation is not completely new, as it is common practice in functional ecology whenever a dimensionality reduction algorithm is used [Schaffer, 1981]. However, in that context, the abstract traits can be expressed as a linear combination of the measured traits, a possibility we drop in our analysis.

The field of phylogenetic comparative methods (see [Garamszegi, 2014] for a recent overview) is based on the realisation that the observations of species' traits are not independent, as every pair of species shares a longer or shorter evolutionary history. In particular, for many traits, closely related species tend to be more similar than distantly related species. In fact, the covariance structure arising from the phylogenetic tree of a group of species is often a good predictor of the covariance structure determined by a measurable trait. This correlation has been repeatedly tested empirically for genetic [Dodsworth et al., 2015], morphological [Naisbit et al., 2011] and behavioural traits [Kamilar and Cooper, 2013], and across different kind of traits, (e.g., behavioural traits are more labile than morphological ones [Blomberg et al., 2003]).

The trait covariance structure we expect from an observed phylogeny depends on the *evolutionary model* [Thomas and Freckleton, 2012] applied and the assumptions on which it is grounded. Although a wide variety of models exists, most models for continuous traits (traits which value range is a (subset) of $\mathbb{R}^d$) can be seen as extension of the elementary branching Brownian motion process (e.g., [Bartoszek, 2013] and references therein).

A common assumption inherited from the Brownian motion model is that of branch independence: the drift process acting on a lineage is independent from the processes occurring on any other concurrent lineage. This rather strong assumption has not received much attention in the literature; an important exception is represented by Nuismer and Harmon [2015]. Nuismer and Harmon showed that the distribution of traits we can expect if species

were influencing each other's evolutionary trajectories is strongly different from that under any classic model of evolution. Building on [Nuismer and Harmon, 2015], the recent works (available as a preprint at the time I am writing) of Drury et al. [2015] and Clarke et al. [2015] provide a likelihood framework for detecting the effect of interspecific competition on the evolutionary distribution of species's traits. The results are limited to competition interaction acting in one clade of species, and thus to the bipartite scenario.

2.2.2 The Webs

Food webs are directed ecological networks describing the flow of energy within an ecosystem; they can be cyclic, looped and weighted, and they are complex [May, 1972; Banašek-Richter et al., 2009]. In a food web, nodes identify species, coarser taxonomic units or guilds (groups of species that are not distinguishable from their interactions); edges identify ecological interactions such as predation, consumption, facilitation, and pollination.

A comprehensive introduction to the theory of food webs is offered by Rossberg [2013]. We will not attempt to enumerate all the proposed food web models here—not even the food web models that have been developed with the aim of unifying all models. The reader can find a classic survey in Drossel and McKane [2003].

Food web history

It would be useful to observe the development over time of a food web, tracing the effects that the origin of a new species, its evolution and eventual extinction have on the structure of the web. Alas, we do not have diachronic data and it is not certain whether we will ever have it.

Precious information can be gathered from the reconstruction of the mammalian community collapse in the ancient Egypt [Yeakel et al., 2014]—although the methods used by the authors could not resolve specific ecological interactions—the inferred species assemblage of the Paleolithic [Roopnarine, 2010, 2012] or the Cambrian [Dunne et al., 2008] periods—but we can not easily compare the inferred food webs with any modern food web, as the temporal sampling is too sparse—the observations of six lakes with widely different ages of origin [Doi et al., 2012]—but they represent six independent food webs, not one diachronic observation. Finally, Abascal-Monroy et al.

[2015] offered three direct reconstruction of the Terminos Lagoon's food web over a time period of 30 years, although the web's interaction topology did not change in those 30 years.

It is therefore necessary to adopt indirect exploratory methods, such as via a phylogenetic comparative analysis of the species' food-web roles and the species' traits that determine their trophic roles.

Ecological traits

An important step in the reconstruction of food web evolution is the identification of those traits that have a role in the shaping of food webs: the "functional traits".

It has been observed that species' body size is enough to inform food web models that capture the global properties of the observed ecological network [Woodward et al., 2005a]. Species' body size has been recognised as having a major role in determining the diet of a species in both marine [Barnes et al., 2008] and land [Reuman et al., 2009] systems, and the body size distribution has a role in shaping the global structure of food webs [Stouffer et al., 2011]. Body size shows a strong phylogenetic signal [Schmidt-Nielsen, 1984; Calder, 1984; Smith and Lyons, 2013] in mammals and across the tree of life, although the data on non-mammalian clades are sparser.

However, the node-level properties of food webs can not be fully explained just by body size [Rohr et al., 2010]. Therefore, we need to find a more complete set of functional traits if we want to give a full picture of food webs. Two major steps in this direction derive from considering the asymmetry of species' interactions, and from moving from directly measurable traits to abstract traits.

Rossberg [2013] labels "foraging" and "vulnerability" traits as the sets of traits that determine the interactions of a species as a predator (a consumer) and a prey (a resource), respectively. We exploit the possibility of decoupling a species' foraging and vulnerability traits in Chapters (3) and (4).

Moreover, the dependency of species' interactions (in terms of propensity or strength) on species' traits is not, in general, simple. For this reason, the identification of a suitable functional response has proven to be crucial in modelling of food webs. To surmount this increasing complexity, it is convenient to consider, instead of directly measured traits, *latent* or abstract traits [Rohr and Bascompte, 2014] that can be indirectly inferred from functional

or topological data.

Extinction, Diversity and Key Roles

Ecological networks are dynamical systems governed by population dynamic processes such as predation, competition and cooperation [Lafferty et al., 2015]. The quest to identify the drivers of stability—the factors that increase or decrease the stability of an ecological community—date at least to Robert May's works [May, 1971, 1972] on the feedback between the complexity and the stability of a community.

Stability may be approached from a whole-network point of view [Solé and Bascompte, 2006] (i.e., focussing on global properties of the food webs, such as nestedness or modularity [Fortuna et al., 2010; Rohr et al., 2014]) or from a species point of view (i.e., assessing the contribution of each species to the stability of a food web).

A food web's stability is defined on the basis of its response to the perturbation of its dynamical regime. The perturbation is commonly assumed to be small (i.e., causing a linear response in the system) and the role of the species is fixed in time. A review of classic approaches for measuring the response of an ecological network to small perturbations is offered by [Neubert and Caswell, 1997].

Two useful measures are the food web's resilience and the food web's resistance. A food web which is able to return to its equilibrium state quickly after a small perturbation is said to have high resilience; a food web requiring a strong impulse to move away from its equilibrium state is said to have high resistance [Vallina and Le Quéré, 2011]. More recently, in the context of bipartite food webs, Saavedra et al. [2015] proposed to focus on the feasibility of the equilibrium states rather than just on their stability.

Both the stability and the feasibility measures depend on the strength of the interaction between the species in a food web (although they are robust to measurement errors [Allesina et al., 2015]); when the dynamical parameters or the topological structure of a food web can not be empirically measured, we need to rely on the definition of a proper model, which is an open problem [Allesina and Tang, 2015; James et al., 2015].

Different species play different roles in a food web and hence contribute differently to the overall stability of the food web. Species having a relatively "high importance" are known as *keystone* species [Mills et al., 1993].

So far, the concept of keystone species has resisted a satisfactory rigorous formalisation and a variety of graph theoretical measures have been adopted as proxies for identifying keystone species [Jordán et al., 2006]. Commonly, local node properties of the species are used as proxies to infer their stability importance. How well local properties map the effect of a species' extinction on the food web's global properties is an interesting question.

Apart from its role in food web stability and feasibility, a species can be valued for its ecological originality (the "distance" between a species food-web role and the roles of all the other species) and its contribution to a food web (functional) diversity (the loss in total diversity we would observe if that species became extinct). Exactly how to define a species' food-web role and how to measure the trophic similarity of a pair of species are matters of ongoing research [Hillebrand and Matthiessen, 2009].

Furthermore, the relationship between a species' trophic originality and its contribution to stability is still an open problem; the results presented in the literature are somewhat contradictory (see Chapter (4)), ranging from a negative correlation [Lai et al., 2012], suggesting that central roles are occupied by redundant species (so that the effect of the extinction of central species is mitigated by the probable survival of similar species), to a positive correlation [Petchey et al., 2008b], suggesting that the keystone species are highly original and thus their extinction will affect ecosystems strongly.

2.2.3 The Web and the Tree

The evolutionary history of a species ensemble has an influence on the species' role in the food webs [Stouffer et al., 2012; Naisbit et al., 2012]. Moreover, it has been observed that the taxonomic classification of a species can be a good predictor of its trophic interactions [Ives and Godfray, 2006; Bersier and Kehrli, 2008; Eklöf et al., 2012]. The hypothesis that the importance of a keystone species to food webs' stability is a consequence of a species' evolutionary history has been proposed [Stouffer et al., 2012], although it is not clear to what extent a species' evolutionary history (and measures such as its evolutionary distinctiveness [Redding and Mooers, 2006]) can be used to predict the species' food-web properties.

However, the phylogenetic signal present in a food web's structure is often low or insignificant [Rohr and Bascompte, 2014]: in other words, the phylogenetic structure of a species community does not explain fully the pair-

wise similarity structure determined by a food web (i.e., its pairwise Jaccard similarities [Naisbit et al., 2012] or the pairwise functional traits distance [Rohr et al., 2010]). The lack of signal can be caused by a weak phylogenetic conservation of species' food-web roles (but see [Naisbit et al., 2012; Stouffer et al., 2012] for evidence of conservation) or the strong influence of species' interactions on their evolution, as this would result in the inadequacy of standard detection techniques [Nuismer and Harmon, 2015].

Chapter 3

Food webs as random dot product graphs

Synopsis: In this chapter we model empirically observed food webs as directed Random Dot Product Graphs. Random Dot Product Graphs extend current food web models beyond the limitations associated to discrete, largely deterministic, graph models. Modelling a food web as the realization of a stochastic process, defined by the Random Dot Product Graphs, allows us to estimate species' functional traits. In other words, we infer a pair of vectorial traits for each species determining the species' interactions as a predator or as a prey. The estimated traits induce a pairwise distance structure on the set of species' as predators, as prey or as both predators and prey. The species' embedding in a metric space enables the detection of clusters of species' ecological roles. The species' distribution in their functional trait space suggests the notion that the food-web evolutionary signature is stronger in the food-web's stochastic backbones, while the phylogenetic conservatism of the food web's fine wiring is weak.

Notes: A version of this chapter has been published in *Oikos* (The Nordic Society): GVDR and Daniel B. Stouffer (School of Biology, University of Canterbury), "Exploring the evolutionary signature of food webs' backbones using functional traits". (first published online 25 September 2015). DOI: 10.1111/oik.02305

Because we are all responsible
for all.

The Brothers Karamazov
Fyodor Dostoyevsky
Translated by Constance Garnett

3.1 Determinism and Stochasticity in food webs

In the classic food-web literature [Coulson et al., 2004; May, 2006] ecological networks are modelled as deterministic objects: an interaction between two species (e.g., a predator and its prey) is either present—with a certain weight defined by its relative importance—or absent; once an interaction is observed between individuals of two species, at a particular point in time and space, that interaction is extended uniformly at the species level.

A growing body of evidence, however, challenges this view and supports the notion that food webs are inherently dynamic objects. The observation of an interaction between two species depends on the concurrence of various events, some of which appear stochastic [Holling, 1973; Mullon et al., 2009; Poisot et al., 2015]. For example, the probability of observing an interaction depends on neutral processes, niche processes, species behaviours and environmental factors [Fortuna et al., 2013; Poisot et al., 2015; Canard et al., 2014]. More specifically, the interaction probabilities depend at least on species' local abundances—determining the probability that an individual od species i encounters and individual of species J—and on species' local phenotypes as characterized by their trait values—determining the propensity that two colliding species do interact [Poisot et al., 2015].

Beyond specific trait values, a species' ensemble of predators and prey—its consumers and its resources—can be regarded as an emergent form of its local phenotype: its *trophic niche*. Within the food-web literature, it is widely acknowledged that the importance of the various traits in determining the species trophic niche is not uniform [Petchey et al., 2008a]. The traits playing a major role in shaping the trophic niche are known as *trophic traits*; in particular, body size is commonly assumed to be the most important (i.e., Jennings et al., 2002). It has also been shown that many emergent properties of food-web structures can often be effectively predicted by models based on just two traits: a predator's body size and the range of body size of that

predator's prey [Williams and Martinez, 2000; Stouffer et al., 2005; Williams and Martinez, 2008; Williams et al., 2010; Stouffer et al., 2011; Zook et al., 2011; Gravel et al., 2013], though this may depend on ecosystem type [Woodward et al., 2005a; Stouffer et al., 2011]. However, the performance of many standard food-web models is reduced when we consider their ability to predict single interactions [Petchey et al., 2008a]. This decrease in performance likely arises because of the models' deterministic nature [Williams et al., 2010; Gravel et al., 2013] and the phenomenological way in which they relate to species' traits [Stouffer, 2010; Eklöf et al., 2013].

3.2 Embedding food webs in a metric space

We consider an observed food web to be the outcome of three distinct stochastic processes: first, ecological and evolutionary factors concur to determine phenotypes(i.e., the set of morphological and behavioural traits of each species in the food web); second, the species' traits—or, more precisely, a subset of traits that depends on the identities of each pair of species—determine which interactions can occur and with which propensity; third, an observer detects some, or all, of the species' interactions, according to the sampling effort and the local abundance of each species in the food web's area.

In our modelling effort, we focus in particular on the second step—linking traits to interactions—and set aside the issues related to the other two processes. *A priori* we do not know the number, the identity or the value of the species' traits that do determine the realization and the propensity of an interactions between two species; we do not know how many and which traits to measure. Hence, we need to estimate this information from the observed food web's topology: we need to estimate the species' functional traits from the observed food web's binary adjacency matrix. We will do that through the estimation, through truncated singular value decomposition of the adjacency matrix, of the parameters of *Random Dot Product Graph* (RDPG) model [Wasserman, 1994]—or, more precisely, of a direct graph extension of RDPG.

3.2.1 Stochastic Block Models

The Random Dot Product Graph model has been developed as a particular family of Stochastic Block Model graphs (SBM). Both models tackle the problem of inferring the presence or absence of non-observed links in a partially observed graph. Under the SBM model, each node of the N nodes in a graph is assigned to one of k, non overlapping, blocks. The model parameters are a vector $\vec{a} \in \{1, \ldots, k\}^N$ specfying the assignment of the nodes to the blocks and a $k \times k$ matrix P which entries P_{ij} define he probability of observing an interaction from a node in the block i to a node in the block j. In practice, the assignment of the nodes to the blocks is not known nor it is the matrix P but it must be inferred by the observed adjacency matrix A (i.e., by the observation of the realized interactions).

The model parameters define a measure of probability on the space of (labelled) direct graphs with N nodes. The probability of sampling a graph G with adjacency matrix A from an SBM with parameters $(\vec{a}, P)$ is simple to compute as the edges of the graph are conditionally independent Bernoulli random variables given the parameters:

$$\mathbf{P}(G) = \prod_{ij} \left[\sum_{kl} \left(\delta_k(\vec{a}_i) \delta_l(\vec{a}_j) P_{kl}^{A_{ij}} \left(1 - P_{kl}^{(1-A_{ij})} \right) \right) \right] \tag{3.1}$$

where $\delta_k(\vec{a}_i)$ is a Kronecker delta with value 1 if the node i is in block k or 0 otherwise (and the convention that 0^0 is 1). To estimate the model parameters through maximal likelihood is known to be an NP problem, even if the number of blocks is known. However, spectral clustering is known to offer a consistent estimator under mild conditions [Lei et al., 2014].

When it is used for detecting community of nodes, a natural assumption is to impose an asymmetry between the within and between blocks linking probability [Abbe and Sandon, 2015], for example requiring the linking probability between two different blocks to be higher than the linking probability within a block. A food web model based on the SBM approach has been introduced by Allesina and Pascual [2009] and applied to the Serengeti National Park's food web [Baskerville et al., 2011].

A necessary task in the estimation of the block assignment vector consists in defining a suitable prior distribution on the number of blocks. Notice that for a graph with N nodes we have at most N partitions. In particular, we

count

$$\sum_{k=1}^{N} \frac{1}{k!} \left(\sum_{i=0}^{k} (-1)^{k-i} \binom{k}{i} i^N \right) \tag{3.2}$$

different assignments of the nodes to the blocks [Holland et al., 1983]. A uniform distribution on the possible partition results in *a priori* probability for the number strongly concentrated on intermediate values; other priors have been proposed, for example Baskerville et al. [2011] the authors propose an exponential hyperprior distribution for the aggregation parameter ξ of a Dirichlet process defining the number of nodes assigned to the blocks. This approach produce a prior probability of having k blocks in a graph with N nodes given by [Holland et al., 1983]:

$$\mathbb{P}(k|\xi) = \frac{|s(N,k)|\xi^k}{\prod_{i=!}^{N}(\xi + i - 1)}, \tag{3.3}$$

where $|s(N,k)|$ is the number of permutations of N elements containing exactly k cycles.

The block model depends on the a prior probability for the number of blocks, which may result difficult to estimate, and considers stochastically equivalent all the nodes assigned to the same block, thus masking any within block variance.

3.2.2 Undirected Random Dot Product Graphs

Simple (undirected) Random Dot Product Graphs [Nickel, 2007] are particular instances of the SBM model where each node is assigned to its own block—a graph G with N nodes has N blocks. Moreover, to each node i it is assigned a vector of *latent traits* $T(i)$. Chosen a model dimension d, T is a function from the set $N(G)$ of the nodes of the graph G to the d-dimensional real space, $T : N(G) \to \mathbb{R}^d$.

The probability of interaction between two nodes i and j is given by a function $\mathcal{F} : \mathbb{R} \to [0,1]$ of the dot product of the nodes' latent trait vectors:

$$\mathbb{P}\left(A_{ij} = 1\right) = \mathcal{F}\left(T(i) \cdot T(j)\right) \tag{3.4}$$

where A_{ij} is the ijth entry of the adjacency matrix A of G.

Given a parameter matrix $\mathbf{T}$—which rows $\mathbf{T}_i$ define the nodes' latent traits—the probability of observing a graph G with adjacency matrix A is

given by:

$$\mathbf{P}(G) = \prod_{ij} \mathcal{F}(\mathbf{T}(i) \cdot \mathbf{T}(j))^{A_{ij}} (1 - \mathcal{F}(\mathbf{T}(i) \cdot \mathbf{T}(j)))^{(1-A_{ij})} \tag{3.5}$$

where the product is other all pairs of nodes.

If the latent traits where sampled from the positive orthant of a unitary ball—so that their dot product is granted to be in $[0, \ldots, 1]$—the function $\mathcal{F}$ can be the identity function. In that case, the probability of observing a graph G simplifies to

$$\mathbf{P}(G) = \prod_{ij} (\mathbf{T}(i) \cdot \mathbf{T}(j))^{A_{ij}} (1 - (\mathbf{T}(i) \cdot \mathbf{T}(j)))^{(1-A_{ij})} \tag{3.6}$$

where the product is other all pairs of nodes.

In practice, the latent traits of the nodes are not known, rather, they must be estimated by one (or multiple) graph observations. It has been proven that, if the latent traits $\mathbf{T}(i)$ are drawn independently from an identic distribution, it is possible to consistently estimate them from an eigen-decomposition of the adjacency matrix of the realized graph [Sussman et al., 2014].

Let $\mathbf{P}$ be the matrix of interaction probabilities determined by the d dimensional latent traits $\mathbf{T}$ of a set of n nodes (i.e., $\mathbf{P} = \mathbf{T} \cdot \mathbf{T}^t$). Let $\mathbf{P} = U \Sigma U^t$ be an eigen-decomposition of $\mathbf{P}$ and $\mathbf{P} = U_d \Sigma_d U_d^t$ its d dimensional truncation, so that $U_d \in \mathbb{R}^{nd}$ are the first d columns of U and $\Sigma_d \in \mathbb{R}^{dd}$ is the diagonal matrix which entries are the first d eigenvalues of d—the entries of Σ are real as $\mathbf{P}$ is symmetric. Then, $\mathbf{T}$ is a rotation of $U_d \Sigma_d^{1/2}$.

Let G be a graph sampled according to the interaction probabilities defined by $\mathbf{P}$ and let A be the adjacency matrix of G. Denote

$$\mathbf{A} \sim W_d \Upsilon_d W_d^t$$

a d dimensional truncated eigen-decomposition of A. When n is large, $\mathbf{P} \sim \mathbf{A}$ [Rohe et al., 2011]. Then, with an error $\epsilon(d, n, g)$—where g is the eigengap of A—bounded above by a function growing as $\sqrt{\log n}$ and a probability greater than $1 - 2\frac{d^2+1}{n^2}$

$$\sum_{ij} \sqrt{\left(W_d \Upsilon_d^{1/2} - \mathbf{T}\right)_{ij}^2} \leq \epsilon(d, n, g) \tag{3.7}$$

up to a rotation of W_d [Sussman et al., 2014]. In particular

$$\lim_{n\to\infty} \frac{\sum_{ij} \sqrt{\left(W_d \Upsilon_d^{1/2} - \mathbf{T}\right)^2_{ij}}}{n} = 0 \tag{3.8}$$

strongly, as $1 - 2\frac{d^2+1}{n^2} \to 0$. A similar bound can be given for the latent traits of any node.

3.2.3 Directed Random Dot Product Graphs

The ecological relationships we are interested in are seldom symmetric. Therefore, we must consider an extension of RDPG to directed graphs [Young and Scheinerman, 2008]. Species are, accordingly, described not by a single vector of traits but by a pair of vectors. We will refer to each species' pair of vectors as the species' *foraging functional trait* and the species' *vulnerability functional trait* vectors. The foraging functional traits of species i will help determine the probability of observing links toward i—the behaviour of i as a predator (or consumer)—whereas the vulnerability functional traits of species i will help determine the probability of observing links from i—the behaviour of i as a prey (or resource). As with undirected RDPGs, the probability of a link from species j to species i (i.e., of i consuming j) will be given by the dot product between the vulnerability functional traits of j and the foraging functional traits of i.

A toy model

To better understand the theory behind directed RDPGs, consider three hypothetical species a, b and c as in Figure (3.1). Here, each species is associated with a pair of two-dimensional functional traits (in this case, the x and y coordinates). For the sake of simplicity in this example, we have imposed their functional trait vectors to have length equal to 1 so that the difference between them is given just by their angular distances. Moreover, we have constrained all of them to be situated in the positive quadrant so that the cosine of the angles between falls in the interval $[0, 1]$.

In this example, the angle between the vectors $a^{(f)}$ and $b^{(v)}$ is smaller than the angle between the vectors $a^{(f)}$ and $c^{(v)}$; mathematically, this implies that the dot product of the vectors $a^{(f)}$ and $b^{(v)}$ is greater than the dot product of the vectors $a^{(f)}$ and $c^{(v)}$. Within the RDPG framework, this also implies that

there is a greater probability of observing a link from b to a—a consuming b—than a link from c to a. Similarly, we can see that the angle between $c^{(f)}$ and $a^{(v)}$ is larger than the angle between $c^{(v)}$ and $a^{(f)}$. This again implies that there is a greater probability of observing a link from c to a than a link from a to c. Considering the pairwise angular distances of all other species, we can directly infer the most likely structure of the three-species food web.

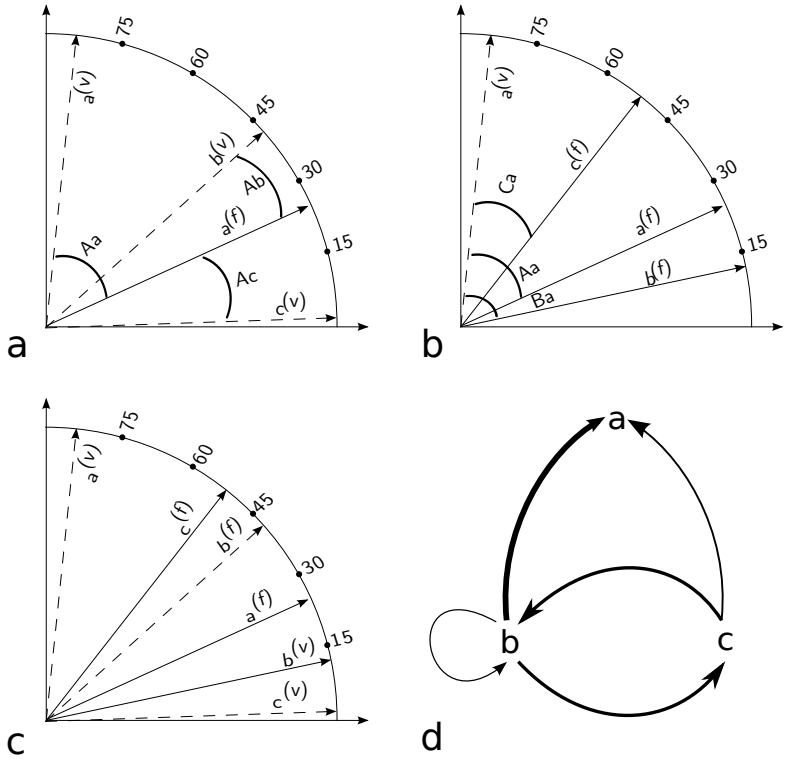

Figure 3.1: The functional trait space of three hypothetical species and their corresponding food web. **a**) The foraging functional traits of species a and the angular distance with the vulnerability functional traits of species b and c. **b**) The vulnerability functional traits of species a and the angular distance with the foraging functional traits of species b and c. **c**) The foraging and vulnerability functional trait vectors for all the species. **d**) The most likely food web, where the width of each interactions is proportional to the probability of the interaction, i.e., the angle between the corresponding foraging and vulnerability functional trait vectors.

Formal definition

Under the directed Random Dot Product Graphs [Young and Scheinerman, 2008] to each node i is assigned a pair of vectors of *foraging* and *vulnerability* (or *outward* and *inward*) traits, denoted $T_f(i)$ and $T_v(i)$. Chosen a model dimension d, T_f and T_v are functions mapping the set of the food web's species to a subset of the d-dimensional real space, $T_{f,v} : N(G) \to \Omega \subset \mathbb{R}^d$, such that the dot product $T_f(i) \cdot T_v(i)$ is in $[0, \ldots, 1]$.

The probability of interaction from a species i to a species j—in other words, j is observed feeding on i—is given by the dot product of the vulnerability traits of i and the foraging traits of j:

$$\mathbb{P}(A_{ij} = 1) = T_v(i) \cdot T_f(j) \tag{3.9}$$

where A_{ij} is the ijth entry of the adjacency matrix A of the food web G.

Notice that

$$\mathbb{P}(A_{ij} = 1) \neq \mathbb{P}(A_{ji} = 1) \tag{3.10}$$

as in general $T_v(i) \cdot T_f(j) \neq T_v(j) \cdot T_f(i)$.

Let $\mathbf{X}$ denote the matrix obtained by multiplying the vulnerability and foraging parameter matrices $\mathbf{T}_f$ and $\mathbf{T}_v$ (i.e., $\mathbf{X} = \mathbf{T}_v \cdot \mathbf{T}_f$). We call $\mathbf{X}$ the model matrix defined by $\mathbf{T}_f$ and $\mathbf{T}_v$. Then, the entries ij of $\mathbf{X}$ give the probability of observing an interaction from i to j:

$$\mathbb{P}(A_{ij} = 1) = \mathbf{X}_{ij} \tag{3.11}$$

Given the vulnerability and foraging parameter matrices $\mathbf{T}_f$ and $\mathbf{T}_v$, and being $\mathbf{X}$ the model matrix they define, the probability of observing a food web G with adjacency matrix A is given by:

$$\mathbf{P}(G) = \prod_{ij} \mathbf{X}_{ij}^{A_{ij}} (1 - \mathbf{X}_{ij})^{(1-A_{ij})} \tag{3.12}$$

where the product is other all pairs of species.

3.2.4 Estimating species' functional traits

The ensemble of all species' traits vectors determine the probability of observing each and every potential link in the food web. As a result, they

determine the probability of sampling a certain food web from the space of all allowable realizations (i.e., its likelihood). In practice, we can not observe directly the process that generates a food web; instead, we usually obtain a single sample from the set of all the possible food web realizations. This implies that we then need to estimate species' foraging and vulnerability functional traits that are most likely to have produced the observed food webs.

Let G be an observed food web composed of S species and A its $S \times S$ adjacency matrix. Let the dimension d be given. Let $\hat{L}$ and $\hat{R}$ be a pair of $S \times d$ matrices such that the Frobenius distance between the adjacency matrix A of G and the product $\hat{L} \times \hat{R}^t$ is minimal, in formula:

$$\left\| A - \hat{L} \cdot \hat{R}^t \right\|_F = \min_{Y,Z \in \mathbb{R}^{S \times d}} \left\| A - Y \cdot Z^t \right\|_F \tag{3.13}$$

where $\|X\|_F$ is the Frobenius norm of the matrix X. As a formula:

$$\|X\|_F = \sqrt{\sum_{ij} X_{ij}^2}\,.$$

The rows of $\hat{L}$ and $\hat{R}$ are the maximum likelihood species vulnerability and foraging traits [Tang et al., 2013; Lyzinski et al., 2013].

To compute a pair of matrices $\hat{L}$ and $\hat{R}$ satisfying the minimization requirement, we first obtain a Singular Value Decomposition of A into three matrices L, Σ, R, such that L and R are real, orthogonal $S \times S$ matrices; Σ is an $S \times S$ diagonal matrix whose non-decreasing ordered entries are the singular values of A; and the three matrices satisfy

$$A = L \cdot \Sigma \cdot R^t\,.$$

Using the SVD of A, we denote L' the $S \times d$ matrix given by the first d columns of L; we denote R' the $S \times d$ matrix given by the first d columns of R; we denote $(\Sigma')^{1/2}$ be the $d \times d$ diagonal matrix defined by the square root of the d greatest singular values of A.

We define $\hat{L}$ the matrix given by

$$\hat{L} = L' \cdot (\Sigma')^{1/2} \tag{3.14}$$

and we define $\hat{R}$ the matrix given by

$$\hat{R} = \left(\Sigma'\right)^{1/2} \times R' \,. \tag{3.15}$$

The rows of $\hat{L}$ and $\hat{R}$ give the species' vulnerability functional and foraging functional traits, respectively. Note that this traits are not uniquely identifiable, as any transformation of the matrix $\hat{L}$ and $\hat{R}$ preserving their dot product would be acceptable.

3.2.5 Choosing the trait dimensionality

The dimension of an RDPG model has direct effects on the variability of the food webs the model produces. In other words, sampling food webs from a RDPG model given parametrised by higher dimensional traits is associated with a lower variance. We can detail this notion more rigorously.

Let A be a (binary) adjacency matrix of a food web G with S species. Choose two S^2-dimensional matrices L and R such that $L \times R^t = A$. For each $d < S$, let us define an RDPG model with functional traits given by L_d and R_d, the first d columns of L and R. As d increases, the variance of the probability distribution given by the RDPG model decreases and the sampled food webs will concentrate around the observed matrix A. Eventually, choosing $d = S$, we can read L and R as the species' traits of dimension equal to the rank of A. The RDPG model with parameters L and R assigns probability null to every adjacency matrix but A.

Hence, a pivotal element of the RDPG approach to food webs is the identification of the model dimensionality. Ideally, one would infer the variability of a food web from empirical data, i.e., through repeated observation of the same ecological network. However, this is not always possible, and repeated observations of food webs are indeed rare. An alternative is given by a graph-theoretical approach: the decreasing sequence of singular values of the observed food web's adjacency matrix A is of great utility in assessing the presence of structure in the graph, and hence in delimiting an appropriate dimensionality interval [Chatterjee et al., 2014].

Different methods to asses a suitable range for the model dimension have been proposed in the statistical literature.

Full rank A first, conservative upperbound for d is given by the number of *non-zero* singular values, Σ_+. This is because every coordinate i after Σ_+ is strictly null and brings no information into the model. Thus, we can safely ignore them.

Each additional coordinated contributes proportionally to the i-th singular value gap (i.e., the distance between the i-th and the $(i+1)$-th singular values, [Andrews and Patterson III, 1976]).

Scree plot We perform an exploratory data analysis by looking at the scree plot of the singular values. The objective is to identify an "elbow"– a large gap—in the sequence of singular values. In fact, we expect it to decrease quickly up to a certain value $\hat{d}$, after which the decrease will slow down [Cattell, 1966]. Although widely used in the literature—and also presented in textbooks [Friedman et al., 2001]—Cattell's graphical approach has the drawback of depending on the researcher's personal judgment and visual acuity. Yet, as in many applications we are not trying to identify the optimal model dimension $\hat{d}$ but rather a suitable interval of model dimension, Cattel's ocular investigation is still a reasonable procedure.

Profile Likelihood We complemented our ocular intuitions with two methods for the estimation of an optimal model dimension d not relying on the researcher judgment. The first method was developed by Zhu and Ghodsi [2006] in the scenario of PCA analysis and is based on the maximization of a profile likelihood function.

Let Σ_q and Σ_Q be, respectively, the set of the first q singular values of A and the set of the last $S-q$ singular values of A. When we ocularly detect an elbow at q in the sequence of singular values we are suggesting that Σ_q and Σ_Q are distributed according to two distribution $f(\sigma|\Theta_q)$ and $f(\sigma|\Theta_Q)$ with different parameters Θ_q and Θ_Q. Let f be known and singular values sequence Σ observed; under the assumption that singular values of Σ_q and Σ_Q are sampled independently, we can write the log-likelihood of the parameters q, Θ_q and Θ_Q as:

$$\log \mathrm{L}\left(q, \Theta_q, \Theta_Q | f, \Sigma\right) = \sum_{i=1}^{q} \log f(\sigma_i|\Theta_q) + \sum_{i=q+1}^{S} \log f(\sigma_i|\Theta_Q)\,. \tag{3.16}$$

Then, for any q we can compute the maximum likelihood estimator of Θ_q

and Θ_Q, which we denote θ_q and θ_Q. Thus, the profile likelihood function of q is:

$$\log \mathrm{L}(q) = \sum_{i=1}^{q} \log f(\sigma_i|\theta_q) + \sum_{i=q+1}^{S} \log f(\sigma_i|\theta_Q). \tag{3.17}$$

We choose the model dimension d maximizing the profile likelihood $\log \mathrm{L}(d)$.

In fact, we can extend Zhu and Ghodsi [2006] method for identifying more than one elbow. Let $b \geq 2$ be the number of elbows we want to identify and define a partition of the singular values Σ into b subsets $\{\Sigma_{q_i}\}_{i=1}^{b}$—each of which has q_i elements—such that each element in Σ_{q_i} is greater than each element in Σ_{q_j} whenever $i < j$. In particular, Σ_{q_1} is the set of the first q_1 singular values of A and Σ_{q_b} is the set of the last q_b singular values of A. As before, the elements of Σ_{q_i} are sampled from a distribution f with parameters Θ_i. Let f be known and singular values sequence Σ observed; under the assumption that singular values of each Σ_{q_i} are sampled independently, we can write the log-likelihood of the parameters $\{q_i\}$, and $\{\Theta_{q_i}\}$ as:

$$\log \mathrm{L}(\{q_i\}, \{\Theta_{q_i}\}|f, \Sigma) = \sum_{i=1}^{b} \left(\sum_{j \in q_i} \log f(\sigma_j|\Theta_{q_i}) \right). \tag{3.18}$$

Then, for any such partition of the singular values we can compute the MLE parameters, which we denote $\{\theta_{q_i}\}$, and its profile likelihood function

$$\log \mathrm{L}(\{q_i\}) = \sum_{i=1}^{b} \left(\sum_{j \in q_i} \log f(\sigma_j|\theta_{q_i}) \right). \tag{3.19}$$

This result allows us to compute increasingly conservative upper bounds for the model dimension.

Following Zhu and Ghodsi [2006], we choose f to be a Gaussian distribution: the optimal d estimated under this choice was compatible with every other method we implemented.

Thresholding The second method is based on the identification of a Universal Singular Value Threshold: the identification of a threshold such that, considering only those coordinates associated with singular values higher than the threshold, the distance between the estimated matrix and the "real" matrix (the matrix given by the "real" model) is asymptotically small [Chatterjee et al., 2014; Gavish and Donoho, 2014]. This latter approach incorpo-

rates the structural hypothesis used in the model (i.e., different random-graph models have different threshold values).

3.3 Empirical food webs

We apply our analysis to nine different food webs, widely varying in location, composition and species' community size. For the majority of our analyses and results, we will focus on the two largest food webs. The first large web was compiled for the Serengeti National Park [Baskerville et al., 2011], and it is made up of 161 species and 592 feeding relationships. Amongst those 161 species, 129 are plants, 23 are herbivores and 9 are carnivores. Most of the links (507) are between herbivores and plants whereas 85 are between animal species. The second large web is a highly resolved food web for the Antarctic Weddell Sea [Jacob et al., 2011]. This food web is composed of 488 taxonomically identified species, 4 distinct non-living source nodes (e.g., detritus), and features more than 16,000 predator-prey interactions. We chose these two food webs because they are both well resolved to the species level which then allows for a robust phylogenetic analysis. We expect that the differences in their latitude, their environment, and their species composition would help ascertain the utility of our approach.

The remaining seven food webs are smaller and were compiled by different authors [Dawah et al., 1995; Harper-Smith et al., 2005; Jonsson et al., 2005; Ledger et al., shed; Memmott et al., 2000; Closs and Lake, 1994; Woodward and Hildrew, 2001; Woodward et al., 2005b]. We analysed the latter webs in order to propose a more complete comparison of the model we are introducing with other well recognized models [Allesina and Pascual, 2009; Petchey et al., 2008b; Rohr et al., 2010]. The sizes of these seven webs vary from 25 to 80 species.

3.4 Assessing model performance

To further corroborate our choice of dimensionality, we observe the model performance as a function of the trait-vector length d. Specifically, we assessed the RDPG model's *fitting performance* in two distinct ways: 1) through its sensitivity, i.e., the ratio of correctly predicted links to observed links, and 2) through its accuracy, i.e., the ratio of correctly predicted observed links and

correctly predicted absent links to the squared size of the community. To compute these ratios, for each model dimensionality d within our estimated optimal interval, we sampled food webs such that each link had an independent probability of being observed (given by the d-dimensional model). Notice that, for the reasons illustrated in the previous section, we expect the performance to grow with d.

Next, we assessed the RDPG model's *predictive performance* in a leave-one-out cross validation test, and we again focused on the sensitivity (correctly predicted links, the "ones" in the observed adjacency matrix), specificity (correctly predicted absent links, the "zeros" in the observed adjacency matrix) and accuracy (correctly predicted entries in the adjacency matrix). In the leave-on-out procedure, we sequentially treated each element of the adjacency as unobserved (i.e., absence of observation, not observation of absence). To do so, we set the entry equal to the *a priori* probability p of observing an interaction in the food web (i.e, the connectivity of the food web *without* that interaction). Then, we estimated the d-dimensional functional traits on the modified adjacency matrix and computed the a posteriori probability p_{ij} of observing an interaction corresponding to that entry. Finally, we classified an entry with value greater than 0.5 as present and an entry with value less than 0.5 as absent. Notice that this is equivalent to averaging the presence/absence of a link over a large sample of randomly sampled food webs where each links is observed with a probability equal to p_{ij}. Finally, we compared the model-estimated food web, which depends on d, with the originally observed one.

Finally, we computed the Akaike Information Criterion value for the RDPG model on all the food webs we analysed. Specifically, the AIC of our model is given by:

$$2 \cdot (S \cdot 2 \cdot d) - 2 \cdot \left(\sum_{ij|A_{ij}=0} \log\left(1 - p_{ij}\right) + \sum_{ij|A_{ij}=1} \log\left(p_{ij}\right) \right) \tag{3.20}$$

where p_{ij} is the probability specified by the model for an interaction from species i to species j, A_{ij} is the entry corresponding to the interaction from species i to species j in the adjacency matrix, S is the number of species, and d is the length of the trait vectors.

In order to compare the RDPG to the other models, we obtained the

fitting performances for the other models—for all but the two largest webs—from the literature [Allesina and Pascual, 2009; Rohr et al., 2010; Allesina, 2011]. For the Serengeti food web, we obtained the species allocation in the 14 groups from the literature [Baskerville et al., 2011] and the estimated link density between each pair of groups ourselves. We computed the likelihood of the group model as described above for the RDPG model, considering the number of parameters equal to $S + \gamma^2$ (i.e., the number of species plus the square of the number of groups). All further details regarding the implementation and fitting performance of these models can be found in the original publications Petchey et al. [2008a]; Allesina and Pascual [2009]; Rohr et al. [2010]; Baskerville et al. [2011].

3.5 Phylogenetic signal

For the two largest webs, we lastly explored the phylogenetic signal of the observed food webs RDPG approximations as a function of the model dimensionality d. Though the upperbound of our analysis is arbitrary, note that it is much less than the full rank of the food webs' adjacency matrices.

We quantified the presence of a phylogenetic signal by comparing the phylogenetic variance-covariance matrix [Revell et al., 2008] between species in a community with the dissimilarity matrix obtained by considering the pairwise Jaccard similarity [Real and Vargas, 1996] computed from that community's adjacency matrix [Rohr and Bascompte, 2014] (as sampled from a d dimensional model or testing single dimensions). The Jaccard similarity of two species in a food web is the number of common predators that consume both focal species divided by the number of predators that consume at least one of the two. Across all pairs of species, this defines a pairwise similarity matrix depending on the model dimension. Similarly, one can also compute the Jaccard similarity based on common prey, or on common predators and prey. For each model dimension considered, we computed the correlation between 99 sampled Jaccard similarity matrices (for species as prey, predators, or both) and the phylogenetic variance-covariance matrix, and we tested for significance using a Mantel test with 999 randomizations.

We also computed Blomberg's K [Blomberg et al., 2003] measure of phylogenetic signal for the foraging (inward) and vulnerability (outward) functional traits using its multivariate extension proposed by Adams [2014].

Notice, however that the analysis of traits obtained through dimensional reduction techniques can be misleading [Uyeda et al., 2015], in particular when the data analysed is inherently high dimensional.

For the Serengeti National Park data, we used a dated phylogenetic tree based on molecular data compiled by De Zwan *et alii*. For the Weddell Sea, we approximated the real phylogeny via a cladogram obtained from the taxonomic classification of the species as given by the Integrated Taxonomic Information System (http://www.itis.gov; information retrieved on 2014-11-11). Given these trees, we estimated the phylogenetic variance-covariance matrix under the assumption of Brownian motion trait evolution [Felsenstein, 1985; Pagel, 1992]. The model assumes that the traits evolved as independent identically distributed Brownian motion along the lineages defined by the phylogenetic tree.

3.6 Results

3.6.1 Trait dimensionality

The optimal value for the model dimension estimated by is $d = 3$ for the Serengeti food web and of $d = 6$ for the Weddell Sea food web. The result is compatible with our ocular examination of the singular values' scree plot (Figure (3.2)). The threshold methods indicates an upperbound of $d = 4$ (or $d = 2$ (Hard Singular Value Threshold) for the Weddell food web, while it failed to indicate a upperbound for the Serengeti food web (the hard singular value threshold is higher than any of the singular values of the Serengeti food web's adjacency matrix).

The upper bound found with the Singular Value Threshold methods for the smaller webs is consistently $d = 1$ or less (the threshold is higher than all singular values). For these webs, the upper bound found with Zhu and Ghodsi's method is consistently $d = 3$ or lower, except for the Grassland food web [Dawah et al., 1995] for which is $d = 8$.

3.6.2 Model Performance

Fitting performance

In terms of sensitivity, the fitting performance was high: more than 60% in a three dimensional model, in both the Serengeti's and Weddell's food

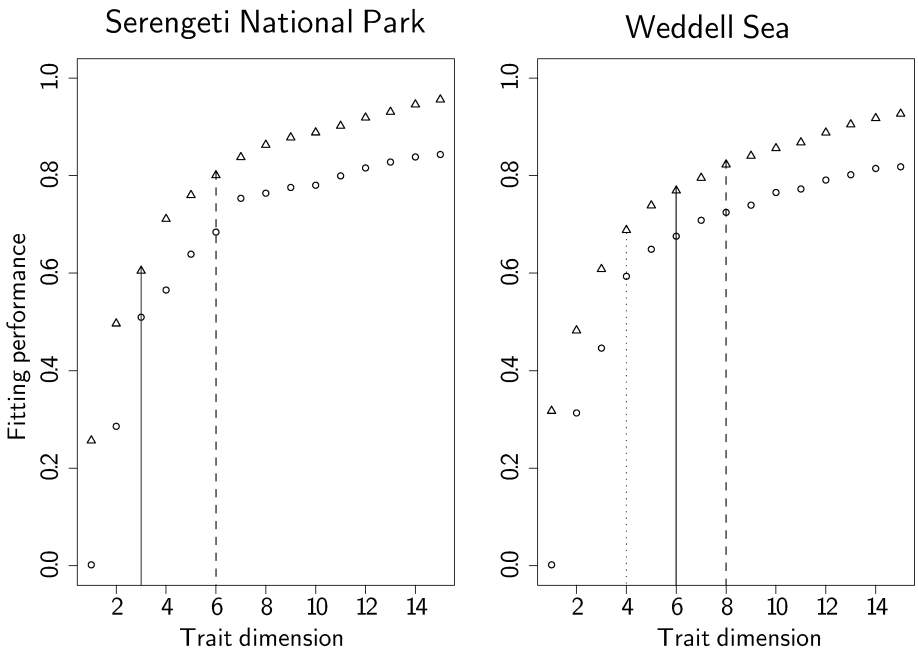

Figure 3.2: Model fitting performance varies with model dimensionality. We show the cumulative sum of the singular value gaps of the food web's adjacency matrix (dots) and fitting sensitivity (triangles) as a function of functional traits' dimension for the Serengeti National Park and Weddell Sea food webs (left and right, respectively). The dotted line corresponds to the dimensionality suggested by the Universal Singular Threshold method, the solid line to Zhu and Ghodsi [2006]'s method, and the dashed line to our visual examination.

webs, and more than 80% in a six (eight) dimensional model in the Serengeti (Weddell) food web. The fitting performance was even higher in terms of accuracy: more than 95% with $d = 3$ in both food webs. On the smaller food webs, the accuracy was consistently above 80% while the sensitivity was more variable, ranging between 20% and 80% at $d = 1$. It was, however, consistently above 80% starting at dimensionalities between $d = 3$ and $d = 8$, with the exception of the Tuesday Lake food web for which the sensitivity never reached 80%).

Predictive power

The predictive power of the RDPG model based on the leave-one-out analysis was high: in the Serengeti's food web more than 60% of the observed links were correctly predicted for models with dimension in the range $d \in \{1, \ldots, 7\}$ and more than 80% of the observed links were correctly predicted for $d \in \{3, 4, 5\}$. The predictive power was even higher in terms of accuracy: more than 95% with $d = 3$ in both food webs. Both accuracy and sensitivity were high on the Weddell sea food web. We could identify a saturating trend in this dataset as well, although we could not detect a peak for values of d between 1 and 16 (and we couldn't extend our analysis further for computational reasons). Nevertheless, we expect a similar overall trend to be present in this case as well.

Performance comparison

The RDPG performed well compared to the other three models we analysed in terms of both fitted and predicted linkwise accuracy. With $d = 1$, the RDPG model's accuracy already exceeded the accuracy of Rohr et al.'s [2010] and Petchey et al.'s [2008a] models for six of the seven smaller webs; in the case of the Broadstone stream food web, this is true starting from $d = 2$ (with $d = 1$ the RDPG model's accuracy roughly matched that of Rohr et al.'s model). The linkwise sensitivity and accuracy of the blockmodel proposed by Allesina and Pascual [2009] is outperformed by the RDPG model on the Serengeti food web starting from $d = 3$ and $d = 2$, respectively.

When amenable to comparison, the RDPG model had a lower AIC than Petchey's Allometric Diet Breadth model and an AIC that was marginally lower or higher than that of Rohr's model and Allesina and Pascual's model

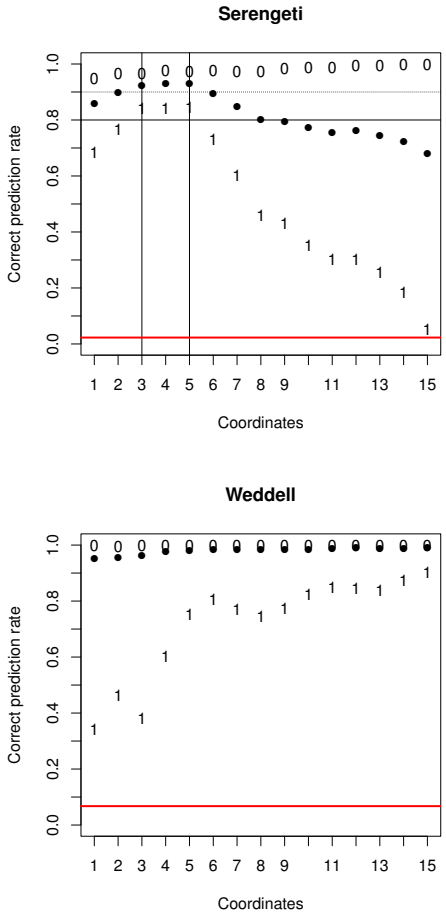

Figure 3.3: Model predictive performance varies with model dimensionality. We show the predictive performance as a function of functional traits' dimension for the Serengeti National Park and Weddell Sea food webs (top and bottom, respectively), for observed links, (1) non-observed links (0), and all pairs of species (full dots). The bottom red line indicates the predictive power of a null model (each link has independent probability of being observed equal to the food web connectance). In the Serengeti plot, we have highlighted the region of peak predictive performance between the two vertical lines.

(Table (3.1)). As one can see from Table (3.2), this is most likely due to the number of parameters, which is considerably higher in the RDPG model than in any other model. For Broom [Memmott et al., 2000] and Grassland [Dawah et al., 1995], two of the smallest webs, the RDPG model assigns a null probability to (at least one) of the observed interactions when d was low. Hence, its log-likelihood in these situations is minus infinity and its AIC is plus infinity.

	Random	Petchey's	Rohr's	Group	RDPG	d
Broadstone stream	809	811	285	272	298	1
Broom	974	1111	657	653	Inf	-
Coachella Valley	866	777	-	411	445	3
Grasslands	1007*	-	944	-	Inf	-
Mill stream	2813	2641	1358	1222	1275	2
Skipwith pond	2529	2654	1491	1360	1485	2
Tuesday Lakes	2893	2513	873	833	1418	3
Serengeti	5647*	-	-	2478*	3416	3

Table 3.1: AIC scores for a directed random graph [Erdös and Rényi, 1960], Petchey's Allometric Diet Breadth (as reported in Allesina, 2011), Rohr's [Rohr et al., 2010], and Allesina and Pascual's [Allesina, 2011, but see Appendix C therein for a caveat about using AIC in this model], and the RDPG model (for the trait length d that minimises the AIC score). The values highlighted by * are computed here on the basis of the data published in [Baskerville et al., 2011, however the caveat discussed in Allesina, 2011 holds here as well].

	Random	Group	RDPG
Broadstone stream	-403.362	-70.941	-91.12
Coachella Valley	-432.108	-115.637	-66.69
Mill stream	-1405.41	-466.776	-477.4
Skipwith pond	-1263.357	-488.002	-458.2
Tuesday Lakes	-1445.359	-199.537	-271.0
Serengeti	-2822.5*	-881.3745*	-742.2*

Table 3.2: Log-likelihood of a Random graph [Erdös and Rényi, 1960], Allesina's and Pascual's [Allesina and Pascual, 2009], and the RDPG model (for the trait length d that minimises the AIC). * from our computation. We omitted the two food webs where we could not choose the RDPG dimension based on AIC.

3.6.3 Species' functional traits

The distribution of species in the functional-trait space can help us explore their ecological role. It would be particularly useful in detecting "outliers", i.e., species with a truly unique role in food web [Petchey et al., 2008b; Jordán, 2009], and clumps, i.e., species with a similar food-web roles [Allesina and Pascual, 2009; Stouffer et al., 2012]. Along these lines, we found that the strongest differentiation in the Serengeti food web was between animals and plants. The phenomenon is clearly visible in the first coordinate of foraging functional and vulnerability functional traits (rightmost column of Figure (3.4)). Top predators and grazers were spread far from the origins of the coordinate axis while plants are stacked upon the axis' origin. We would fully expect this behaviour as they do not have any incoming link (i.e., they do not feed on any other species that is present in the analysed food web).

Similarly, two Hyracoidea species (*Heterohyrax brucensis* and *Procavia capensis*) appeared unique in the foraging functional trait space of the Serengeti web, suggesting that their behaviour as predators is "peculiar". This unique role of Hyracoidea was also observed by the species grouping proposed by Baskerville et al. [2011] based on the identity of species' interactions. Notably, the closest species in terms of foraging functional traits was the elephant (*Loxodonta africana*), which also happen to be the closest evolutionary relative of the Hyracoidea in the Serengeti National Park.

The low-dimensional functional trait space of the Weddell Sea food web also exhibited a complex structure. In particular, the foraging functional traits distribution showed a split of the species into two well-defined groups. As we show in Section (3.6.4), this separation was strongly predicted by the phylogeny. In addition, it is related to the species' feeding behaviour and type. While the Serengeti food web showed a strong separation between plants and animals, the Weddell Sea trait space appeared to be more blurred across trophic guilds.

3.6.4 Phylogenetic signal

We tested for phylogenetic signal of species' functional roles estimated from the Serengeti and Weddell Sea food webs. In general, species' roles exhibited significant phylogenetic signal both for species as predators, as prey, or for both combined. Moreover, in both of these food webs, we observed a

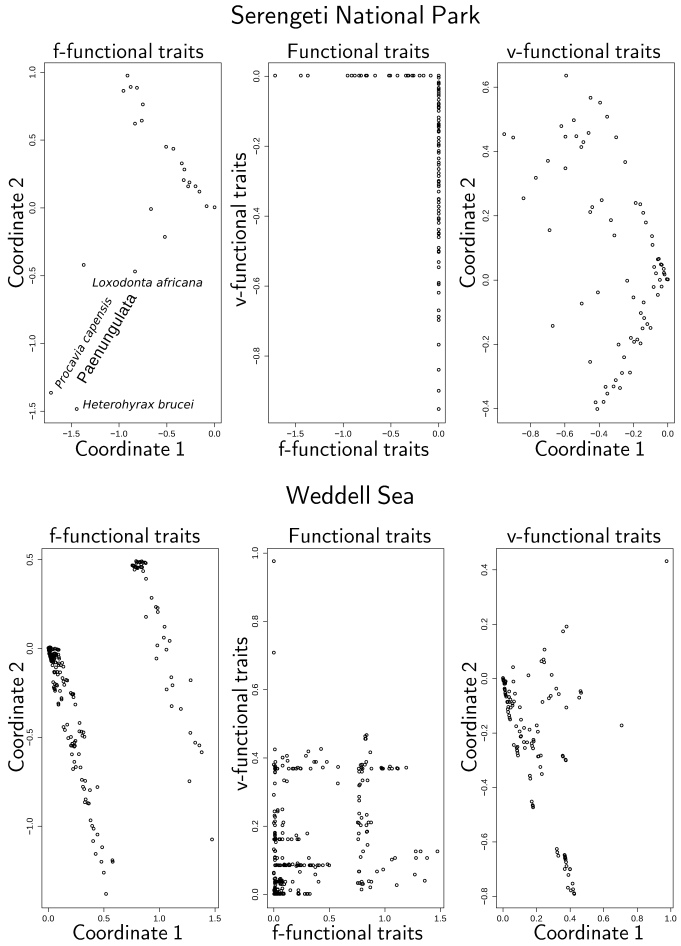

Figure 3.4: The distribution of functional traits for species in the Serengeti National Park and Weddell Sea food webs In the left column we show the first two coordinates of the foraging functional traits, and in the right column we show the first two coordinates of the vulnerability functional traits. In the middle, we show the first foraging functional-trait coordinate against the first vulnerability functional-trait coordinate. We can notice the outlier position of the Hyracoidea (and of *Loxodonta africana*, their closest evolutionary relative) in the Serengeti National Park. The deep distinction between plants and animals in the Serengeti is also visually apparent (central panel).

saturation effect in the correlation between the Jaccard similarity matrix and the phylogenetic variance-covariance matrix as we considered increasing model dimensions from $d = 1$ to $d = 20$ (Figure (3.5)). The trend is stronger if we considered the contribution of single coordinates, as we have a decreasing signal (which is non significant for $d = 4$ and above in the Serengeti).

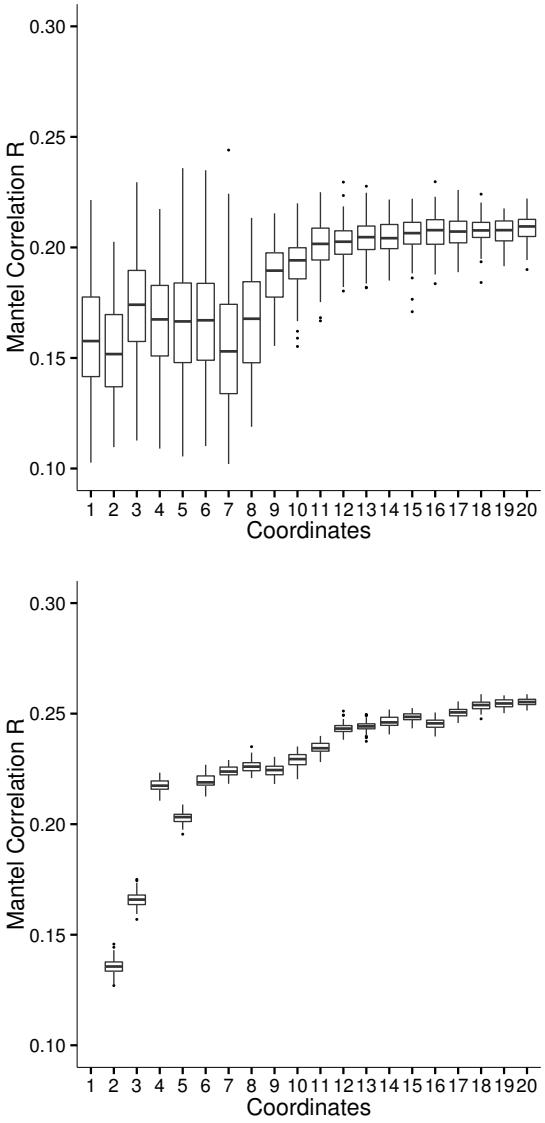

Figure 3.5: Correlation between the similarity of species' roles (as both predator and prey) and the phylogenetic variance-covariance matrix for the Serengeti National Park (top) and Weddell Sea (bottom) food webs. In both panels, we show the (significant at the level $p < 0.01$) correlation for 99 sampled food webs as a function of the length of species' trait vectors. Notice that the model with $d = 1$ for the Weddell Sea is not significant and we don't show the correlation value.

Looking at one coordinate at a time, we detected a decreasing phylogenetic signal (Blomberg's K) for the vulnerability and foraging functional, see

Figure (3.6).

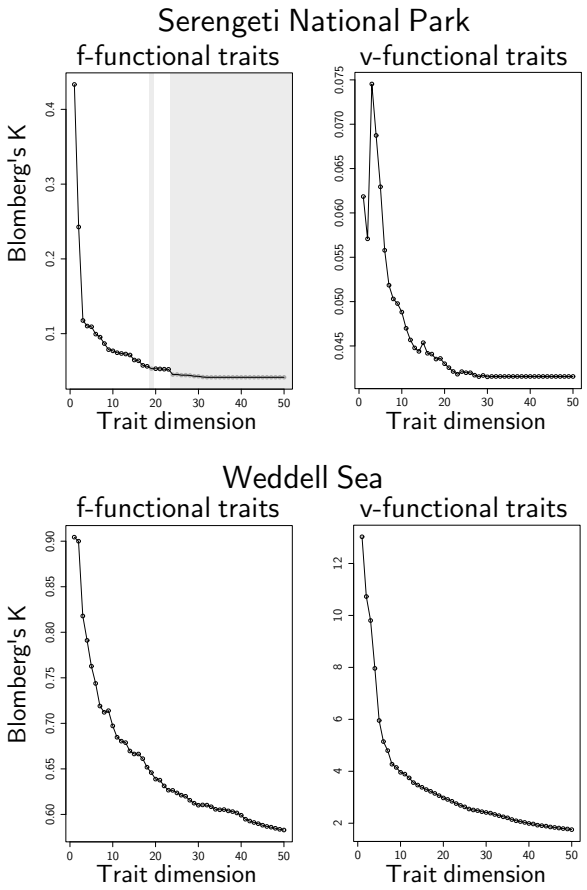

Figure 3.6: Phylogenetic signal (Blomberg's K) across the estimated trait coordinates for the vulnerability (i) and foraging (f) functional traits.

3.7 Discussion

Previous research has indicated that simple, phenomenological food-web models can be successful but are unable to account for all the observed variance of food-web structure [Allesina et al., 2008; Rohr et al., 2010; Williams et al., 2010]. Therefore, to explain the structure of food webs more accurately, we need to adopt a different or improved approach. Here, we introduce one such possibility, the directed random dot product graph model, and study its behaviour for nine food webs (two larger one from the Serengeti National Park and the Weddell Sea and seven smaller food webs). Having estimated

the functional traits for the species in the food webs, we demonstrate that our model can fit observed interactions with considerable link-wise accuracy. We show also that the model can predict interactions for which we simulated absence of observation. While the enumeration and identification of the minimum or sufficient number of traits to "explain" a food web is still an open problem [Eklöf et al., 2013; Capitán et al., 2013], our results support the argument that food webs are inherently low dimensional.

In our approach, we distinguished between species' vulnerability and foraging traits with the former defining their "role" as *preys* and the latter their role as *predators*. This distinction is not uncommon in the available literature [Bersier and Kehrli, 2008; Rossberg et al., 2010; Rossberg, 2013] and may help to explain an element of its success. The way in which we identify these trait values is quite different to earlier approaches in the following way: previous research had attempted to define a suitable function $\mathcal{F}$ that maps a pair of vulnerability and foraging traits to the probability or occurrence of an interaction [Rossberg et al., 2006; Rossberg, 2013]. Typically, the shape of $\mathcal{F}$ was proposed based on some natural assumption of species behaviour e.g., $\mathcal{F}$ should increase with respect to the similarity of the prey's vulnerability and predator's foraging traits [Petchey et al., 2008a] or $\mathcal{F}$ should allow for a certain dietary plasticity [Williams et al., 2010].

Actual traits involved in the process of food web assembly may differ across a web or for each pair of species. For instance, the traits determining the predation habits of an eagle may not be the same as those that determine the grazing preferences of a gazelle. Defining a suitable function $\mathcal{F}$, many prior approaches had to face this problematic complexity. Imposing ad hoc variables and rules for each pair of species is a truly ambitious task, to say the least. Instead, we propose the use of "abstract" *functional* traits that express the combined effect of many species-specific traits that would be measured empirically. Furthermore, our RDPG model adopts an extremely simple function $\mathcal{F}$—a dot product—still able to satisfy key criteria [Rossberg, 2013] while being remarkably predictive. A key consequence of this simplicity is that the complexity of explaining empirical interactions is shifted from identifying a suitable function $\mathcal{F}$ to the functional traits of the species themselves.

Similar approaches are not without precedent [Matias and Robin, 2014]. For example, the functional grouping of species proposed by Allesina and

Pascual [2009] aims to identify *groups* of species that have distinct within- and between-group interaction probabilities. Under the stochastic block model [Holland et al., 1983; Wang and Wong, 1987], the species in a network are partitioned into groups (blocks) such that every group is non-empty and no node sits at the intersection between groups. As this clustering into groups is based solely on the observed food-web structure, the RDPG approach may be considered a generalization of stochastic block models that extends the upper bound on the number of blocks to the number of species in the community. Furthermore, if we consider a model where the block each species belongs to is determined by its position in *functional space* [Rohe et al., 2011; Xu et al., 2014], we can recover the undirected RDPG model by assuming that the probability of a link between two nodes is given by their distance in this space. However, as we have seen comparing the fitting performance of our model and Allesina and Pascual's 2009 model, information is lost forcing the species into k blocks (groups) and assuming that species in blocks behave homogeneously.

3.8 Conclusions

Here, we have shown that complex food webs can be modelled with high fidelity based on a parsimonious stochastic model. Based on the food webs' sequence of singular values, we consistently estimated a dimensionality upperbound much lower than the full rank of the food webs' adjacency matrix. The RDPG model outperformed other classic models both in terms of fitting performance—how many observed present/absent interactions were accurately captured—and in terms of predicting performance—how many non-observed interactions where accurately predicted. On this basis, we believe is important to distinguish the two performance frameworks and to explicitly consider unobserved interactions. We argue this may be best achieved by adopting a probabilistic view of species interactions.

Moreover, we detected a low but significant phylogenetic signal in the species' food-web roles—a result that echoes the conclusions of previous research [Bersier and Kehrli, 2008; Stouffer et al., 2012; Rohr and Bascompte, 2014]. Here, however, we could distinguish between the contribution given by food webs' *backbones*—the relative lower dimensional model structure—and food webs' fine wiring—the relative higher dimensional model structure. In

particular, our results suggest that most of the evolutionary signal is already present in the structure of food webs' stochastic backbones. The importance of the food-web backbones was consistently found when we considered independently species as consumers (or predators) and species as resources (or prey). Moreover, the saturating trend we detected when considering dimensionally increasing models was backed up by the analysis of single coordinates.

The fact that the predictive power of phylogeny varies as function of the choice of model dimensionality begs the question of whether deterministic food-web models are really able to convey information about the evolutionary character of species-rich community. Confirming the presence of evolutionary signal in food webs, our results may be considered a first step in the direction of investigating more of the detailed nature of this signal.

Appendix

Synopsis: In the previous Chapter we saw that the (abstract) functional traits of the species in a food web exhibit an evolutionary signal. The signal was detected under the assumption that branches do evolve independently. In other words, the interactions between species do not affect the species' evolutionary trajectories. However, lineage independence is a strong assumption when we are modelling the evolution of those traits that determine species interactions. In this Appendix, I introduce a model for the evolution of traits that takes the effect of species' interactions on the evolution of species' traits into account, which we label branching interacting traits evolution (BITE) model. BITE is defined for species for which the probability of interactions is distributed according to an RDPG model. It represents an explicit attempt to deal with lineages' non-independence. We will define it rigorously and show how, under the condition that the species community is large enough, it can be interpreted as an extension of the Ornstein–Uhlenbeck model for the evolution of traits.

3.A Evolutionary histories in a community of interacting species

A central assumption of the evolutionary models used in phylogenetic comparative methods (see [Garamszegi, 2014] for a recent introduction) is that the evolutionary processes occurring on different branches of the phylogeny are independent. This allows for a fast estimation of the optimal model's parameters [Revell, 2012; Pennell et al., 2014].

However, the results presented in this thesis as well as other already published studies [Freckleton and Harvey, 2006; Pennell et al., 2015] support the notion that the species' functional traits may have not evolved according

to a simple branching Brownian motion.

Despite the recent advances in the modelling of functional trait evolution in complex ecological networks, a general model is still missing.

3.A.1 The evolution of traits in a fish-bowl

We observe a *phylogeny*, $\mathcal{T}$, in which the tips are a given group of species $\mathbf{S}$ and, for each species $i \in \mathbf{S}$, a d-dimensional vector of traits $\mathbf{i}$. For convenience, we restrict our focus to phylogenies given that are given by rooted ultrametric binary trees: all internal nodes have exactly one parent node and two daughter nodes, tips have exactly one parent node and no daughters, and all tips are observed at the present time T. We model the evolution of species' traits as a stochastic process occurring on the branches of $\mathcal{T}$ (starting from its root).

Branching Brownian motion To start, let us consider species' traits as one-dimensional real variables. The most elementary model we define is commonly named the *branching Brownian motion* model (BBM); the BBM builds on a simple Brownian motion model. The one-dimensional Brownian motion with variance σ (a positive real parameter) is a continuous-time stochastic process $B_\sigma(t)$ into the real line, $\mathbb{R}$, and satisfying the following conditions [Mörters and Peres, 2010]:

1. The process starts at the origin (i.e., $B_\sigma(0) = 0$).
2. The increments are independent from the past (i.e., $B_\sigma(t + \delta t) - B_\sigma(t)$ does not depend on the values assumed by $B_\sigma(t)$ in the past).
3. Any increment $B_\sigma(t + \delta t) - B_\sigma(t)$ is normally distributed with mean 0 and variance $\sigma\delta t$:

$$B_\sigma(t + \Delta t) - B_\sigma(t) \sim \mathcal{N}(0, \sigma\Delta t)\,;$$

4. The process $B_\sigma(t)$ is almost surely continuous:

$$\lim_{s \to t} B_\sigma(s) - B_\sigma(t) = 0\,.$$

The existence of such a stochastuc process has been proved by Wiener [1923].

Let N_t denote the number of extant species at each time t. We express the values of the traits in S at time t by a column vector of dimension N_t $\mathbf{X}(t) \in \mathbb{R}^{N_t}$. Each row, $\mathbf{X}_i(t)$, of $\mathbf{X}(t)$ evolves, between two speciation events, as a Wiener process. In other words, $\mathbf{X}(t + \Delta t) - \mathbf{X}(t)$ is distributed as an indipendently and indentically distributed multinomial random variable with mean 0 and variance $\sigma\Delta t$. As a formula:

$$\mathbf{X}_i(t + \Delta t) - \mathbf{X}_i(t) \sim \mathcal{N}(0, \sigma\Delta t), \tag{3.21}$$

as long as the interval $[t, t + \Delta t]$ does not include a speciation event. Let s be the time at which the ancestral lineage i speciated. In that moment, the row i of $\mathbf{X}(s)$ is substituted by two rows that have identical values to $\mathbf{i}(s)$ and the evolution process continues independently henceforth. If we ignore all the other lineages and focus on one lineage from the root to a tip i, the value of $\mathbf{i}(t)$ describes a Brownian motion.

It is convenient to write the Brownian motion as a diffusion process (see Section 12.4 in [Bosq and Nguyen, 2013]) defined by a stochastic differential equation:

$$\mathrm{d}\mathbf{X}(t) = \sigma \, \mathrm{d}B_t. \tag{3.22}$$

In fact, what we mean is that the increments of $\mathbf{X}(t)$ are given by the integral equation:

$$\mathbf{X}(t + \Delta t) - \mathbf{X}(t) = \sigma \int_t^{t+\Delta t} \mathrm{d}B_u, \tag{3.23}$$

where the integral has to be interpreted as an Itô integral [Itô, 1944] with respect to the Brownian process B_u. Under this notation, σ is known as the diffusion coefficient.

The BBM model is thoroughly detailed in the literature and has been extended in different directions: it is possible to (a) incorporate a drift imposing a non-zero mean to the distribution of the underlying Wiener process (i.e., defining a new stochastic process $V(t) = \mu t + W(t)$); (b) to relax the hypothesis of identical distribution, letting σ depend on the lineages (i.e., $\sigma = \sigma(i)$); (c) to let the parameters depend on the absolute time (i.e., $\sigma = \sigma(t)$), the age of the lineage (i.e., $\sigma = \sigma(i, t - s(i))$, where $s(i)$ is the time to the most recent ancestor of the lineage $s(i)$) or the speciation rate of (a subtree of) the phylogeny. See [Thomas and Freckleton, 2012] for a review of the above and other models.

This generalisations does not affect the independence of the lineages: after a speciation event, all the species evolve independently.

Branching Ornstein–Uhlenbeck model An important extension of the BBM is based on a stochastic process introduced in the 1930s by Leonard Ornstein and George Eugene Uhlenbeck that models the motion of a particle (here a species) that is attracted toward an *optima* position Θ and diffuses according to a Brownian motion (see [Wax, 1954]). Using the notations introduced above, we can write Ornstein's and Uhlenbeck's model (the Ornstein–Uhlenbeck model or OU) as:

$$\mathrm{d}\mathbf{X}(t) = \alpha\left[\Theta - \mathbf{X}(t)\right]\mathrm{d}t + \sigma(t)\,\mathrm{d}\mathbf{B}\,\mathrm{d}t, \tag{3.24}$$

where Θ is a column vector in which the rows are the trait optima of the species in $\mathbf{S}(t)$ and α is a column vector in which the rows are given by parameter that determine the strength of attraction toward the species' (theoretical) optimum [Doob, 1942]. We call the term $\alpha\left[\Theta - \mathbf{X}(t)\right]$ the drift term of the stochastic process. Rigorously, the OU stochastic process is defined as stochastic integral equation:

$$\mathbf{X}(t+\Delta t) - \mathbf{X}(t) = \alpha\int_t^{t+\Delta t}\left[\Theta - \mathbf{X}(t)\right]\mathrm{d}t + \sigma\int_t^{t+\Delta t}\mathrm{d}B_u, \tag{3.25}$$

where the first integral has to be interpreted in the classic Riemann sense and the second is the Itô stochastic integral [Itô, 1944].

The branching Ornstein–Uhlenbeck model (BOU) [Hansen, 1997] is defined as the BBM, but the independently and indentically distributed processes occurring on the lineages between speciation events are Brownian motion with drift (OU) processes instead of pure Brownian motion processes. When a mother lineage speciates, her daughter lineages inherit the mother traits.

As for the BBM model, various generalisations have been considered (see [O'Meara and Beaulieu, 2014] for an overview): α can depend on the lineages and on the time, where as the optima Θ can be fixed and equal for all species, or depend on time and lineages $(\Theta)_i(t) = \Theta(i,t)$.

The branching Ornstein–Uhlenbeck model and the named generalisations assume lineage independence.

3.A.2 Expected species' covariance

In practice, we do not observe the evolutionary trajectories of species' traits; instead, we can reconstruct the species' phylogeny from molecular data and observe the distribution of the traits among its tips.

The problem is to compare the distribution of the traits as observed empirically with what we would expect to observe under a certain evolutionary model (e.g., BBM, BOU or one of their extensions) to fit the model parameters and assess if the fit is significant or not. Thus, the evolutionary models are distinguishable as long as they produce different expected trait's distribution (see [Kaliontzopoulou and Adams, 2016] for a discussion of the limitations imposed by this request).

Consider, at time T, a pair of species i and j for which the most recent common ancestor speciated at time S. The species i and j have evolved independently for a time $s = T - S$. Hence, the expected variance–covariance structure for the species' traits is given by:

$$\mathbf{V}_{BBM} = \sigma \begin{bmatrix} T & S \\ S & T \end{bmatrix} \tag{3.26}$$

under a BBM model of evolution [Felsenstein, 1985] with variance σ and by:

$$\mathbf{V}_{BOU} = \sigma \begin{bmatrix} 1 - e^{-2\alpha T} & e^{-2\alpha s}\left(1 - e^{-2\alpha S}\right) \\ e^{-2\alpha s}\left(1 - e^{-2\alpha S}\right) & 1 - e^{-2\alpha T} \end{bmatrix} \tag{3.27}$$

under a BOU model of evolution [Hansen, 1997] with variance σ and an attraction strength α. Notice that for a BOU with a unique selection regime (i.e, the α and θ for the same for all the lineages), the trait optimum does not appear in the covariance matrix.

Given a dated phylogeny $\mathcal{T}$, we can fully specify the expected variance–covariance matrix of an indefinitely large group of species using Equations (3.26) and (3.27), as the pairwise covariance of each pair of species is independent from that of all the other species. Thus, given the trait's distribution and the species' phylogeny, we can compute the likelihood of a BBM [Pagel, 1999] or BOU [Butler and King, 2004] evolutionary model, even in the presence of measurement errors in the trait [Ives et al., 2007; Silvestro et al., 2015] or the phylogenetic [Huelsenbeck et al., 2000; Rangel et al., 2015] data.

3.B The evolution of traits when species interact

All the models discussed in the previous section assume the independence of concurrent lineages. As we are interested in studying the evolution of the traits that determine the probability of interactions between the species, we may want to abandon that assumption. Indeed, Nuismer and Harmon [2015] have shown that the presence of evolutionary effects due to species interactions, in the form of either a repulsion or an attraction between species with similar traits, leads to trait distributions that are strikingly different from what would be expected in the absence of interactions effects.

Here, we begin to sketch a food-web model of traits evolution. We explicitly include in the model the effect of ecological interactions among the species of a food web: the evolution of a lineage will depend on the traits of all other interacting lineages. Theoretical [Doebeli, 2011] and empirical [Abrams, 2000] results regarding the adaptive radiation and diversification of predator–prey (resource–consumer) systems support the notion that species' traits adapt to increase their trophic fitness, which is the ability of a species to prey (consume) or escape predation (consumption) [Nosil and Crespi, 2006; Nosil, 2012].

3.B.1 Adaptive dynamics and coupled differential equation

3.B.2 Functional traits

Let $\mathbf{i}(t)$ and $\mathbf{j}(t)$ be the real d-dimensional functional traits of the species i and j at time t. Let m_{ij} be a scalar function mapping the functional traits of i and j into the interaction propensity between i and j; in other words, $m_{ij}\left(\mathbf{i}(t), \mathbf{j}(t)\right) \in [0, 1]$ is the probability of species i interacting with species j. Similarly, let d_{ij} be a vectorial function from the traits of i and j to the direction that the evolution of the traits of i would take if there were no other species except j (and if the evolution of the traits had no stochastic motion component); specifically, $d_{ij}\left(\mathbf{i}(t), \mathbf{j}(t)\right) \in \mathcal{S}^d_{0,1}$, where $\mathcal{S}^d_{0,1}$ is the unitary d-sphere, which expresses the direction of the displacement of the traits of species i caused by species j. We will often drop the traits $\mathbf{i}(t)$ and $\mathbf{j}(t)$ from the notation, and write $m_{ij}(t)$ and $d_{ij}(t)$ for $m_{ij}\left(\mathbf{i}(t), \mathbf{j}(t)\right)$ and $d_{ij}\left(\mathbf{i}(t), \mathbf{j}(t)\right)$ respectively.

We can combine the magnitude m_{ij} and the direction d_{ij} into a function

f_{ij} describing the effect of species j on species i:

$$f_{ij}(t) = m_{i,j}(t)\, d_{i,j}(t), \tag{3.28}$$

If $\mathbf{i}(t)$ and $\mathbf{j}(t)$ are vectors in $\mathbb{R}^d$, then f_{ij} maps the functional traits into the closed unitary d-ball, $f_{ij} : \mathbb{R}^d \times \mathbb{R}^d \to \mathcal{B}^d_{0,1}$. Each species j that is extant at time t affects the evolution of species i's traits in accordance with $f_{ij}(t)$ and a parameter $\alpha_i(t)$, giving the sensitivity of species i to the ecological pressure at time t.

Using the notation we introduced in Section 3.A.1, we assume that the evolutionary effect of the ecological interactions are additive and define the evolution of species i's traits as:

$$\mathrm{d}\mathbf{i}(t) = \alpha_i(t) \sum_{j \in \mathbf{S}(t)} f_{ij}(t)\, \mathrm{d}t + (1 - \alpha_i(t))\, \mathrm{d}\mathbf{B}(t), \tag{3.29}$$

where $\mathbf{S}(t)$ are all the species extant at time t and $\mathbf{B}(t)$ is a d-dimensional Brownian motion with vector of variance $\vec{\sigma}$ (in other words, each coordinate l of $\mathbf{B}(t)$ has variance $\vec{\sigma}_l$).

In general, the three forces f_{ij}, m_{ij} and d_{ij} need not be the same for all pairs of species; neither, in practice, is it always possible to estimate $m_{ij}(t)$ and $d_{ij}(t)$.

3.B.3 The random dot product graph case

The BITE model can be specified for the food-web model defined in this chapter. Indeed, I propose a definition of the magnitude and direction component of f_{ij} grounded on the species' functional traits as estimated by RDPG.

The RDPG model considers asymmetric interactions between species determined by a pair of vector traits for each species, where each vector is of length d. If i is a prey of the predator j, then the vulnerability traits of i are affected by the foraging traits of j (and vice versa). The interaction probabilities are defined by the proximity of the vulnerability traits ($\mathbf{i}^{(out)}(t)$) and the foraging traits $\mathbf{i}^{(out)}(t)$ in a d-dimensional Euclidean metric space.

Accordingly, we can decompose the magnitude of the ecological pressure of j on i, m_{ij}, into the magnitude of the ecological pressure of j on the vulnerability traits of i ($m_{i^{(out)},j^{(in)}}$, which depends just on the foraging

traits of j) and the magnitude of the ecological pressure of j on the foraging traits of i ($m_{i^{(in)},j^{(out)}}$, which depends just on the vulnerability traits of j).

We can write an explicit formula for the magnitude of the evolutionary effect between each pair of species in a food web:

$$m_{i^{(out)},j^{(in)}}(t) = \mathbf{i}^{(out)}(t) \cdot \mathbf{j}^{(in)}(t). \tag{3.30}$$

As the dot product is symmetric, the magnitude of the evolutionary effect is symmetric:

$$m_{j^{(in)},i^{(out)}}(t) = m_{i^{(out)},j^{(in)}}(t) \ . \tag{3.31}$$

We can define the directional component of the ecological pressure of j on i similarly, distinguishing the effect on the vulnerability ($d_{i^{(out)},j^{(in)}}$) and the foraging ($d_{i^{(in)},j^{(out)}}$) traits of i. The key modelling assumption is that the traits of the prey i evolve to maximise the angular distance to the predator j's foraging traits and hence decrease the magnitude of the effect of j; conversely, the traits of the predator j evolve to minimise the angular distance to the prey i's vulnerability traits and hence increase the probability of an interaction with i (e.g., the probability that i is preyed or consumed by j). In particular, left by themselves, a pair of predator and prey species would evolve in the same direction, entering into an arms race [Vermeij, 1987]:

$$d_{i^{(out)},j^{(in)}}(t) = d_{j^{(in)},i^{(out)}}(t) \tag{3.32}$$

Let $\mathbf{j}^{(in)}(t) -_w \mathbf{i}^{(out)}(t)$ be the projection of the vector $\mathbf{j}^{(in)}(t) - \mathbf{i}^{(out)}(t)$ onto the sphere which has the origin as its centre and a radius $\|\mathbf{i}^{(out)}(t)\|$. We can now write the direction component $d_{i^{(out)},j^{(in)}}$ as:

$$d_{i^{(out)},j^{(in)}}(t) = \frac{\mathbf{j}^{(in)}(t) -_w \mathbf{i}^{(out)}(t)}{\|\mathbf{j}^{(in)}(t) -_w \mathbf{i}^{(out)}(t)\|} \, . \tag{3.33}$$

Let $\mathbf{pP}\left[\mathbf{i}^{(out)}(t), \mathbf{X}^{(in)}(t)\right]$ and $\mathbf{Pp}\left[\mathbf{i}^{(in)}(t), \mathbf{X}^{(out)}(t)\right]$ be the total interaction effects on the evolution of i as prey and as a predator, respectively. Specifically:

$$\begin{cases} \mathbf{pP}\left[\mathbf{i}^{(out)}(t), \mathbf{X}^{(in)}(t)\right] & = \sum m_{i^{(out)},j^{(in)}}(t)\, d_{i^{(out)},j^{(in)}}(t) \ ; \\ \mathbf{Pp}\left[\mathbf{i}^{(in)}(t), \mathbf{X}^{(out)}(t)\right] & = \sum m_{i^{(in)},j^{(out)}}(t)\, d_{i^{(in)},j^{(out)}}(t) \ . \end{cases} \tag{3.34}$$

We now have a fully specified model for the evolution of the traits in a group of species that interact according to an RDPG-like food web model. We can write the traits evolution of each species i in a food web as a couple of stochastic differential equations:

$$\begin{cases} \mathrm{d}\mathbf{i}^{(out)}(t) & = \vec{\alpha}_i \mathbf{pP}\left[\mathbf{i}^{(out)}(t), \mathbf{X}^{(in)}(t)\right] \mathrm{d}t + (1-\vec{\alpha}_i)\,\mathrm{d}\mathbf{B}(t) \\ \mathrm{d}\mathbf{i}^{(in)}(t) & = \vec{\alpha}_i \mathbf{Pp}\left[\mathbf{i}^{(in)}(t), \mathbf{X}^{(out)}(t)\right] \mathrm{d}t + (1-\vec{\alpha}_i)\,\mathrm{d}\mathbf{B}(t)\,, \end{cases} \tag{3.35}$$

where $\mathbf{B}(t)$ is a d-dimensional Brownian motion with variance $\vec{\sigma}$.

Notice that $\mathbf{pP}[\cdot,\cdot]$ and $\mathbf{Pp}[\cdot,\cdot]$ are completely determined by the distribution of the species' functional traits in the functional space of the food web. Hence, the only free parameters of the models are the variance of the of the Brownian motion $\vec{\sigma}$, the species' sensitivity to the ecological pressure $\vec{\alpha}$ and the RDPG model dimension d.

3.B.4 BITE as an Ornstein–Uhlenbeck process

Our definition of the Ornstein–Uhlenbeck process can be generalised further by introducing lineage-specific trait optima, denoted $\Theta(i,t)$, which are a function of the time [Bartoszek, 2013]. In particular, $\Theta(i,t)$ can itself be a stochastic process, such as a Brownian motion. This kind of model has been considered in phylogenetic comparative methods. For example, Beaulieu et al. [2012] analysed a family of evolutionary models where the optima $\Theta(i,t)$ were stepwise constant functions, which could differ from lineage to lineage.

In a complementary direction, the BOU model has been generalised by introducing global optima that are themselves stochastic process: the Ornstein–Uhlenbeck with Brownian optima (OUBM) model [Hansen et al., 2008] consider optima drifting as a Brownian motion; the Ornstein–Uhlenbeck with Ornstein–Uhlenbeck optima (OUOU) model [Jhwueng and Maroulas, 2014] consider optima that evolve as an Ornstein–Uhlenbeck process (independent from the main Ornstein–Uhlenbeck process) where optima are centred on zero.

We can express the BITE model in the form of an Ornstein–Uhlenbeck model with lineage-specific and drifting trait optima. Indeed, we can define

the optima for the vulnerability traits of species i at time t, $\Theta_i^{(out)}(t)$, as:

$$\Theta_i^{(out)}(t) = \mathbf{i}^{(out)}(t) - \mathbf{pP}\left[\mathbf{i}^{(out)}(t), \mathbf{X}^{(in)}(t)\right], \tag{3.36}$$

and the optima for the foraging traits of species i at time t, $\Theta_i^{(in)}(t)$, as:

$$\Theta_i^{(in)}(t) = \mathbf{i}^{(in)}(t) - \mathbf{Pp}\left[\mathbf{i}^{(in)}(t), \mathbf{X}^{(out)}(t)\right]. \tag{3.37}$$

The optima for the vulnerability traits and the foraging traits are both completely determined by the food-web distribution of the vulnerability and foraging traits. We can now rewrite the evolutionary Equation (3.35) as:

$$\begin{cases} \mathrm{d}\mathbf{i}^{(out)}(t) &= \vec{\alpha}_i \left[\Theta_i^{(out)}(t) - \mathbf{i}^{(out)}(t)\right] \mathrm{d}t + (1 - \vec{\alpha}_i)\, \mathrm{d}\mathbf{B}(t) \\ \mathrm{d}\mathbf{i}^{(in)}(t) &= \vec{\alpha}_i \left[\Theta_i^{(in)}(t) - \mathbf{i}^{(in)}(t)\right] \mathrm{d}t + (1 - \vec{\alpha}_i)\, \mathrm{d}\mathbf{B}(t), \end{cases} \tag{3.38}$$

where $\mathbf{B}(t)$ is a d-dimensional Brownian motion with variance $\vec{\sigma}$ and sensitivity to the ecological pressure $\vec{\alpha}$.

In general, we cannot apply the usual techniques to compute the traits' covariance (see, for example, the Appendix in [Beaulieu et al., 2012]), as the increments of $\Theta_i^{(out)}(t)$ and $\Theta_i^{(in)}(t)$ are not independent from the traits of i.

However, let us choose a species i from $\mathbf{S}$ uniformly at random. At each time t of the evolutionary process, the maximum effect that can be applied by any species j on i is bounded by the norm of j's trait vectors. Moreover, suppose that the traits of each species j that fall into a cone $\mathcal{C}_r(i)$ (a hyperconic subset of the functional space, determined by all the point of the functional space having angular distance to the species i at most equal to r) are symmetrically distributed around i; in other words, suppose that the probability of finding a species j is the same in each direction around i. We can approximate the total ecological pressure on i (for either its foraging or vulnerability traits) by the sum of all the effects applied by the species j in the cone $\mathcal{C}(i)$; in fact, the magnitudes of the effect applied by the species decrease with the angular distance from i, and thus the species l falling outside the cone $\mathcal{C}_r(i)$ contribute relative less than the species falling into the cone. We can, under the hypothesis that the species' traits in $\mathcal{C}_r(i)$ are distributed independently[1], invoke the central limit theorem for bounded

[1] We could, in fact, weaken this hypothesis and require only *weak* independence [Billingsley, 2008], namely that the traits of species that are distant enough in the functional space

variables (see, for example, exercise 27.4 in [Billingsley, 2008] and conclude that the sum of the effects of the species in the cone converges weakly to a multinomial distribution centered in zero[2].

Hence, in the scenario with low d and high $\mathbf{S}$, we expect the evolution of the species' functional traits to be described by an Ornstein-Uhlenbeck process with lineage-specific optima drifint as an independent Brownian motion process. However, further analysis is needed to confirm this conjecture.

3.C Discussion

We cannot yet provide a closed expression akin to Equation (3.26) for the traits' covariance under the BITE model. In fact, the expected trait variance of any species and the expected trait covariance of any pair of species depend on the trait distribution of the whole community of species. However, at least for relative simpler models [Drury et al., 2015], it has been shown that the covarinace between each pair of species can be obtained as a solution to a differential equation.

Analytical insights such as those that close the previous section may help us to understand—at least qualitatively—what network structure and trait distribution we should expect when the species' interactions affect the evolution of the species' traits [Nuismer and Harmon, 2015]. In Chapter (4), we define a family of species' centrality measures and we estimate their empirical distribution in a five observed food webs. We will see that the distribution of those centralities appears to derive from an Ornstein–Uhlenbeck evolutionary process, compatible with the indications of this Appendix.

Large community-evolution models [Loeuille and Loreau, 2009] have been proposed from different perspectives, such as individual-based models [Melián et al., 2011] and the analysis of *adaptive dynamics* [Brännström et al., 2012]. The results obtained are encouraging. These models are, in general, burdened by an explicit description of population dynamics (based on linear or non-linear demographic responses [Drossel et al., 2004]), and are defined on a low-dimensional [Itô and Ikegami, 2006; Itô et al., 2009; Allhoff et al., 2015; Drury et al., 2015; Clarke et al., 2015] or discrete space [Caldarelli et al., 1998;

are independently distributed.

[2]However, the convergence on the number of species in $\mathbf{S}$ is slow [Hall and Barbour, 1984] and its speed decreases with d, because the probability of picking a species i from $\mathbf{S}$ that is peripheral in the functional trait space increases.

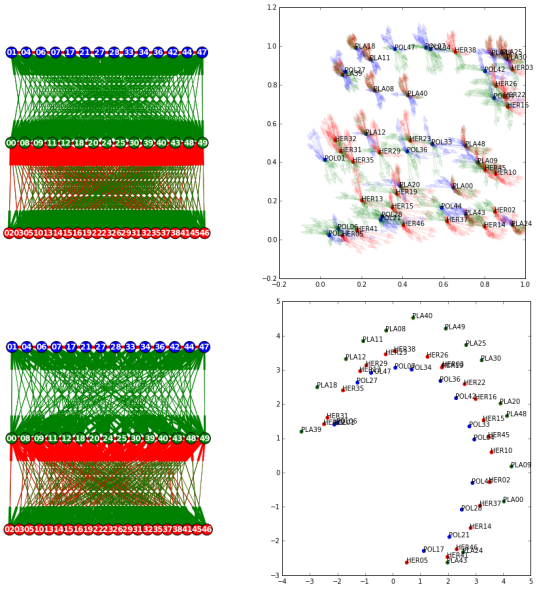

Figure 3.C.1: A time lapse of the evolution of a food web under the Bite model. Here, three guilds of species (plants in green, pollinators in blue and herbivores in red) interact according to the Bite model.

Drossel et al., 2001; Rossberg et al., 2006]. Generalising these models to higher dimensions in a continuous space is not trivial, neither mathematically nor biologically. It has been shown by Doebeli and Ispolatov [2010] that the dimension of the trait space plays a key role in species evolution, as there is a trade–off between stability and diversity [Débarre et al., 2014; Doebeli and Ispolatov, 2014; Ispolatov et al., 2016]. It is interesting to notice that the dimensionality we estimated from the RDPG model is in line with this result. The functional space dimension is an easily tuneable parameter of the BITE model; the model is also easier to simulate, as it does not depend explicitly on the species' demographic dynamics. The relationship between BITE, individual-based and adaptive dynamics models requires further investigation.

We mentioned in Section (2.2.2) that information about food webs' diachronic assembly is sparse. The available topological definition is not adequate for directly reconstructing the evolutionary trajectories of species' RDPG traits. Hence, we have to rely on comparative and indirect methods if we are to assess the relevance of ecological interactions for the evolution of species in food webs. The use of computer simulation for testing evo-

lutionary models has a long history [Garland et al., 1993]. Recent results [Allhoff et al., 2015] have shown that accounting for species' interactions when simulating the evolution of food webs produces realistic ecological networks. This result support the notion that there is an important feedback between the ecological and evolutionary processes. Similarly, our preliminary exploratory simulations (see Figure 3.C.1 for a typical outcome of a short time simulation) seem to suggest that the BITE model for the evolution of a food web can recover some of the properties of empirical food webs, such as their modular structure and their nestedness.

Chapter 4

Centrality and uniqueness in random dot product graphs

Synopsis: Estimating species' relative importance in their ecosystems—in terms of their contribution to ecosystems' stability and diversity—is a crucial task at the core of all scientifically informed efforts to preserve the planet's biodiversity. This task is commonly grounded on the measurement of the species'—morphological, behavioural and trophic—characters, or through their evolutionary history. However, collecting enough homogeneous data to assess each species' importance across a large ecosystem is labour-intensive and is not always feasible. Thus, the description of ecosystems as food webs—the graphs of who-eats-whom—allowed the adoption of graph-theoretical proxies for species' importance depending just on the food webs' topological structures. These measures derive from rigid, deterministic graph models. Therefore, their applicability to complex food webs, which are characterized by stochastic behaviours, can be limited. Here, we assess species' ecological relevance while accounting for food webs' stochasticity. To do so, we model food webs as RDPGs and identify their stochastic backbones: the most statistically persistent interactions. The RDPG model allows us to estimate a species' position in a low-dimensional abstract functional trait space, either for a species as prey, as a predator or as both predator and prey. The representation of a species in this functional space offers a unified framework in which to estimate the species' importance for food web stability, their contribution to the food web's functional diversity and their ecological uniqueness, relying only on topological data. We compare the species' ordering based

on their relevance, as determined by our novel measures and six classic measures, and explore the distribution of species relevance among the tips of the Serengeti National Park food web's phylogeny. Although we do not detect a linear correlation between evolutionary and ecological relevance, we find a clade of species that are both ecologically and evolutionarily distinctive. Our results highlight the importance of considering both evolutionary and ecological factors when valuing species for conservation purposes.

Notes: A version of this chapter has been submitted to *Royal Society Open Science* (The Royal Society Publishing): GVDR and Carey Priebe (Department of Applied Mathematics and Statistics, Whiting School of Engineering, John Hopkins University), "Important, Unique and Central: Species' Relevance in Food Webs".

I go for all, because someone
must go for all.

The Brothers Karamazov
Fyodor Dostoyevsky
Translated by Constance Garnett

4.1 Introduction

The need for scientifically informed conservation policies boosted the attempts to estimate species' relative importance in food webs: the graphs describing the flows of energy between species in an ecosystem [May, 2009]. A sound approach to assess a species' contribution to an ecosystem is based on the concept of functional diversity. As summarised by Petchey and Gaston [2006, pg. 742],

> [...] measuring functional diversity is about measuring functional traits diversity, where functional traits are components of an organism's phenotype that influence ecosystem level processes.

In this context, the contribution of a species to the functional diversity of a food web is captured by the traits diversity loss that we would observe after the removal of that species [Villéger et al., 2008; Fontana et al., 2015]. However, identifying suitable phenotypic traits and collecting all the necessary data across a full food web is often ambitious. The tangled intricacy of food webs, where there are often thousands of interactions between hundreds of plants and animals, motivates the use of complex-network tools for solving ecological problems [Proulx et al., 2005]. Centrality measures—graph theoretical measures developed in economic, social, technological and theoretical scenarios to identify crucial nodes in a network [Newman, 2009]—have been proposed to assess a species' centrality and to identify the species that play a crucial role within an ecosystem [Estrada, 2007; Lai et al., 2012].

The evolutionary distinctiveness of species (i.e., the amount of *exclusive* evolutionary information hinging on a species) is an intrinsic component of biodiversity [Mace et al., 2003] and the evolutionary diversity of species is used as a proxy for a species' functional diversity [Winter et al., 2013]. Evolutionary diversity has been shown to promote ecosystem stability [Cadotte

et al., 2012]. Accordingly, it has been argued that the evolutionary distinctiveness of species should be one of the factors grounding conservation efforts [Faith, 1992; Redding and Mooers, 2006; Isaac et al., 2007]. However, the exact relationship between the evolutionary and food-web distinctiveness of a species is an open problem [Gerhold et al., 2015; Miranda and Parrini, 2015].

In the previous chapter, we introduced directed RDPG for food webs: from the classic binary description of a food web—its adjacency matrix—we estimate species' position in an *abstract functional trait* metric space so that the species' interaction probabilities are determined by the pairwise distance structure: the probability of observing an interaction from species i to species j (e.g., j feeding on i) is given by the dot product of the vulnerability functional traits of i and the foraging functional traits of j.

This motivates the distinction between a food web's backbone—its most statistically persistent structure—and its fine wiring, which is more sensitive to contingent ecological factors or stochastic noise [Grady et al., 2012; Bellingeri and Bodini, 2015]. A robust ordering of species based on their ecological relevance should not be too sensitive on the fine wiring of a food web [Livi et al., 2011].

Here, we show how the abstract functional trait space, estimated by the RDPG model, offers a unified framework in which to assess species' importance, uniqueness and diversity. We propose three measures, relying only on topological food-web data, which can serve as proxies for measures based on phenotypic data.

Building on the existing measures of trophic similarity [Yodzis and Winemiller, 1999; Luczkovich et al., 2003; Jordán et al., 2009], we will define the *uniqueness* of a species' food-web role as its isolation (i.e., the average distance to all the other species) in the abstract functional traits space estimated by the RDPG model. To measure the species' relative importance in a food web, we define a species' *strain* as the effect that removing that species has on the estimated abstract functional trait space: for each focal species in the food web we measure the total distance between the remaining species' positions in the abstract functional trait space before and after the removal of the focal species. The strain of a species captures a global effect at the whole food-web scale, rather than a local property of its interactions structure. Borrowing from the functional diversity literature, we estimate

the functional diversity of a food web as the volume of the convex hull enclosing all the species' abstract functional traits. Accordingly, we define the contribution of a species to the functional diversity of a food web as the loss in diversity caused by the removal of that species. Focussing on the vulnerability, on the foraging or both the vulnerability and foraging abstract functional traits, we can assess a species' relevance as prey, as a predator or as both predator and prey. We distinguish among the species' strain, uniqueness, and contribution to the functional diversity as prey (*outward* strain, uniqueness, and contribution to the functional diversity), as a predator (*inward* strain, uniqueness, and contribution to the functional diversity) or as both a predator and prey (*total* strain, uniqueness, and contribution to the functional diversity).

We correlate these novel measures among each other as well as with six classic network centrality measures, and we explore their distribution among the clades present in the food web. In particular, we test whether the distribution of ecological relevance among the tips of the Serengeti National Park food web's phylogeny is compatible with an evolutionary model of traits evolution. Finally, we examine the hypothesis that the species' ecological relevance and evolutionary distinctiveness are indeed correlated.

4.2 Food-web relevance

Random dot product graphs Let A be a food web including S species. Given a dimension d, under the RDPG model, each species i in A is associated to a pair of abstract functional trait vectors of dimension d. The two vectors are the *rank-d vulnerability* traits (or outward traits), which describes the species as a prey or a resource, and the *rank-d foraging* traits (or inward traits), which describes the species as a predator or a consumer. The probability of observing an interaction from species i to species j is given by the dot product of the out traits of i and the in traits of j. For an observed food web A, the species' traits are estimated through a scaled, truncated, singular value decomposition of the adjacency matrix of A (see the previous chapter for more details).

4.2.1 Strain

The strain of species i measures the effect that the removal of i from the food web has on the remaining species' abstract functional traits, as estimated from the RDPG model. The effect is measured for species either as predators, as prey or as both. Let $X(A)$ be the matrix of either the inward, outward or total rank-d abstract functional traits (the last one being the matrix in which the first d columns are given by the inward traits and the next d columns are given by the outward traits). We use $X(A)^{r(i)}$ to denote the matrix of the (inward, outward or total) functional traits for all the species in the food web A except i (i.e., the matrix obtained by $X(A)$ removing the ith row). The matrix $X\left(A^{d(i)}\right)$ is the matrix of traits for the species in the food web A that has been computed after having dropped the species i from the food web with all its interactions (i.e., the matrix of traits computed after removing the ith row and column from A). Both $X(A)^{r(i)}$ and $X\left(A^{d(i)}\right)$ are matrices with $S-1$ species (each species in A but i) and d columns (the model's dimension). In $X(A)^{r(i)}$, the functional traits are computed before removing i, in $X\left(A^{d(i)}\right)$ they are computed after the removal event.

In the previous chapter we noticed that the parameter matrix of and RDPG model is defined up to an orthogonal transformation. Thus, the distance between $X(A)^{r(i)}$ and $X\left(A^{d(i)}\right)$ is given by both the species removal effect and, possibly, a different basis for the RDPG parameters. Let M and W denote two $S \times d$ matrix. We denote $M_{proc}(W)$ the Procrustes transformation[1] [Borg and Groenen, 1997] of M of minimal distance to W (we drop the argument (W) from the notation whenever it is clear from the context). Then, the Frobenius norm of the two matrices differences, $||M_{proc}(W) - W||_F$, is called the Procrustes distance between M and W [Dryden and Mardia, 1998]. We denote

$$\hat{X}\left(A^{d(i)}\right) = \left[X\left(A^{d(i)}\right)\right]_{proc}\left(X\left(A\right)^{r(i)}\right),$$

the Procrustes transformation of $X\left(A^{d(i)}\right)$ of minimal distance to $X(A)^{r(i)}$. We define the rank d **strain** of the species i as the sum of squared entries of the differences between $X(A)^{r(i)}$ and $\hat{X}\left(A^{d(i)}\right)$. Being $X(A)$ the matrix

[1] A Procrustes transformation is a geometric transformation given by a combination of a translation, a rescaling and a rotation. Notice that a Procrustes transformation preserves angles.

of either the inward, outward or total rank-d functional traits, we will speak of species' *inward*, *outward* or *total* strain, respectively. In formula:

$$\text{strain}(i) := ||X(A)^{r(i)} - \hat{X}\left(A^{d(i)}\right)||_F \tag{4.1}$$

We are interested in the use of RDPG-based measures to value species in a way that is robust to model parameters. Therefore, we tested whether the species' ordering by strain was sensitive to the choice of model dimensionality and performed a pairwise correlation test for each pair of dimensions in the range $[1, \ldots, 15]$. Notice that the latter upper range limit is much greater than the suitable upper bound for model dimensionality found in the previous chapter.

4.2.2 Uniqueness

We define the rank-d *uniqueness* of a species in a food web, either as a predator, prey or both, as the average of its Euclidean distance to every other species in the d-dimensional (inward, outward or total) abstract functional trait space.

Let $d(p, q)$ denote the d dimensional Euclidean distance between the point p and q; let $\langle f(i,j)\rangle_j$ be the mean of the function f over all the species j except i. That is, $\langle f(i,j)\rangle_j = \frac{1}{S}\sum_{j\neq i}(f(i,j))$. Then, the **uniqueness** of species i is defined as:

$$\text{uniqueness}(i) := \langle d\left(X(A)_i, X(A)_j\right)\rangle_j . \tag{4.2}$$

The relative uniqueness of the species in a food web is robust to orthogonal transformations of the food web's abstract functional space: indeed, the pairwise distance structure is invariant to rotations and translation, while uniform rescaling leaves unchanged the ratio

$$\frac{\text{uniqueness}(i)}{\text{uniqueness}(j)}$$

for every pair of species i and j.

4.2.3 Diversity

The volume of the convex hull of a community of species in the traits space is a proxy for its functional diversity [Villéger et al., 2008]. Here, we define the contribution of species i to a food web's abstract functional diversity as the difference in volume between the convex hull of the species traits, in the (inward, outward or total) abstract functional space, before and after species i is removed.

Let $\mathcal{H}^{(d)}(X)$ be the convex hull of a set of points X in the real space $\mathbb{R}^d$. Then, we define $V\left(\mathcal{H}^{(d)}(X)\right)$ its d dimensional volume—or the area of the convex hull of X if $d = 2$. We identify $X(A)$ with the set of points of the species in A and $X(A)^{r(i)}$ with the set of points of the species in A but i. Then, the contribution to the food-web functional diversity of a species i is the difference in volume between the two convex hulls

$$\text{diversity}(i) := V\left(\mathcal{H}^{(d)}(X(A))\right) - V\left(\mathcal{H}^{(d)}\left(X(A)^{r(i)}\right)\right) \tag{4.3}$$

and we define its normalized version as

$$\text{normdiversity}(i) := \frac{V\left(\mathcal{H}^{(d)}(X(A))\right) - V\left(\mathcal{H}^{(d)}\left(X(A)^{r(i)}\right)\right)}{V\left(\mathcal{H}^{(d)}(X(A))\right)} \tag{4.4}$$

Again, the relative diversity and normalized diversity of a species is robust to orthogonal transformations of the abstract functional space.

In this sense, all the three RDPG based measures we defined are robust to the non identifiability of the (inward, outward and total) abstract functional traits.

4.2.4 Topological centralities

We assessed the keystone centrality of a species i in a food web A by using six different (topological) network measures following Estrada [2007] (see [Jordán et al., 2009] for more details about their ecological interpretation). We choose these topological measures as their evaluation does not necessitate morphological trait data nor interaction weights.

- the betweenness (BC [Freeman, 1979; Brandes, 2001]) of species i, given by the number $s_{jij'}$ of shortest paths connecting every pair j, j' of species in the food web traversing species i, weighted by the total

number $s_{jj'}$ of paths between j and j':

$$BC(i) := \frac{s_{jij'}}{s_{jj'}}$$

- the closeness (CC [Bavelas, 1950; Freeman, 1979]) of species i, defined as the reciprocal of the sum of the path distances, $d_p(\cdot)$, from i to every other species j in the food web:

$$CC(i) := \left(\sum_{j \neq i} d_p(j, i) \right)^{-1}$$

- the degree (DC) of species i, measuring the number of interactions involving the species i (both as a predator or as a prey):

$$DC(i) := |\{j \in A | i \to j \text{ or } j \to i\}|$$

- the eigenvector centrality (EC [Bonacich and Lloyd, 2001]) of species i, that is a graph centrality satisfying the request that the score of each species i in the food web is proportional to the sum of the centrality scores of the species interacting with i. The values of EC are computed as the entries of the first eigenvector of A.

- the information centrality (IC [Stephenson and Zelen, 1989]) of species i, that is the harmonic mean of the resistance distances [Klein and Randić, 1993] toward the species i. Let I_{ji} denote the resistance distance from j to i, then:

$$IC(i) := \frac{S}{\sum_{j \neq i} (I_{ji})^{-1}}$$

- the subgraph centrality (SC [Estrada and Rodriguez-Velazquez, 2005]) of species i, which counts the number of returning loops starting from species i, discounted exponentially by their size. It is possible to give a closed expression for IC in terms of the exponential of the adjacency matrix A:

$$SC(i) := \left[e^A \right]_{ii}$$

We will discuss more these topological measures in the next chapters.

4.3 Phylogenetic diversity

The concept of "phylogenetic diversity" [Faith, 1992; Hartmann and Steel, 2007] constitutes an alternative point of view from which to evaluate the diversity of a community of species. The phylogenetic diversity of an evolutionary tree is the total sum of branch lengths in that phylogeny. This concept has been applied in the prioritisation of species for conservation purposes [Faith, 1992; Mace et al., 2003]. We each estimated species' evolutionary distinctiveness by measuring its fair proportion value [Isaac et al., 2007], equal splits value [Redding and Mooers, 2006] and the length of the terminal phylogenetic branch leading to that species, following Faye et al. [2015]. The fair proportion and equal split scores attempt to apportion the total evolutionary history of a phylogeny among the extant species.

4.4 Comparative analysis

Because of their shared evolutionary histories, we would expect to observe more similar traits for more closely related species [Cavalli-Sforza and Edwards, 1967; Felsenstein, 1985]. The evolutionary dependency of species arises the statistical issue of controlling and correcting for the phylogenetic covariation structure of the observed species' traits. To select the appropriate evolutionary model, we compute the relative Akaike information criterion corrected for finite sample size (AICc, see Hurvich and Tsai [1989]) of four distinct models [Garamszegi and Mundry, 2014]. We consider an uncorrelated null model, a Brownian motion model [Felsenstein, 1985], a Brownian motion with attraction toward an optimum (Ornstein–Uhlenbeck) model [Hansen, 1997] and a model with early burst of differentiation [Harmon et al., 2010]. We test for linear correlations among the (inward, outward and total) novel measures (of strain, uniqueness, and contribution to functional diversity) and among (inward, outward and total) strain and uniqueness and the six keystone centralities.

4.5 Results

We computed the species strain for $d \in [1, \ldots, 15]$ (Figure (4.1 a)). In the previous chapter we estimated a suitable model dimension $d = 3$ for the

Serengeti National Park food web. The species' strain (model dimension $d = 3$) has an average value of 0.032 and a variance of 0.017; a small number of species have a high strain (Figure (4.1 b)). The three species with the highest strain are all in the Afrotheria clade (and represent the totality of that clade in the food web). These are *Procavia capensis* (rock hyrax, strain = 1.316), *Heterohyrax brucei* (yellow-spotted rock hyrax, strain = 0.884) and *Loxodonta africana* (the African bush elephant, strain = 0.317). The ordering of species based on their strain is robust to the choice of model dimension, in the range $d \in [1, \ldots, 15]$ (Figure (4.1 c)). Every pairwise ordering correlation in the analysed interval is significant at $p < 0.01$ (this result is also confirmed by the analysis of the independent assembly of the Serengeti National Park food web by de Visser et al. [2011]).

The Afrotheria are also characterized by high uniqueness in terms of their mean distance to the other species in the abstract functional trait space. The observation can be extended the species' phylogeny, noticing that the two measures are non-uniformly distributed among the tips of the phylogenetic tree (Figure (4.2 a)). There is also support for an Ornstein–Uhlenbeck (Brownian motion with attraction toward an optimum) model of evolution for both strain and uniqueness (Figure (4.2 b)).

The correlation between species' (outward and total) strain and uniqueness is significant at $p < 0.01$, while the species' inward strain and uniqueness are not consistently correlated for $d > 4$ (Figure (4.3 a)). The computation of the species' contribution to the abstract functional diversity for $d > 4$ (species as both predators and prey) and $d > 7$ (species as either predators or prey) was not possible because of software limitations. However, in the feasible range of d, the species' total strain is significantly positively correlated with both the species' total uniqueness and their contribution to the total functional diversity (Figure (4.3 b)). The correlations for the partial (either inward or outward) measures are not consistently significant and depend on the measure considered.

The strain and mean distance of species in the Serengeti National Park are, in general, positively correlated with the common keystone centralities (Figure (4.4)). The significance and strength of the correlations depend on the particular combination of the centrality measure, the model dimension and the functional space considered (either inward, outward or total). We observed the most consistent correlations with the Betweenness, Subgraph and

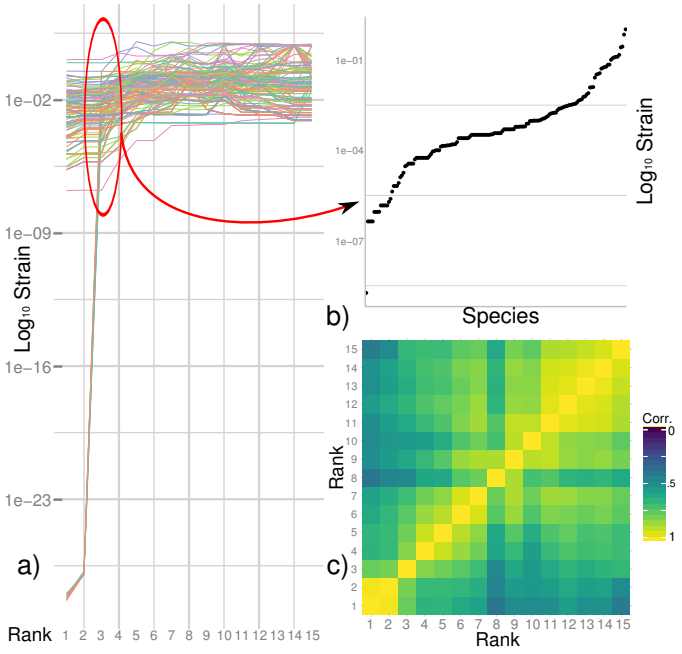

Figure 4.1: The distribution of species' strain in the Serengeti National Park food web [Baskerville et al., 2011]. (a) The line trace strain of each species ($\texttt{Log}_{10}$ transformed) along an increasing model dimension ($d \in [1, \ldots, 15]$). The strain has been computed for species as both predators and prey. (b) A cross-section of (a) for $d = 3$ (corresponding to the suitable model dimension). (c) Pearson product-moment correlation coefficients for the species ordering induced by the species' total strain across the model dimensions $d \in [1, \ldots, 15]$. The ordering is robust to the choice of the model dimension d: the Pearson's r is consistently above 0.5 (and all the pairwise correlations are significant at $p < 0.01$).

Degree centralities. The correlation results are qualitatively confirmed by performing the regression analysis either accounting for or ignoring the species' phylogenetic covariance structure. Hence the correlations hold whether or not we consider the phylogenetic structure of the food web. This general agreement between our novel measures and the common graph-theoretical indices used to identify keystone species supports the applicability of the RDPG model for food webs.

Although there are species with both high phylogenetic distinctiveness and high strain or uniqueness (Table (4.1)), we did not detect any significant linear correlation between the species' evolutionary and ecological relevance measures.

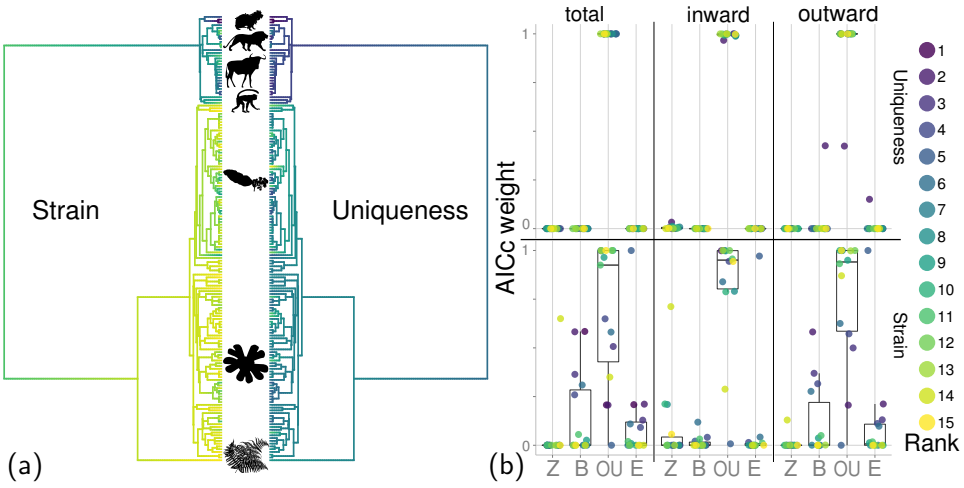

Figure 4.2: (a) Distribution of rank-3 species' strain and uniqueness in the phylogeny (lighter yellow for lower values; darker blue for higher values) for species as both predators and prey (all). The silhouettes (from phylopic.org) mark the corresponding clades: Afrotheria (hyraxes and elephants) are the species with the highest strain and uniqueness. (b) Akaike Information Criterion (corrected for sample size) weights for four models of species' (inward, outward and total) strain and uniqueness evolution: uncorrelated, Z; Brownian motion, B [Felsenstein, 1985]; Ornstein-Uhlenbeck, OU [Hansen, 1997]; Early Burst, E [Harmon et al., 2010]. The data consistently supports an OU model, except for the low-dimension strain evolution, in which there is also good support for the B model.

4.6 Discussion

For each species in the food web, we researched its position in the (inward, outward and total) abstract functional trait space for $d \in [1, \ldots, 15]$ and computed three measures of ecological relevance (strain, uniqueness and contribution to functional diversity). We verified that species' ordering based on the measures we introduced is robust to the choice of the model's dimension d. The RDPG model for food webs allows us to distinguish between the low-dimensional, stochastic backbone of a food web and its fine wiring. The stochastic backbone is robust to food web variability and to misspecifications of the food web structure, such as a missed observation of an interaction or an erroneous recording. Being based on the estimated (low-dimensional) structural food-web backbone, the measures we introduced are themselves robust to the variability of complex food webs. Other classic

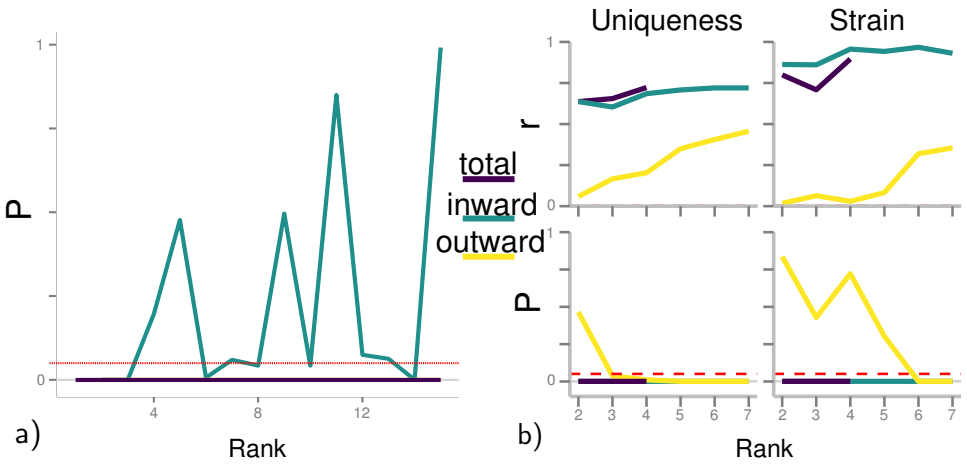

Figure 4.3: (a) There is a significant correlation between a species' uniqueness and strain for the species as prey (outward) and as predators and prey (total). For model dimensions $d > 3$, the correlation is not consistently significant for the species as a predator (inward). (b) There is a significant correlation between the species' (inward and total) strain and uniqueness and the species' contribution to the functional diversity (the loss of abstract functional diversity after the removal of a species). The correlation between a species' outward strain and contribution to functional diversity is not significant for low dimensions. The dashed red lines correspond to $p = 0.05$.

measures of trophic uniqueness [Yodzis and Winemiller, 1999; Luczkovich et al., 2003; Jordán et al., 2009] do not make this distinction.

The RDPG model allows us to estimate the abstract functional diversity of a food web by relying solely on topological data. It remains to be ascertained whether there is a correspondence between the classic morphological functional diversity and our novel concept of abstract functional diversity. If verified, the abstract functional diversity may serve to estimate the (classic) functional diversity without the burden of identifying suitable phenotypic traits with a functional role across all the species in a food web—an ambitious task, given species' heterogeneity. Our results appear to point toward a positive answer. The range of suitable abstract space dimensions estimated under the RDPG model, is in good accordance with the number of (classic) functional traits that Maire et al. [2015] estimated for an optimal (classic) functional diversity analysis.

We showed that a species' abstract functional trait uniqueness is positively correlated with its classic centrality in the Serengeti National Park

Species	Strain	Uniqueness	Diversity	Equal Splits
Procavia capensis	1.32	1	3	6.5
Heterohyrax brucei	0.88	2	1	6.5
Loxodonta africana	0.32	7	6	2
Panthera pardus	0.31	3	10	148.5
Panthera leo	0.18	6	4	148.5
Eudorcas thomsonii	0.17	8	19	150.5
Nanger granti	0.16	5	13	150.5
Connochaetes taurinus	0.15	4	14	138
Madoqua kirkii	0.15	11	2	100
Aepyceros melampus	0.12	13	0	100

Table 4.1: The 10 species in the Serengeti National Park food web [Baskerville et al., 2011] with the highest strain (as both predators and prey) and their ordering based on ecological uniqueness (as both predators and prey), contribution to functional diversity (diversity, as both predators and prey) and equal splits (a measure of evolutionary distinctiveness). Strain, uniqueness and contribution to functional diversity are positively correlated. However, although there are species (e.g., the Afrotheria clade) with a high score in all four measures, in general, there is no significant linear correlation between ecological relevance and evolutionary distinctiveness.

food web. The result was also confirmed for the Weddell Sea food web [Jennings et al., 2002], the Caribbean Sea food web [Opitz, 1996] and the independent compilation of the Serengeti National Park food web by de Visser et al. [2011]. A positive correlation between classic functional uniqueness, *sensu* Yodzis and Winemiller [1999], and the degree centrality—the number of trophic interactions—has already been established by Petchey et al. [2008b]. The result is even more interesting if read in comparison with the negative correlation found by Lai et al. [2012] between the classic centralities and the trophic uniqueness of a species *sensu* Luczkovich et al. [2003] and Jordán et al. [2009]. Further comparative analyses are therefore needed to explain this difference and explore the relationship between the abstract functional uniqueness of a species and its trophic uniqueness as otherwise defined. Similarly, a species' strain is positively correlated with its classic centrality and that a species' uniqueness predicts its strain. In addition, both strain and uniqueness are positively correlated with a species' contribution to the abstract functional diversity of the food web. Petchey et al. [2008b] have shown that trophically unique species are exposed to a higher risk of secondary extinction, highlighting their fragility. Conversely, the correlation

between uniqueness and strain supports the notion that food webs are particularly fragile to the extinction of functionally unique species, as already suggested by O'Gorman et al. [2010].

The ecological relevance—strain and uniqueness—of the species in the Serengeti food web is not uniformly distributed across the phylogeny (in fact, it is compatible with the distribution we would expect under a Ornstein-Uhlenbeck model of evolution). We did not detect a significant correlation between the species' ecological relevance and their evolutionary distinctiveness. However, a small number of species have both high ecological relevance and high evolutionary distinctiveness. This is the case in the Afrotheria clade (i.e., the African elephants and two hyrax species). The peculiarity of the Afrotheria clade has already been suggested by Baskerville et al. [2011] on the basis of the particularity of the hyrax's trophic role. Our results confirms the importance of considering both ecological and evolutionary factors in the evaluation of species for conservation purposes.

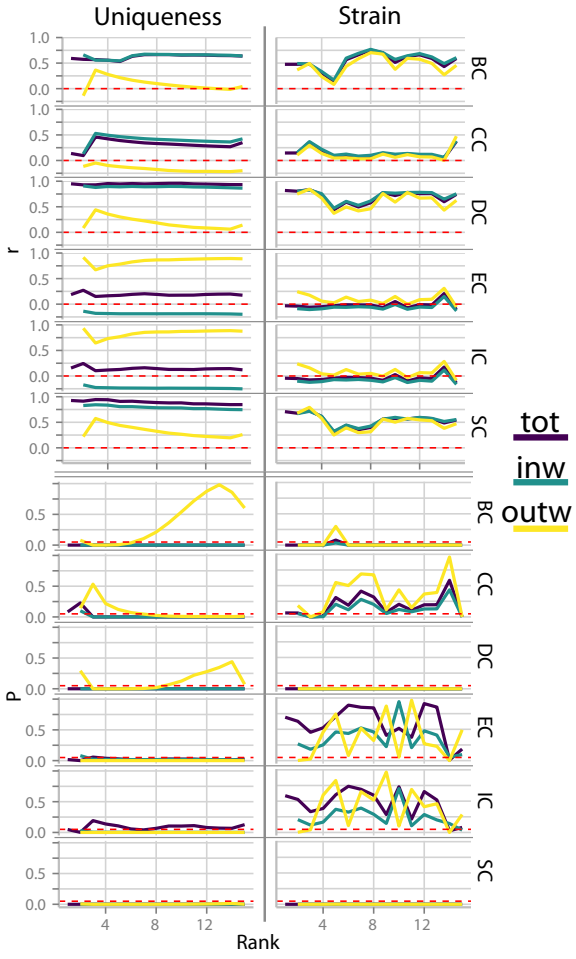

Figure 4.4: Correlation between a species' strain and uniqueness (as a predator, inward; prey, outward; predator and prey, total) and the species' betweenness (BC), closeness (CC), degree (DC), eigenvector (EC), information (IC), and subgraph (SC) centralities. Strengths and significances depend on the combination of the centrality index (the correlation is significant for most centralities except EC and IC), functional space (the correlation with the outward strain and uniqueness is weak) and model dimension (the correlation is stronger for low d). The dashed red lines correspond to $r = 0$ and $p = 0.05$.

Appendix

4.A Food webs representation

Here we present a graphical depiction of the five food webs we analysed in the chapter. In particular, nodes (species) are disposed in a plane space where the horizontal axis represents the omnivory index of the species (plus a small noise to avoid superposition) and the vertical axis represents the trophic level of the species; the area of the nodes correspond to the species' degree centrality (the total number of their interactions, the bigger the higher) while their colour indicates the ranking of the species based on their total strain, computed at $d = 3$ (deep blue for lower values, light yellow for higher values). For each web we also show the distribution of outward, inward and total strain, computed at $d = 3$.

The Trophic level [Pauly et al., 2000] of a consumer species i, TL_i, is defined as:

$$TL_i = 1 + \frac{1}{d_i^{in}} \sum_{j \to i} TL_j \tag{4.5}$$

where the sum is over all the species j consumed by i and d_i^{in} is the number of resources of i. Thus, the trophic level of a basal species (such as a plant) is one.

The omnivory index [Pauly et al., 2000] of a species i, OI_i, is defined as the variance of the trophic level the species' resources:

$$TL_i = \frac{1}{d_i^{in}} \sum_{j \to i} \left(TL_j - (TL_i - 1) \right)^2 . \tag{4.6}$$

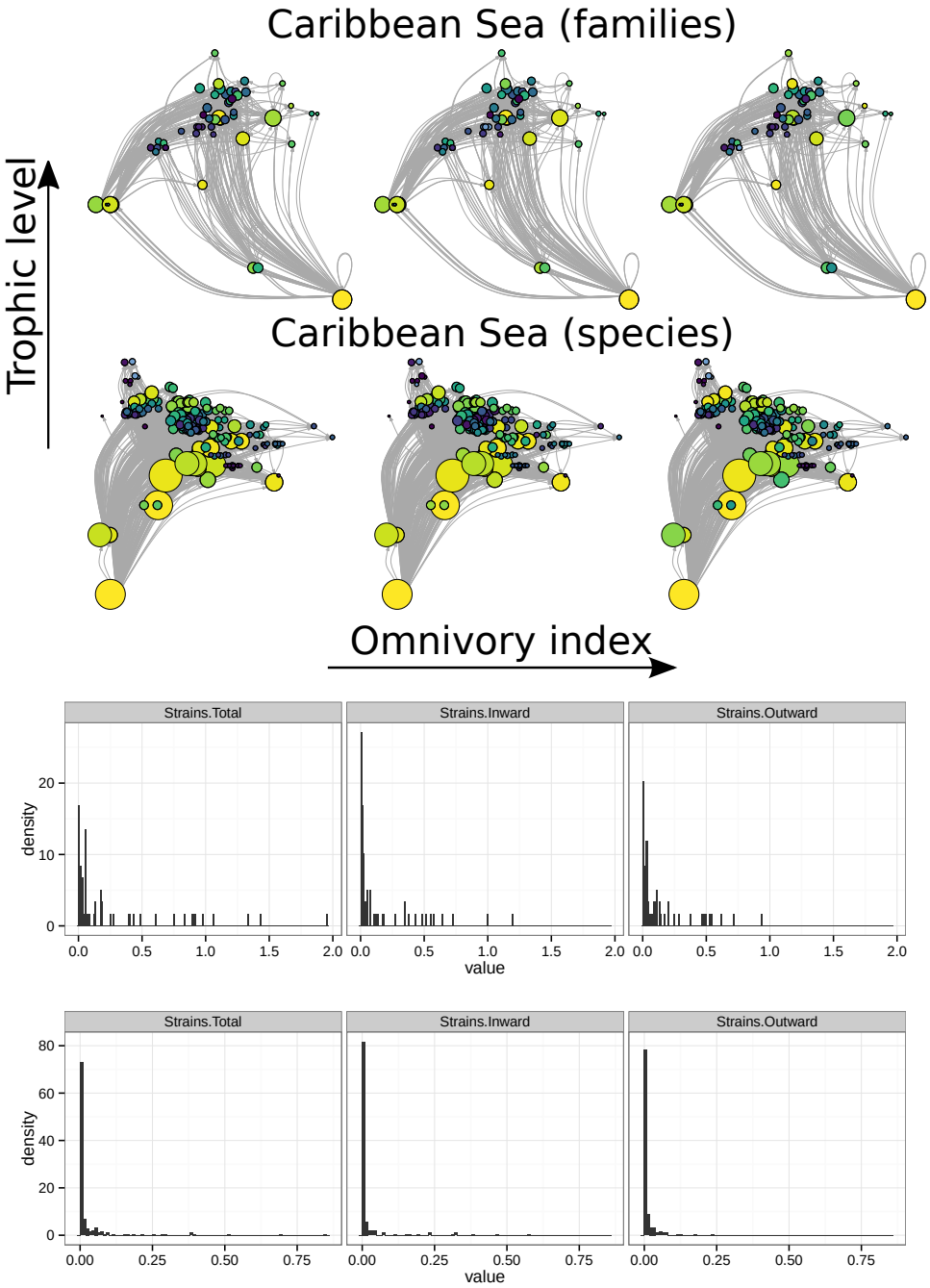
Caribbean Sea (families)
Trophic level
Caribbean Sea (species)
Omnivory index
Strains.Total
Strains.Inward
Strains.Outward
density
value

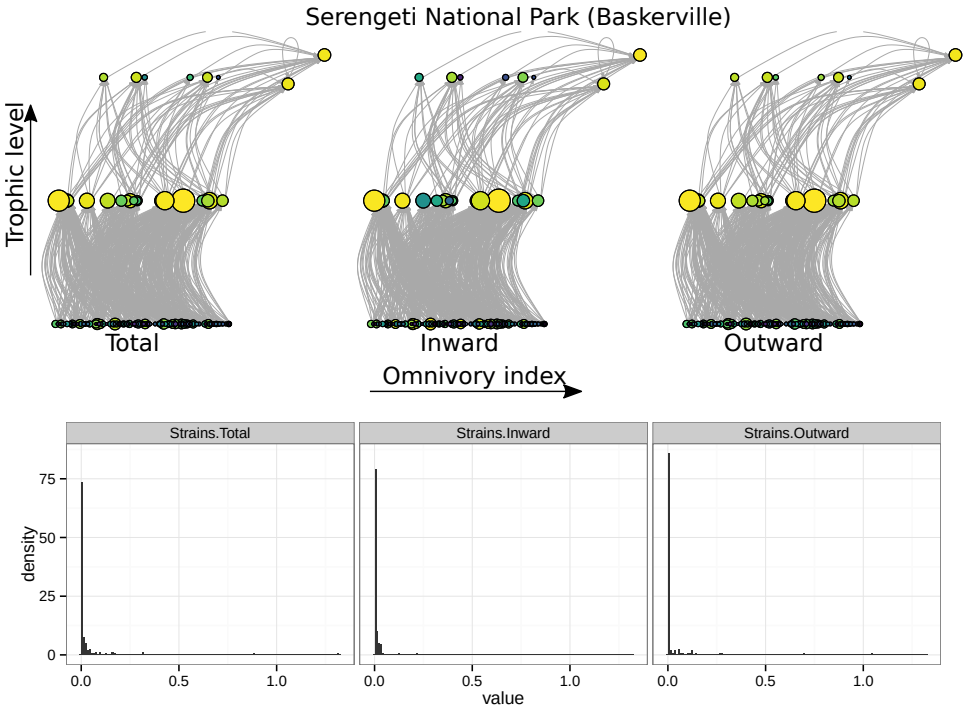
Serengeti National Park (Baskerville)
Trophic level
Total
Inward
Outward
Omnivory index
Strains.Total
Strains.Inward
Strains.Outward
density
75
50
25
0
0.0
0.5
1.0
value

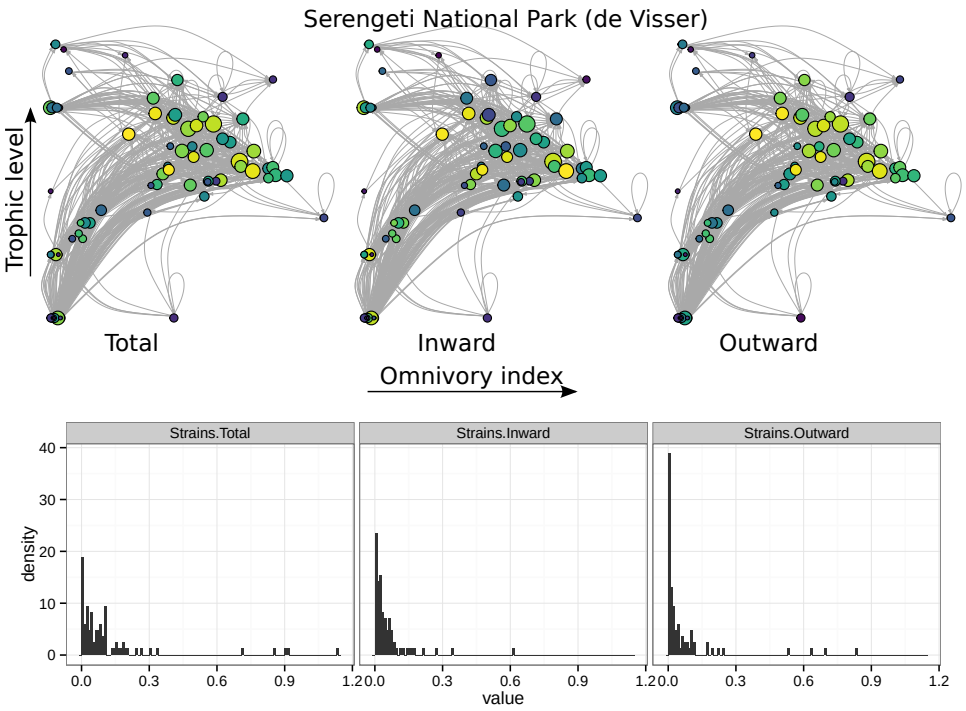
Serengeti National Park (de Visser)
Trophic level
Total
Inward
Outward
Omnivory index
Strains.Total
Strains.Inward
Strains.Outward
density
40
30
20
10
0
0.0
0.3
0.6
0.9
1.2
value

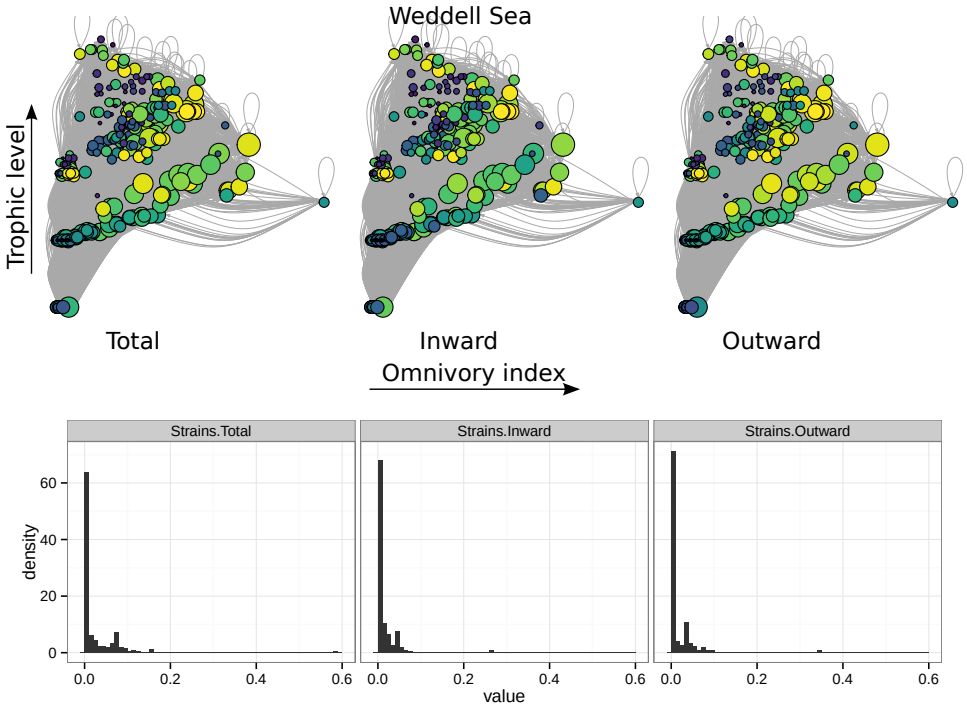

4.B Weighted networks

In the previous chapter we computed species strain from topological food webs' data only. In fact, obtaining estimates for the amount of energy flowing between a pair of species is often difficult. Therefore, we usually have a more reliable knowledge of the topological structure of an interaction network rather than of its weighted version. However, the components of the species' diets are not equally important. Thus, if the species' ranking we estimated from the topological data were extremely sensitive to the interactions' weight its applicability would be limited. On the other hand, if the topological species' ranking were not affected at all by the specification of interactions weights, that would rise doubt about its ecological meaning.

To test the extent to which our *strain* and *mean distance* measures are robust to the specification of interactions' weights, we compared the ranking of the species based on topological data with the rankings we obtained by simulating interactions weights. To do so, we sampled the interactions weights from a Log-Normal distribution, truncated so that their minimum value was 10^{-6} and normalised so that the maximum value was 1.

The results we obtained show that the correlation between the topological

and the weighted rankings were significant and positive for more than 95% of the simulations. However, the amount of variation in the weighted ranking explained by the topological ranking had a large variance (i.e., it spanned the range from almost null to almost one). Yet, the set of species with higher *strain* and the set of species with higher *mean distance* as estimated from the topological data was consistent across the simulated weighted networks, indicating that our measures are able to identigy the species with distinctively high ecological importance.

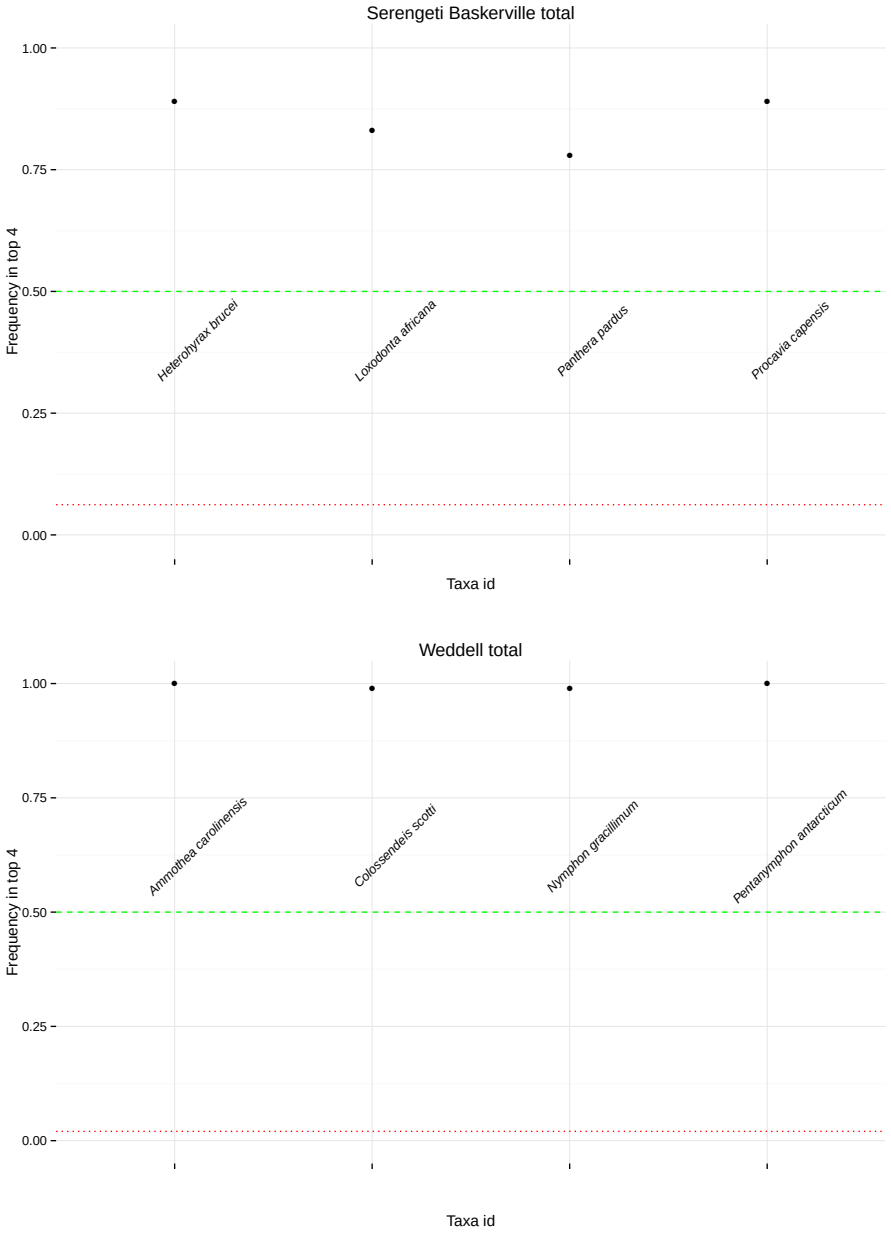

Figure 4.B.1: Frequency of presence in the set of four species with the highest strain as estimated by the simulated weighted networks for the four species with the highest strain as estimated by the topological networks. Baskerville's Serengeti National Park food web (top) and Weddell Sea food web (bottom).

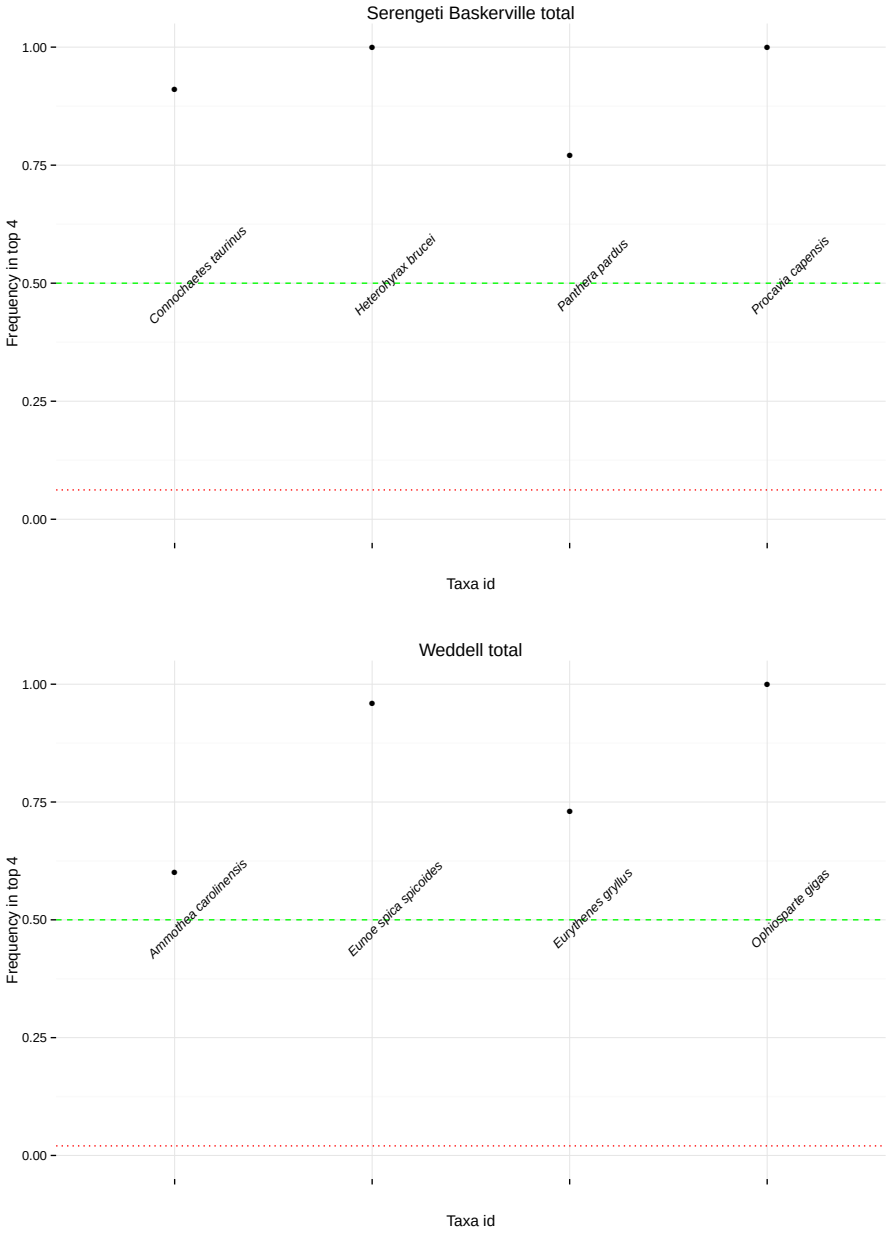

Figure 4.B.2: Frequency of presence in the set of four species with the highest mean distance as estimated by the simulated weighted networks for the four species with the highest mean distance as estimated by the topological networks. Baskerville's Serengeti National Park food web (top) and Weddell Sea food web (bottom).

Chapter 5

Evolutionary hypothesis in a metric trait space

Synopsis: Tropical rainforests are a hotspot of animal and plant biodiversity. It has been suggested that the coexistence of such a rich ensemble of species is the outcome of an interplay between ecological and evolutionary processes—the diversification of species into finely resolved niches with low overlap—supported by long-term environmental stability and the high productivity of the tropical forest. Here, we test these ideas across a guild of frugivorous birds at two sites in the tropical Andes of Peru, a global hotspot of avian diversity.

We introduce a niche model that combines a recently published functional space representation [Dehling et al., 2016] of species' foraging niches and a related novel measure of niche overlap. We embed the frugivore bird–fruit plant interaction networks into a pair of multidimensional metric spaces (one for the resources and one for the consumers) and identify a frugivore's foraging niche with the convex hull enclosing its plant resources.

We introduce a null model of niche evolution where the niche boundaries and preferences evolve in unison. We define two alternative trajectories, modelling the hypothesis that frugivore diversification at short evolutionary distances is dominated by a modification of the frugivores' consumption propensities or by the redefinition of the frugivores' diets (i.e., by the introduction of new plant species in their niches or the exclusion of old plant species from their niches).

We test this hypothesis and provide evidence of a different coexistence

strategy for recently speciated frugivores and distantly related ones: fine-scale differences in foraging preferences are apparently sufficient to reduce competition between ecologically very similar species. Our results provide a straightforward explanation for the mechanisms underpinning the origin and maintenance of species' coexistence in megadiverse communities.

Notes: A version of this chapter has been submitted to the *Proceeding of the National Academy of Science* as: GVDR, Matthew C. Hutchinson, Daniel B. Stouffer, D. Matthias Dehling (School of Biology, University of Canterbury) "Coexistence in a megadiverse foraging guild is explained by short-term resource-use modification and long-term niche shifts"

> [...] a vast number of animals can be found in even a small district. It is natural to ask: "What are they all doing?" [...] Animals are not always struggling for existence, but when they do begin, they spend the greater part of their lives eating.
>
> *Animal Ecology*
> **Charles Sutherland Elton**

5.1 Biodiversity and niche overlap

The Peruvian Manú National Park holds an extraordinary richness of "endless forms most beautiful and most wonderful", as biodiversity was described by Darwin [1859]. It is, indeed, an hotspot of animal and plant diversity [Dehling et al., 2014a]; more than 1000 bird species [Walker et al., 2006] thrive in the Manú reserve, finding ecological conditions that meet their survival and reproductive requirements—the set of which compose a species' "niche" [Hutchinson, 1957]. A key facet of niches is given by a species' feeding requirements [Elton, 1927; Pianka, 1981; Winemiller et al., 2015]: however flourishing it may be, any habitat can offer only a limited pool of resources; thus in a megadiverse group of species, such as the Manú's birds, the species' diets inevitably overlap [Gause, 1934; MacArthur, 1972] and may cause competition [Cody, 1974; Lara et al., 2015].

The competition for shared resources between a pair of species can result in either the complete exclusion of one species from the system [Gause, 1934], the evolutionary movement of their niches away from the shared resources [Grant and Grant, 2011; Ellis et al., 2015] or the ecological avoidance of the shared resources [Maret and Collins, 1997]. Competitive interactions between species often lead to the specialisation of one or more species on a subset of the resources available and thus the evolutionary divergence of lineages based on their resource use [Sale, 1974; Futuyma and Moreno, 1988]. Given the different competitive abilities of each species, the persistence of rich biodiversity depends on the ecological and evolutionary partitioning of the available resource space [Gause, 1934; MacArthur, 1972; Pianka, 1981]:

indeed, differences among species' niches is considered to be essential for their coexistence [Chesson, 2000; Chase and Leibold, 2003].

It has been widely observed that evolutionarily close species exhibit more similar traits than distantly related ones [Darwin, 1859; Felsenstein, 1985]; as they depend, at least in part, on heritable traits, species' diets show a significant phylogenetic signal [Böhning-Gaese and Oberrath, 1999; Pearman et al., 2014], as does their role in trophic networks [Stouffer et al., 2012]. In fact, in Chapters (3) and (4), we found that closely related species have similar food-web functional traits. However, the extent to which a neutral model is adequate for describing the evolution of species niches [Wennekes et al., 2012; Joly et al., 2013; Münkemüller et al., 2015; Winemiller et al., 2015] and, ultimately, the origin of biodiversity [Rosindell et al., 2012; Fisher and Mehta, 2014] is an open question: for example, the evidence of niche phylogenetic *conservatism* (the tendency of phylogenetic near species to resemble each other more than what expected under a neutral model of evolution, where traits evolve as a BBM process, see Section (3.A.1)) is ambiguous [Losos, 2008; Ingram et al., 2009; Wiens et al., 2010]; similarly, the exact nature of the relationship between ecological and evolutionary processes in shaping species' niches is an open problem [Post and Palkovacs, 2009; Stuart and Losos, 2013; Nuismer and Harmon, 2015].

We adopt a food-web perspective to study the evolution of frugivore bird niches as consumers of fruit plants in two sites of the Manú National Park. Nevertheless, the concepts we introduce here can easily be adapted to other systems. We exploit the embedding of an ecological network into a suitable metric space, where, as in Chapter (3), the proximity between two species reflects their ecological similarity, and define the *foraging niche* of a consumer species in that network as the portion of the space occupied by the species' resources. We consider the foraging niche as a proxy for the functional, Eltonian [Elton, 1927], interaction niche of a consumer. Notice that foraging niches are based solely on food webs' topology; in other words, they are defined regardless of how much a certain consumer relies on a certain resource. We define a niche *centroid* as the weighted centre of its niche, where the weights are given by consumption propensity: a consumer's centroid will be closer to those resources that are more frequently consumed, controlling for resource availability.

Here, we test whether the overlap of the foraging niches and the distance

between their centroid are linearly correlated across the bird species' phylogenetic distances. In doing so, we can gather insight into the evolution of foraging niches and the mechanisms supporting biodiversity in a large bird community.

5.1.1 Niche differentiation in the functional trait space

Whatever the mechanism driving it, we can distinguish two main patterns in the differentiation of a foraging niche (see [Sale, 1974]). A niche can evolve by:

1. the inclusion of a new resource in a consumer's diet or the removal of an old, shared, resource from the consumer' diet, producing a modification of the foraging niche boundary, which we name *niche redefinition*[1] (not to be confused with "niche shift" [Pearman et al., 2014]). Niche redefinition results in reduced (potential or realised) competition between two frugivores through the reduction of their dependency on commonly shared resources. Morphological adaptive evolution is likely to be associated with niche redefinition, as different resources may require slightly different toolsets to be exploited [Silvertown et al., 2001; Grant and Grant, 2011];

2. the redistribution of a consumer's relative propensities toward its resources [Connell, 1961; Willis, 1966; Alatalo et al., 1986], which we name *frequency modification*; frequency modification may result in reduced competition through a relative reduction of the consumption load on shared resources in favour of other resources in the existing niches of frugivores.

If a consumer relies lightly on newly added components of its diet, we can assume that the consumption frequencies and thus the niche centroids change only marginally under niche redefinition: species that diversify through niche redefinition alone will decrease their relative niche overlap. Conversely, a change in the consumption frequencies of a species does not, in general, affect

[1] In general, the inclusion of a new resource in a consumer's diet or the removal of an old resource from a consumer's diet does not necessarily modify the consumer's niche. In fact, such event modifies the consumer's niche only if the representation of the resource species in the functional space is outside the convex hull enclosing the consumer's diet (i.e., its foraging niche). We define as niche redefinition only to those events that modifies the consumer's niche boundaries.

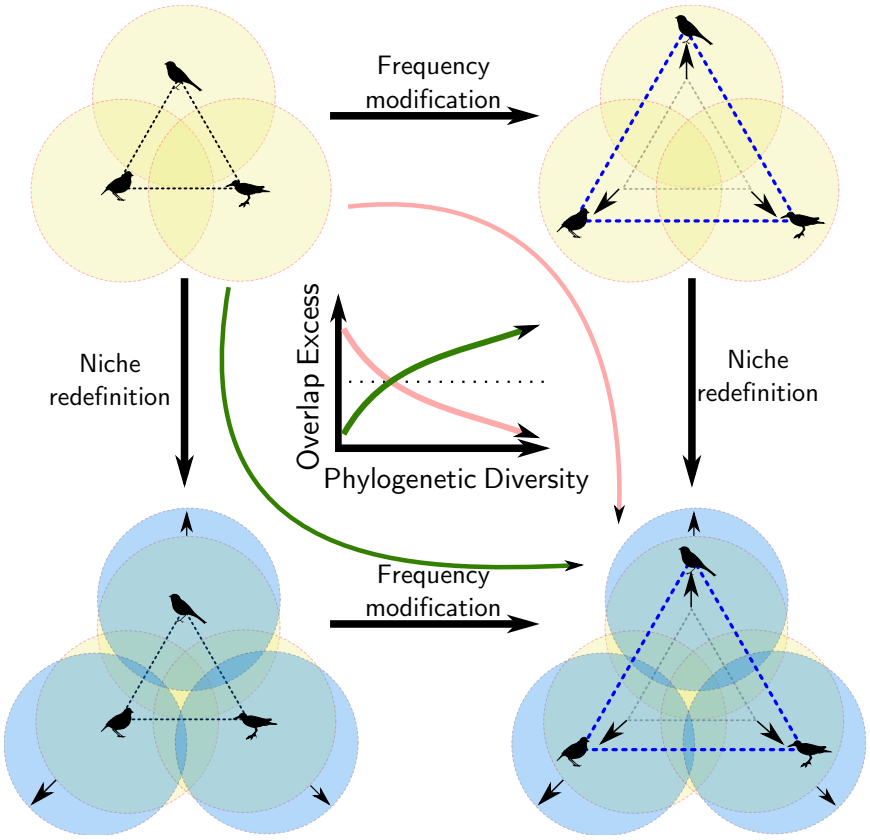

Figure 5.1: The two patterns of niche differentiation that we distinguish and their trajectories in the correlation between niche overlaps and centroid distances. The horizontal movement corresponds to **frequency modification**, where species change their consumption propensities, leaving the boundaries of their foraging niches untouched; the vertical movement corresponds to **niche redefinition**, where species reduce their foraging niche overlap by either adding or removing resources in their diet. Under the **null model** of niche evolution, the niche overlap and the centroid distance change consistently with the phylogenetic distance separating two species (dotted trajectory). We consider two alternative hypothesis: if the differentiation between closely related species results in frequency modification, while niche redefinition is dominant for further related species, we observe a relative overlap that is higher than expected under the null model for short phylogenetic diversities (light **red trajectory**); conversely, if the differentiation between closely related species happens mostly through niche redefinition and frequency modification follows, we detect a relative overlap that is lower than expected under the null model for short phylogenetic diversities (dark **green trajectory**).

that species' foraging niche boundaries: species that diversify by frequency modification alone will increase their centroids' distance (see Figure (5.1)).

We consider a null model of niche evolution and we contrast it with two alternative hypotheses:

Null model: the patterns of frequency modification and niche redefinition act concurrently—and at the same evolutionary pace—during the diversification of the species in a community.

Red trajectory: at the beginning of the evolutionary divergence of a pair of species, the species diversify mostly through the modification of their consumption propensities; the redefinition of the foraging niches follows only afterwards, becoming more evident over long evolutionary times.

Green trajectory: the species diversify first by redefining their foraging niches; the centroids' divergence becomes prominent only afterwards.

In all three cases, we would expect the foraging niche overlaps to correlate with the centroid distances. To test the previous claim, we fit a linear model of the niche overlaps against the centroid distances, controlling for the absolute volume of the bird foraging niches and their degree of frugivory.

We define the *overlap excess* of a pair of bird species as the difference between the observed and predicted pair's overlap. The *overlap excess* therefore represents the deviation from the null model of the foraging niche overlaps: a positive overlap excess means that two species overlap more than expected and a negative overlap excess means that two species overlap less than expected.

Under the null model of niche evolution, we do not expect to detect a significant correlation between the phylogenetic distance and the overlap excess of a pair of species, as these move consistently during evolutionary differentiation. The two alternative differentiation hypotheseis yield contrasting expectations of the overlap excesses along the phylogenetic distance: in both cases, we expect a significant correlation between the species' overlap excess and their phylogenetic distance, and we expect the correlation to be positive under the red trajectory and negative under the green trajectory (see Figure (5.1)).

5.2 Methods and Materials

5.2.1 Interaction, trait and phylogenetic data

To estimate the degree of overlap between a group of species' niches, we need to identify a set of traits that are of ecological relevance across the considered community and which can be expressed in commensurable coordinates [Holt, 1987].

We used the dataset of bird–plant interactions published by Dehling et al. [2014a]. We investigated resource use in a foraging guild (all species use similar resources). All species occur in same habitat. We sampled plant–bird interaction networks at two sites in the Manù Biosphere Reserve in the Andes of south east Peru (hereafter "Manù"): Wayqecha, which is located at 13.2S, 71.6W a 3000m above sea level in an upper montane rainforest with 26 bird and 51 plant species, and San Pedro which is located at 13.1S, 71.6W a 1500m above sea level in a lower montane rainforest with 61 bird and 53 plant species. Details of the sampling procedure can be found in [Dehling et al., 2014b].

We built the resource functional space by projecting plant species into a four-dimensional metric space estimated from the following plant traits: fruit size, fruit diameter, crop mass, and plant height [Dehling et al., 2014b]. We assessed the foraging preference of a bird species by calculating the interaction centroid, defined as the weighted mean of its resource positions in the trait space, weighted by the plant abundances [Dehling et al., 2016].

We obtained 1000 dated phylogenetic trees from birdtree.org [Jetz et al., 2012, 2014] for each of the two community of birds: Wayqecha and San Pedro. The trees were sampled from the pseudo-posterior distribution estimated on the phylogenetic backbone given by Hackett et al. [2008]. See Figure (5.1) for a graphical representation of one sample from the combined phylogeny.

5.2.2 Estimating birds' foraging niches

We let $\mathcal{S}$ denote the functional trait space as estimated in [Dehling et al., 2014b]. For each bird species i in the plant–bird interaction network W, we let $c(i)$ denote the centroids of i and $W_i = \{x_{i1}, \dots\}$ be the set of plants i consumes. We define the *observed* foraging niche of a bird species i as the smallest convex (closed) subset of $\mathcal{S}$ containing W_i—its *convex hull*—and denote it as $h(i)$. To account for the possibility that we did not detect some

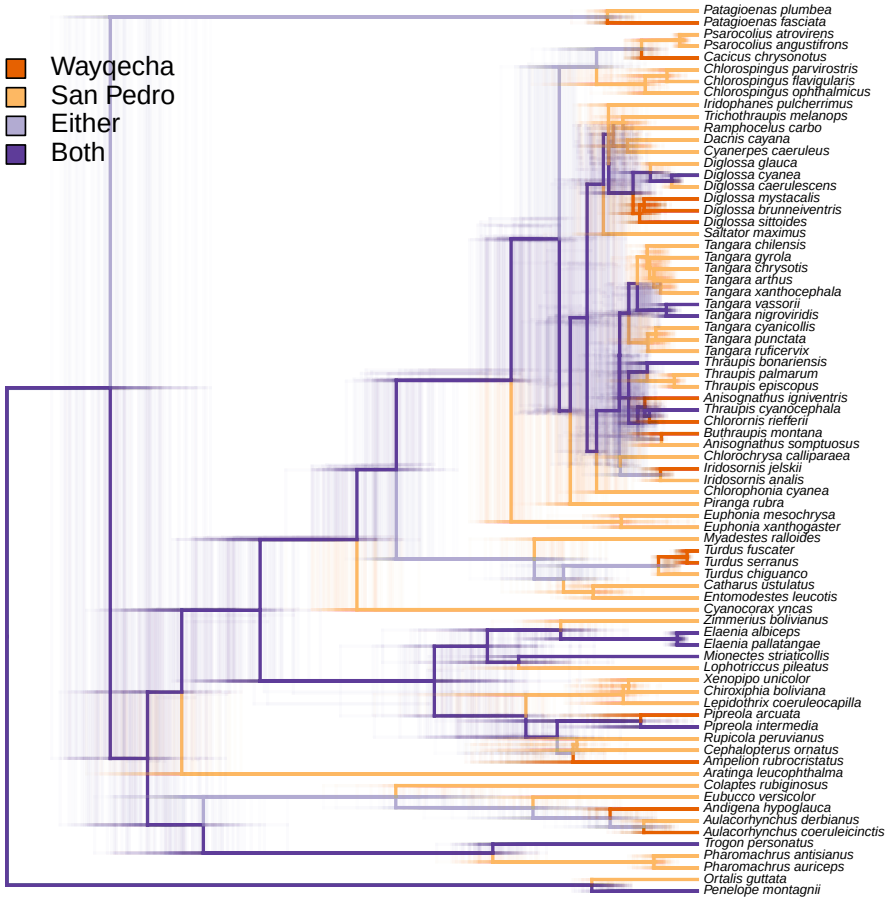

Figure 5.1: Empirical distribution of the combined Manú phylogeny, as sampled from birdtree.org [Jetz et al., 2012]. The lineages are coloured according to the presence of a descendent in the two network communities: dark purple if they have at least one descendant in both the Wayqecha and San Pedro networks, light purple if they have a descedant in each of the two networks but none in both, dark orange if they have a descedant only in the Wayqecha network, and light orange if they have a descedant only in the San Pedro network.

of the interactions between birds and plants, we introduce two enveloping algorithms for the observed foraging niches.

Under the first algorithm (*centroid enveloping*), for each bird species i and plant species x that is not in W_i, we compute the Euclidean (four-dimensional) distance from x to $c(i)$ and we let $d_c(x,i)$ denote this. We set $d_c(x,i) = 0$ for all the species x that are in W_i. Next, we assign to each species x a probability $\mathbb{P}_c\left(x|c(i), W_i, \alpha, \beta\right)$ defined as:

$$\mathbb{P}_c\left(x|c(i), W_i, \alpha, \beta\right) = \begin{cases} e^{-\frac{1}{\alpha} d_c(x,i)^\beta} & \text{if } x \notin W_i \\ 1 & \text{if } x \in W_i, \end{cases} \tag{5.1}$$

where α and β are two positive real valued parameters determining the shape of the envelope. Then, for each bird i we sample each plant x in W with probability $\mathbb{P}_c\left(x|c(i), W_i, \alpha, \beta\right)$ and we denote the set of sampled plants $\dot{W}_i$, which we label the *centroid augmented* diet of bird i. Finally, we define the *centroid augmented* foraging niche, $\dot{h}_i$, as the smallest convex (closed) subset of $\mathcal{S}$ containing $\dot{W}_i$.

Under the second algorithm (*vertex enveloping*), for each bird species i and plant species x that is not in W_i, we compute the minimum of the Euclidean (four-dimensional) distances from x to the plant species that are in the observed diet W_i and we let $d_W(x,i)$ denote this. We set $d_W(x,i) = 0$ for all the species x that are in W_i. Next, we assign to each species x a probability $\mathbb{P}_W\left(x|W_i, \alpha, \beta\right)$ defined as:

$$\mathbb{P}_W\left(x|W_i, \alpha, \beta\right) = \begin{cases} e^{-\frac{1}{\alpha} d_W(x,i)^\beta} & \text{if } x \notin W_i \\ 1 & \text{if } x \in W_i, \end{cases} \tag{5.2}$$

where α and β are two positive real valued parameters determining the shape of the envelope. Then, for each bird i we each plant x in W with probability $\mathbb{P}_W\left(x|W_i, \alpha, \beta\right)$ and we denote the set of sampled plants $\bar{W}_i$, which we label the *vertex augmented* diet of bird i. Finally, we define the *vertex augmented* foraging niche, $\bar{h}_i$, as the smallest convex (closed) subset of $\mathcal{S}$ containing $\bar{W}_i$.

Higher values of α increase the probability of the plant resources being included in the augmented niches, whereas β controls the speed with which the probability decays as the distance (from the observed interactions or the centroid) grows.

We let $\hat{W}_i$ and $\hat{h}_i$ denote the diet and the foraging niche of i without distinguishing among the observed, centroid augmented or vertex augmented definition of the diet and of the foraging niche, respectively. None of the following analyses depends strictly on the definition adopted. We use $V(X)$ to denote the four-dimensional volume of a convex subset of $\mathcal{S}$. If any of the foraging niches contains less than five resources, or if it contains a set of resources that lies in a degenerate subset of $\mathcal{S}$ of null-four dimensional volume, we drop the corresponding bird species from the analysis.

Niche overlap We define the overlap space of a pair of bird species i and j as the intersection between their foraging niches:

$$O(i,j) = \hat{h}_i \cap \hat{h}_j \tag{5.3}$$

As it is an intersection of convex hulls, an overlap space is convex and possibly empty.

Moreover, for each pair of consumer species i and j, we propose three measures of the niche overlap:

Symmetric overlap: the volume of $O(i,j)$:

$$so(i,j) = V\left(O(i,j)\right) . \tag{5.4}$$

Relative overlap: the volume $V\left(i,j\right)$ normalised by the sum of the volume of i's and j's foraging niches:

$$ro(i,j) = \frac{V\left(O(i,j)\right)}{V(\hat{h}_i) + V(\hat{h}_j)} . \tag{5.5}$$

Egoistic overlap: the volume $V\left(i,j\right)$ normalised by the volume of i's foraging niche:

$$eo(i,j) = \frac{V\left(O(i,j)\right)}{V(\hat{h}_i)} . \tag{5.6}$$

Using qhull [Barber et al., 1996] in the R package *geometry* [R Core Team, 2013; Habel et al., 2014], we compute the convex hulls of the observed and augmented diets of for every bird species in the two interaction networks. For each pair of consumer species, we computed their symmetric, relative and egoistic overlap.

We tested for a linear correlation between niche overlap and phylogenetic distance, and between centroid distance and phylogenetic distance in the Wayqecha and San Pedro interaction networks, both by using the function *lm* in R [R Core Team, 2013] and by using a Mantel Test using the function *mantel* in the *vegan* package [Oksanen et al., 2015] (999 permutations of the dissimilarity matrices).

5.2.3 Null model evolution

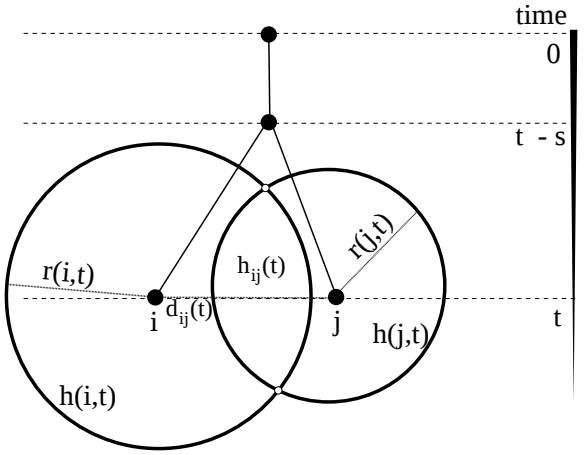

Figure 5.2: A graphical explanation of the notation used in Section (5.2.3), as projected in a two-dimensional space. The lineages i and j of the phylogeny W_τ, extant at time t, speciated at time $t-s$. With each of these, we associate a niche centroid ($c(i,t)$ and $c(j,t)$), and a niche radius ($r(i,t)$ and $r(j,t)$). The centroids and radii define their niches ($h(i,t)$ and $h(j,t)$), their centroid distance ($d_{ij}(t)$) and their niche overlap (the area $h_{ij}(t)$).

We will define our null model of niche evolution in detail and explore its behaviour. Figure (5.2) shows a diagram of the notation we introduce.

Let $\mathcal{S}$ be the four-dimensional Euclidean space. We consider a clade of birds W, whose phylogeny we denote as W_τ. At every time t in the history of the phylogeny, with every lineage i in W_τ is associated a niche centroid $c(i,t) \in \mathbb{R}^4$ and a radius $r(i,t) \in \mathbb{R}$. Under the null model, the lineages' centroid coordinates evolve as independently and identically distributed Brownian motions with mean 0 and variance σ:

$$\mathrm{d}c(i,t)_j = \mathrm{d}\mathbf{B}_t(0,\sigma)\,\mathrm{d}t \tag{5.7}$$

for each lineage i and each coordinate j. The centroid of the phylogeny's root starts at the origin, $c(i,0) = \vec{0}$. Similarly, the lineages' radii evolve as independently and identically distributed Brownian motions with mean 0, variance ρ and constrained to $\mathbb{R}_+$ (the positive reals):

$$\mathrm{d}r(i,t) = \mathrm{d}\mathbf{B}_t(0,\rho)\,\mathrm{d}t \tag{5.8}$$

for each lineage i. The radius of the phylogeny's root starts at an arbitrarily chosen value r_0; in other words, $r(i,0) = r_0$. Here, we assume the ratio $\frac{\rho}{r_0}$ to be small enough that the probability that any radius hits 0 is negligible. In other words, if we let $r_-(i)$ be the minimum value of $r(i,t)$ between $t = 0$ and the present $t = T$, and $\Phi(x)$ be the cumulative distribution function of the standard normal distribution, then we assume the probability

$$\mathbb{P}\left(r_-(i) \leq 0\right) = 2\Big(1 - \Phi\left(\frac{r_0}{\sqrt{\rho T}}\right)\Big) \tag{5.9}$$

to be small (see [Karatzas and Shreve, 2012] for a proof of the previous equation).

The foraging niche of each lineage i at time t is defined as the four dimensional ball with a centre in $c(i,t)$ and a radius $r(i,t)$:

$$h(i,t) = \mathcal{B}\left(c(i,t), r(i,t)\right), \tag{5.10}$$

for which the volume is given by:

$$V\left(h(i,t)\right) = V\Big(\mathcal{B}\left(c(i,t), r(i,t)\right)\Big) = \frac{\pi^2}{2} r(i,t)^4\,. \tag{5.11}$$

As the Brownian motion governing the lineage radius is centred in 0, we have $\mathbb{E}(r(i,t)) = r_0$ for each lineage i and each time t. Thus we have:

$$\mathbb{E}\Big(V\left(h(i,t)\right)\Big) = \frac{\pi^2}{2}\mathbb{E}(r(i,t)^4) = \frac{\pi^2}{2} r_0^4\,. \tag{5.12}$$

For each pair i and j of lineages in W, let $d_{ij}(t)$ denote the distance between i's and j's niche centroids (i.e., $d_{ij}(t) = \|c(i,t) - c(j,t)\|$). We let $h_{ij}(t)$ denote the intersection of their niches at time t:

$$h_{ij}(t) = h(i,t) \cap h(j,t) = \mathcal{B}\left(c(i,t), r(i,t)\right) \cap \mathcal{B}\left(c(j,t), r(j,t)\right)\,. \tag{5.13}$$

If $d_{ij}(t) > r(i,t) + r(j,t)$, the intersection $h_{ij}(t)$ is empty; otherwise, it is a convex subset of $\mathcal{S}$ (in general, it is not a ball). We can now define the niche overlap of i and j at time t as the volume of $h_{ij}(t)$ if it is not empty (or 0 otherwise) and we denote this as $V_{ij}(t)$. The volume $V_{ij}(t)$ can be expressed as a polynomial function of the niche radii and the centroid distance; this motivates the regression modelling we propose in the next section.

In the rest of this paragraph, we give an explicit formula for the intersection volume that will be used in the null model simulations.

The niche intersection $h_{ij}(t)$ is delimited by two hyperspherical caps, one bounded by $h(i,t)$, which we denote η_{ij}, and the other bounded by $h(j,t)$, which we denote η_{ji}. We compute the volume of the intersection as the sum of the two hyperspherical cap volumes. Following Li [2011], the volume of a n dimensional cap is given by:

$$V(\eta) = \frac{\pi^{\frac{n-1}{2}} r^n}{\Gamma\left(\frac{n+1}{2}\right)} \int_0^{\arccos\left(\frac{h}{r}\right)} \sin^n(t)\,\mathrm{d}t, \tag{5.14}$$

where r is the radius of the bounding sphere, n is the dimension of the cap and h is the height of the cap. We can reduce the dimensionality of the problem by noticing that the heights of the caps η_{ij} and η_{ji}, determined by the intersection of two four-dimensional sphere, is equivalent to the heights of the caps defined by the intersection of their projection to a two-dimensional plane containing the line segment between joining the i's and j's centroid. We let ζ_{ij} and ζ_{ji} denote the heights of the cap η_{ij} and η_{ji}, respectively. We now have:

$$\begin{aligned} \frac{\zeta_{ij}}{r(i,t)} &= \frac{d_{ij}^2 + r(i,t)^2 - r(j,t)^2}{2 d_{ij} r(i,t)}\,; \\ \frac{\zeta_{ji}}{r(j,t)} &= \frac{d_{ij}^2 + r(j,t)^2 - r(i,t)^2}{2 d_{ij} r(j,t)}\,. \end{aligned} \tag{5.15}$$

We let θ_{ij} denote the angle $\arccos\left(\frac{\zeta_{ij}}{r(i,t)}\right)$ and we let θ_{ji} denote the angle $\arccos\left(\frac{\zeta_{ji}}{r(j,t)}\right)$. Thus the volume of $h_{ij}(t)$ is:

$$\begin{aligned} V_{ij}(t) &= \frac{\pi^{\frac{3}{2}}}{\Gamma\left(\frac{5}{2}\right)} \left(r(i,t)^4 \int_0^{\theta_{ij}} \sin^4(t)\,\mathrm{d}t + r(j,t)^4 \int_0^{\theta_{ji}} \sin^4(t)\,\mathrm{d}t \right) \\ &= K\left(r(i,t)^4 g(\theta_{ij}) + r(j,t)^4 g(\theta_{ji}) \right), \end{aligned} \tag{5.16}$$

where the $K = \frac{1}{24}\pi$ is a numeric constant and the function g is defined as:

$$g(x) = 12x - 16\cos(x)\sin(x) + 4\cos(x)^3\sin(x) - 4\cos(x)\sin(x)^3\,. \quad (5.17)$$

We can express, at least at the first approximation, $g(\theta_{ij})$ and $g(\theta_{ij})$ as rational functions of the niche radii and the centroid distances. In fact, for the first of the two summands in Equation 5.16, we have:

$$\cos(\theta_{ij}) = \cos\left(\arccos\left(\frac{\zeta_{ij}}{r(i,t)}\right)\right) = \frac{\zeta_{ij}}{r(i,t)}\,, \quad (5.18)$$

and:

$$\sin(\theta_{ij}) = \sqrt{1 - \left(\frac{\zeta_{ij}}{r(i,t)}\right)^2}\,, \quad (5.19)$$

and finally:

$$\theta_{ij} \sim \frac{\pi}{2} - \frac{\zeta_{ij}}{r(i,t)} + o\Big((\frac{\zeta_{ij}}{r(i,t)})^2\Big)\,. \quad (5.20)$$

5.2.4 Deviation from the null model

We adopt the notation introduced by Wilkinson and Rogers [1973] to define as a formula the linear model of the variable x with the variables $y_1, y_2, \ldots$ as predictors:

$$x \sim y_1 + y_2 + \ldots\,. \quad (5.21)$$

With this, we mean that each observation x_i of the variable x is modelled as:

$$x_i = \eta_0 + \eta_1 y_{1i} + \eta_2 y_{2i} + \cdots + \epsilon_i\,, \quad (5.22)$$

where $y_{1i}, y_{2i}, \ldots$ express the values of the predictor variables associated with the observation x_i, ϵ_i is the residual associated with the observation x_i and $\eta_0, \eta_1, \eta_2, \ldots$ are the model parameters estimated from the set of observation. We let $y_i : y_j$ denote the interaction terms of the predictor variables y_i and y_j, and $y_i * y_j$ denote $y_i + y_j + y_i : y_j$.

We test the fit of the null model of niche evolution by fitting a linear model of the (symmetric, relative and egoistic) niche overlap (for observed and augmented niches) with the niche volumes and the fourth power of the centroid distances as predictors. Expressed as formula, for the egoistic

overlap, we have:

$$eo(i,j) \sim d_{i,j}^4 + V\left(h(i)\right) + V\left(h(j)\right). \tag{5.23}$$

The model definition would be the same for the other measures of niche overlap. In order to control for higher-order effects and the role of other variables, such as an effect of the birds' order or their degree of frugivory, we consider also more parameter-rich linear mixed effects models (see Appendix (5.A)).

Next, we define the overlap excess between species i and j as the standardised residual associated with their niche overlap. We test the correlation between overlap excess and phylogenetic distance by fitting a linear regression model and testing the permutational significance of a Mantel Test [R Core Team, 2013; Oksanen et al., 2015] (999 permutations). We also controlled for the effect of degree of frugivory.

5.3 Results

For the sake of expository simplicity, we present the results for the outcome of one randomisation. We augmented the foraging niches via centroid enveloping with the parameters $\alpha = 1/4$ and $\beta = 1$ for the Wayqecha network, and $\alpha = 2/3$ and $\beta = 1$ for the San Pedro network, which we chose as these parameters conserve the foraging niche shapes while reducing the number of degenerate foraging niches (0 out of 26 birds for Wayqecha; 2 out of 61 birds for San Pedro). For each interaction network, we selected the first of the phylogenetic trees downloaded from birdtree.org [Jetz et al., 2012]; the R random seed was set to 42.

The analysis across different randomisation settings (see Appendix (5.B) for more details of all the combinations we tested) produced results that were fully consistent with the ones we show here; although the regression slopes changed numerically, they preserved significance and sign. The conclusions we draw are based on these.

We will provide simulation and analysis code in a publicly accessible repository (see http://gvdr.github.io) to allow the readers run the analsys pipeline on the presented and other datasets with user-defined parameters.

5.3.1 Ecological and evolutionary distance

There is a significant linear correlation between the centroid distance and the phylogenetic distance (see Figure (5.1)), and between the niche overlap and the phylogenetic distance (see Figure (5.2)), in both the Wayqecha and San Pedro interaction networks. The correlation between the centroid distance and the phylogenetic distance is significant (at the level of $p < 0.001$) and positive (Wayqecha slope 0.002 ± 0.001; San Pedro: slope 0.007 ± 0.001). In other words, the consumption propensities of distantly related consumer species are more dissimilar than those of closely related ones. The correlation between the niche overlap and the phylogenetic distance is significant and negative: the foraging niches of closely related consumer species intersect over a larger functional trait space than those of distantly related species; it is significant (at the level of $p < 0.001$) for the symmetric (Wayqecha: slope -0.0061 ± 0.0011; San Pedro: slope -0.0023 ± 0.0006), relative (Wayqecha: slope -0.0013 ± 0.0001; San Pedro: slope -0.00101 ± 0.00006) and egoistic (Wayqecha: slope -0.0020 ± 0.0003; San Pedro: slope -0.0010 ± 0.0001) overlap. All the results are confirmed by a Mantel Test's permutational significance over 999 permutations.

5.3.2 Overlap Excess

There is a significant and negative linear correlation between the overlap excess and the species' phylogenetic distance in both interaction networks: controlling for their niche volumes and centroid distances, closely related species tend to overlap more than what would be expected under a null model of niche evolution, whereas distantly related ones overlap less than expected (see Figure (5.3)). The correlation is significant (at the level of $p < 0.001$) for the symmetric (Wayqecha: slope -0.004 ± 0.001; San Pedro: slope -0.0016 ± 0.0003), relative (Wayqecha: slope -0.006 ± 0.001; San Pedro: slope -0.0033 ± 0.0003) and egoistic overlap (Wayqecha: slope -0.005 ± 0.001; San Pedro: slope -0.0018 ± 0.0003). This negative correlation is confirmed when controlling for the birds' degree of frugivory.

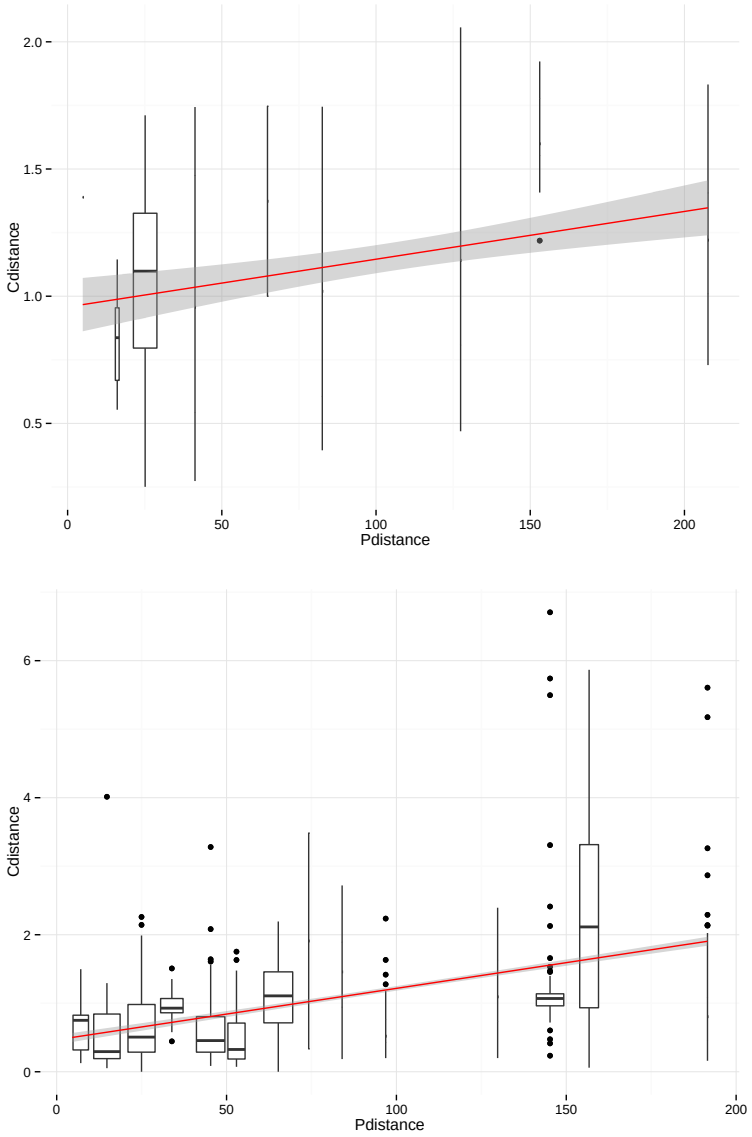

Figure 5.1: The species' niche centroid distances versus their phylogenetic distances in the Wayqecha (top) and San Pedro (bottom) interaction networks. The continuous red line represents the linear regression of the centroid distance versus the phylogenetic distance. In both networks, the slope is significant and positive: the consumption propensities of closely related species are more similar than those of distantlt related species.

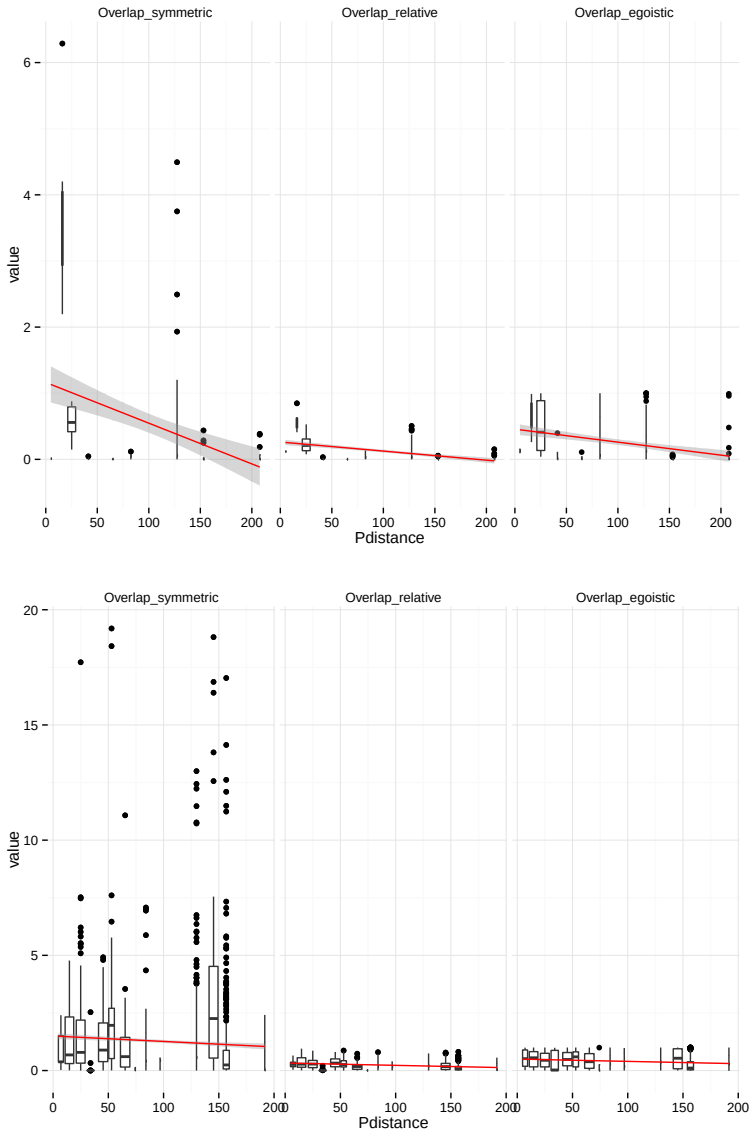

Figure 5.2: The species' niche overlaps versus their phylogenetic distances in the Wayqecha (top) and San Pedro (bottom) interaction networks. From left to right: the symmetric, relative and egoistic overlaps. The continuous red line in each facet represents the linear regression of the niche overlap versus the phylogenetic distance. In all cases, the slope is significant and negative: the foraging niches of closely related species overlap more than those of far related species.

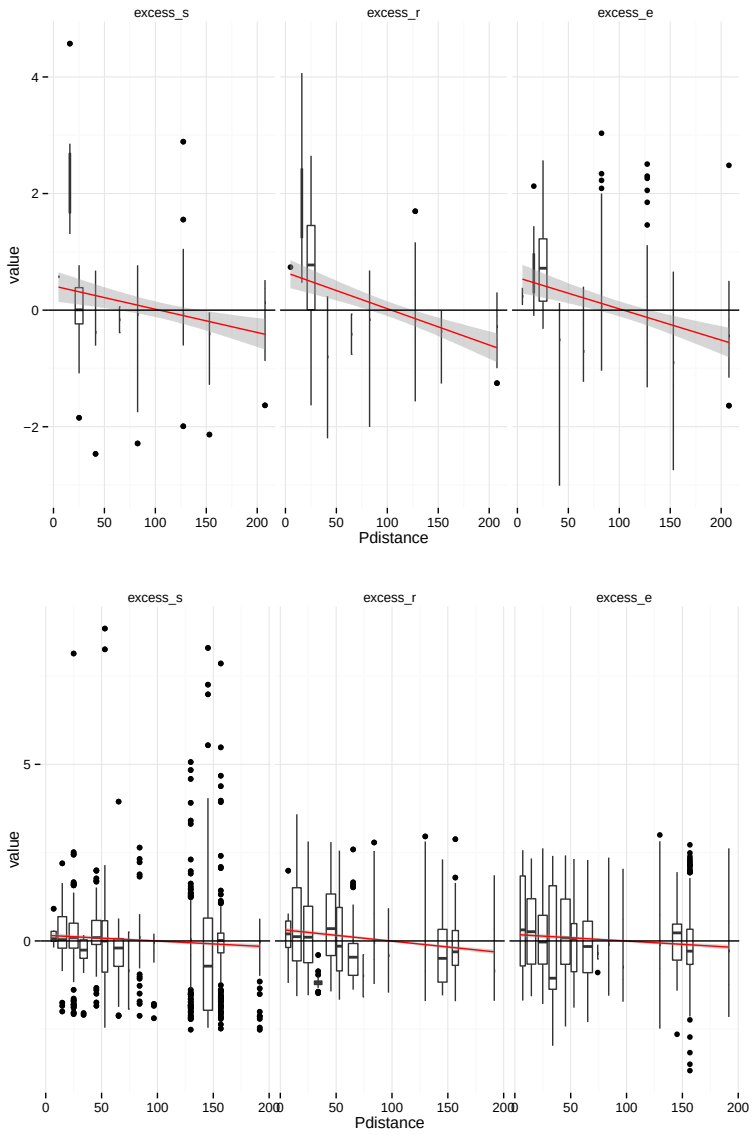

Figure 5.3: The species' overlap excesses versus their phylogenetic distances in the Wayqecha (top) and San Pedro (bottom) interaction networks. From left to right: the excesses for the symmetric, relative and egoistic overlaps. The red continuous line in each facet is the linear regression of the overlap excess versus the phylogenetic distance. In all the cases the slope is significant and negative: closely similar species tend to overlap more than expected.

5.4 Conclusions

Ecological and evolutionary diversification correlate Our results support the notion that the ecological role of the species is shaped by their evolutionary history. Closely related species share a larger portion of the resource space and have more similar consumption propensities than species that diverged a long time ago. Thus the evolutionary similarity of a pair of species is a predictor of their ecological similarity.

Both the processes of frequency modification and niche redefinition appear to have a role in reducing the competition between coexisting species and, ultimately, in supporting the biodiversity of Wayqecha and San Pedro. In diverse ecological assemblages, it is these processes that maintain ecological coexistence and affect the evolutionary trajectories of the constituent species [Alatalo et al., 1986; Gavrilets and Losos, 2009]. For example, in tropical regions, it has been suggested that up to 90% of woody plants produce fruits [Fleming, 1979], which, in turn, supports a diverse frugivorous fauna. Therefore, the coexistence of these frugivore species is likely to be determined by their ecological (frequency modification) and evolutionary (niche redefinition) response to the competition for food resources.

Niche differentiation: centroid first, boundary later The excess in niche overlap decreases with increasing phylogenetic distance between the species. In other words, species that diverged recently tend to overlap more than what we would expect, given the differences in their consumption propensity and overall foraging niche volume. This trend suggests that the coexistence strategies of recently speciated frugivores and distantly related ones may be different. Species that have diverged recently share similar morphologies; hence, they can gather resources from a similar pool of plants. As a consequence, they can reduce their mutual competition by redistributing their consumption efforts away from each other. Frequency differences in foraging preferences appear to play a key role in the coexistence of closely related species. On the other hand, those species that have diverged a long time ago have evolved ecological traits that are different enough to result in a reduced intersection of their foraging niche. Therefore, they do not need to ecologically adapt their consumption preferences to coexist.

We need to understand better the evolutionary history of species' foraging

traits in order to be in the position to provide a more detailed interpretation of the observed correlations between niche and phylogenetic dissimilarity. In particular, whether the trend we detected expresses an ecological differentiation induced by natural selection or is instead mainly consequence of ecological processes it depends on the degree of ecological plasticity of the niche centroids.

Appendix

5.A Higher complexity models

We tested the effect of the interaction terms and the significance of other categorical variables—namely, the taxonomical order of the bird species and their degree of frugivory—by considering more complex models. In particular using the function lmer in the R package *lme4* [Bates et al., 2015] we fitted a complete model with and additive random effect for each level of birds' dietary dependence on fruits:

$$\begin{aligned} eo(i,j) \sim & d^4_{i,j} * V\left(h(i)\right) * V\left(h(j)\right) + \\ & + (d^4_{i,j}|F_i/F_j) + (V\left(h(i)\right)|F_i) + (V\left(h(j)\right)|F_j), \end{aligned} \tag{5.24}$$

where F_i and F_j are categorical variables expressing the degree of frugivory (either "obligate" or "partial") of species i and j, respectively (see [Wilkinson and Rogers, 1973] for the notation). Similarly, we fitted a complete model with and additive random effect for each level of birds' taxonomical classification:

$$\begin{aligned} eo(i,j) \sim & d^4_{i,j} * V\left(h(i)\right) * V\left(h(j)\right) + \\ & + (d^4_{i,j}|O_i/O_j) + (V\left(h(i)\right)|O_i) + (V\left(h(j)\right)|O_j), \end{aligned} \tag{5.25}$$

where O_i and O_j are categorical variables accounting for the order of the bird species i and j, respectively (see [Bates et al., 2015] for the notation).

We also tested models containing the possible subsets of the predictor variables present in the two complete models. The results we show in Section (5.3) are robust to all the choices of predictors we considered.

5.B Randomisations

To assess the robustness of our results, we conducted series of 42 randomisations spanning the possible combinations of:

1. different algorithms for enveloping the observed foraging niche, either based on the distance of the species from the birds' centroid or based on the plants in the observed birds' diet, as defined in Section (5.2.2);

2. different parameters for the enveloping algorithms: we ran the randomisations for the combination of α in $\{1/100, 1/4, 1/2, 1, 2\}$ and β in $\{1, 1.5, 2\}$ (see Section (5.2.2) for the definitions of the enveloping parameters);

3. different trees from the 1000 phylogenies' pseudo-posterior distribution offered by birdtree.org [Jetz et al., 2012];

4. different definitions of the overlap measure: we computed the overlap excess for the symmetric, relative and egoistic niches as defined in Section (5.2.2);

5. different regression models, as explained in Appendix (5.A).

In order to control for dimensionality issues (such as the sparsity of the plants in the functional space) and to test the hypothesis that the observed trends were driven by only some of the functional space dimensions, we performed a jack-knifing procedure on the space's dimensions. We removed each of the axes and reran the analysis by projecting the centroid and the niches onto the remaining three-dimensional space, and by modifying the regression models accordingly to the reduced dimension (e.g, considering the third power of the centroid distance instead of the fourth power).

Finally, to control for the effect of empty intersections—which produce null overlaps—we performed the analysis by filtering any pair of birds with an overlap (either symmetric, relative or egoistic) smaller than an abitrary threshold (set at 10^{-3}) from the dataset.

The correlations between centroid distance and phylogenetic distance, between niche overlap and phylogenetic distance, and between overlap excess and phylogenetic distance were confirmed across all the combinations, except only for the randomisations with $\alpha = 2$ and $\beta = 1$. We attribute this to the

fact that at the highest values of α, the augmented foraging niches saturate the functional space, yielding meaningless results for the niche overlap.

5.C Centroid phylogenetic analysis

Here, we show the scattergram of the centroids for the Wayqecha and San Pedro species community obtained by using the function *fancyTree* in the R package *phytools* [Revell, 2012] (see Figures (5.C.1) and (5.C.2)).

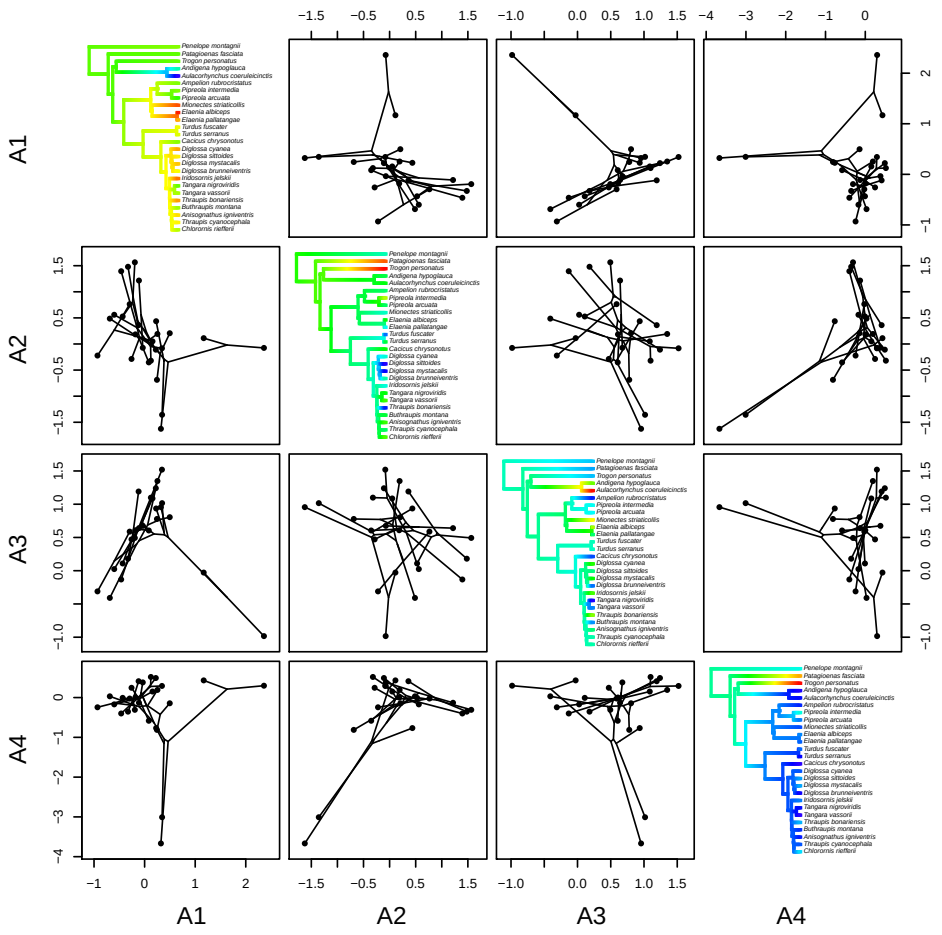

Figure 5.C.1: The scattergram of the niche centroids in the Wayqecha plant–birtd interaction network, obtained by using *phytools* [Revell, 2012].

We consider two hypotheses for the distribution of the species' niche centroids: (1) the null hypothesis, H_0, that the centroids are distributed as a Multinomial independent of the phylogenetic history of the species in

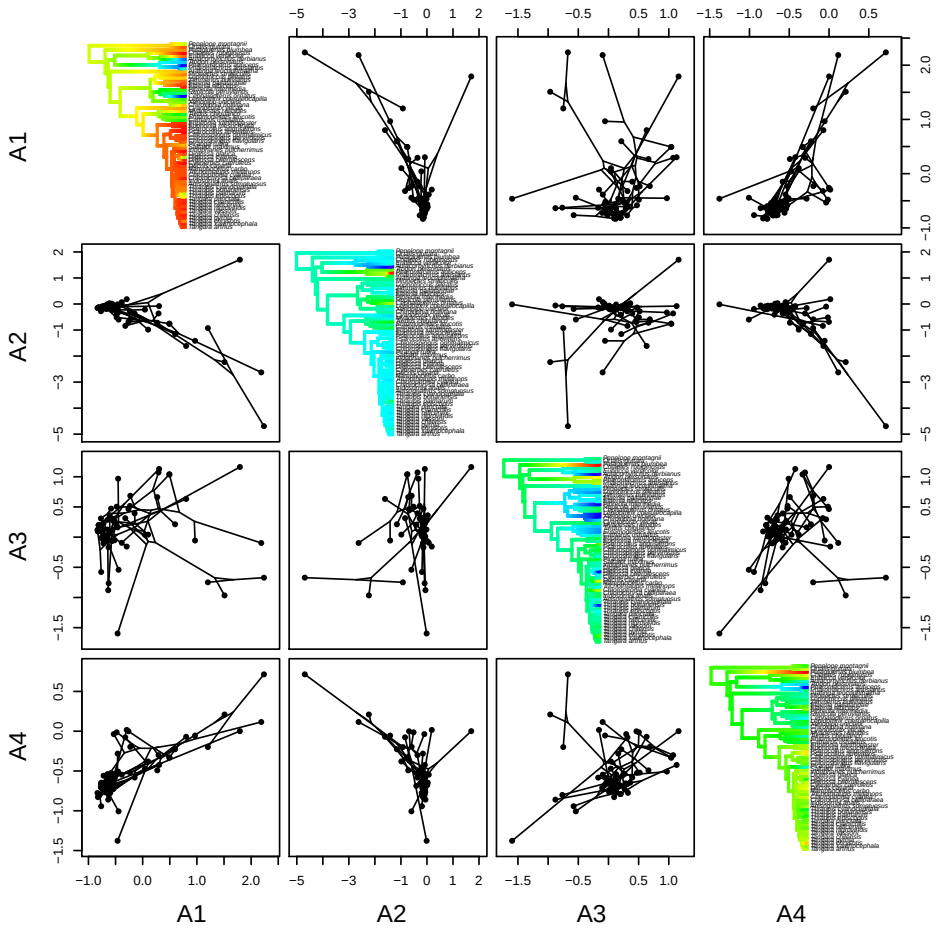

Figure 5.C.2: The scattergram of the niche centroids in the San Pedro plant–birtd interaction network, obtained by using *phytools* [Revell, 2012]. On the diagonal the distribution of the centroids' coordinates across the bird phylogeny. Out of the diagonal, the two-dimensional scatter plot of the coordinate pairs.

each interaction network: and (2) the alternative hypotesis, H_1, that the centroids are the outcome of an evolutionary processes taking place on the phylogeny according to a branching (multivariate) Brownian motion.

To test the hypothesis H_0, we estimate the variance covariance matrix of the centroid coordinates and their means from the observed centroids (ignoring the phylogenetic covariance). To test the hypothesis H_1, we estimate the BBM parameters taking into account the correlation between species determined by their shared evolutionary history (we use mvBM from mvMORPH to accomplish this task). Then, in both case we fit the simulated centroids to a multivariate Brownian motion and compare the Log-Likelihood of the empirical centroids to the simulated one.

We can refute the null hypothesis H_0 but not the alternative hypothesis H_1. In fact over 1000 simulations none of the multinomial had a higher likelihood than the observed centroid distribution; on the other hand, 17% (for the Wayqecha community) and 28% (for the San Pedro community) of the centroids simulated according to a BBM model had a lower likelihood than the observed ones.

5.D Niche intersections in the evolutionary null model

5.D.1 Upper and lower bounds

We provide upper and lower bounds for $V_{ij}(t)$ that hold for non-spherical convex hulls. The intersection volume is bounded from above by the volume of the smallest of the two niches and is bounded from below by the volume of the largest sphere that is fully contained in the $h_{ij}(t)$. As a formula:

$$\max_{\mathcal{B}(x,r)\subset h_{ij}(t)} V\Big(\mathcal{B}(x,r)\Big) \leq V_{ij}(t) \leq \min\Big(\left(V\left(h(i,t)\right), \left(V\left(h(j,t)\right)\right)\Big), \quad (5.26)$$

where the maximum is over the four-dimensional balls $\mathcal{B}(x,r)$ contained in $h_{ij}(t)$. If one niche is contained in the other (i.e., $h(i,t) \subseteq h(j,t)$ or $h(j,t) \subseteq h(i,t)$) then the largest ball $\mathcal{B}(x,r)$ is the largest ball contained in the smallest niche itself.

We analyse the case where for two niches, one is not a subset of the other.

Consider the left-hand side of Equation (5.26). Let $r_{ij}(t)$ be the radius

of the largest ball in $h_{ij}(t)$. If the two niches are balls, then:

$$r_{ij}(t) = \frac{1}{2}\big(r(i,t) + r(j,t) - d_{i,j}(t)\big)\,. \tag{5.27}$$

However, in general

$$|r_{ij}(t) - \frac{1}{2}\big(r(i,t) + r(j,t) - d_{i,j}(t)\big)| = \epsilon_{ij}(t)\,. \tag{5.28}$$

The error $\epsilon_{ij}(t)$ depends non-trivially on the shape of the convex hulls. Thus the left hand side of Equation (5.26) is difficult to approach, at least for niches which shape is strongly non spherical.

If the two niches are not too different from a sphere, we can express the left-hand side of Equation (5.26) as a function of the lineages' radii and centroid distances:

$$\begin{aligned}\max_{\mathcal{B}(x,r)\subset h_{ij}(t)} V\Big(\mathcal{B}(x,r)\Big) &= \max\Big(0, \frac{\pi^2}{2}\Big(r(i,t) + r(j,t) - d_{i,j}(t)\Big)^4\Big) \\ &= \frac{\pi^2}{2}\max\Big(0, \Big(r(i,t) + r(j,t) - d_{i,j}(t)\Big)\Big)^4\,.\end{aligned} \tag{5.29}$$

Let s be the time since the divergence of lineages i and j, and be r_s and c_s the radius and centroid of the most recent common ancestor of i and j. In this case, we have $\mathbb{E}(r_s) = r_0$ and $\mathbb{E}(c_s) = 0$. Remember that, as the Brownian motion governing the radii is centred on 0, we have:

$$\mathbb{E}\left(r(i,t)\right) = \mathbb{E}\left(r(j,t)\right) = r_0 \tag{5.30}$$

and thus:

$$\mathbb{E}\left(r(i,t) + r(j,t) - d_{i,j}(t)\right) = 2r_0 - \mathbb{E}\left(d_{ij}(t)\right). \tag{5.31}$$

We can compute $\mathbb{E}\left(d_{ij}(t)\right)$ by remembering that the coordinates of the centroids evolve as independently and identically distributed Brownian motions; hence, for each coordinate k, following [Letten and Cornwell, 2015], we have an expected centroid distance that is proportional to the square root of the time since s and to the variance σ. As a formula:

$$\mathbb{E}\left(d_{ij}(t)_k\right) = \mathbb{E}\left(c(i,t)_k - c(j,t)_k\right) = \sigma\sqrt{s}\,, \tag{5.32}$$

so that:

$$\mathbb{E}\left(d_{ij}(t)_k\right) = \sqrt{4\rho^2 s} = 2\sigma\sqrt{s}\,. \tag{5.33}$$

Moving our attention to the-right hand side of Equation (5.26), using the volume formula of Equation (5.11), the value of the minimum niche volume is a function of the lineages' radii:

$$\begin{aligned}\min\Big(\left(V\left(h(i,t)\right),\left(V\left(h(j,t)\right)\right)\Big) &= \min\left(\frac{\pi^2}{2}r(i,t)^4, \frac{\pi^2}{2}r(j,t)^4\right)\\ &= \frac{\pi^2}{2}\min\Big(r(i,t), r(j,t)\Big)^4\\ &\leq \frac{\pi^2}{2}\left(\frac{r(i,t)+r(j,t)}{2}\right)^4.\end{aligned} \tag{5.34}$$

For linearity, we have:

$$\mathbb{E}\left(\frac{r(i,t)+r(j,t)}{2}\right) = r_0\,. \tag{5.35}$$

Notice that in Equations (5.29) and (5.34) that, again, we can bound the niche overlap of a pair species from above and from below, at least in the first approximation, with a polynomial function of their radii and the centroid distance—which depends on the evolutionary history of the two species.

5.D.2 Simulation results

We simulated the null model evolution of spherical niches (defined in Section (5.2.3)) for Wayqecha and San Pedro interaction networks. To do so, we used the function *mvSIM* in the R package *mvMORPH* [Clavel et al., 2015]. In particular, the evolution of the centroids was simulated according to a four-dimensional Brownian motion with coordinate covariance structure set equal to the one estimated from the observed distribution of the traits by using the function *mvBM* in the R package *mvMORPH*.

Here we present the result of one random simulation. The results were consistend across 100 simulation: the regression of the centroid distance versus the phylogenetic distance, and of the niche overlap versus the phylogenetic distance were significant on all the simulations.

Under the null model of evolution, the correlation between overlap excess

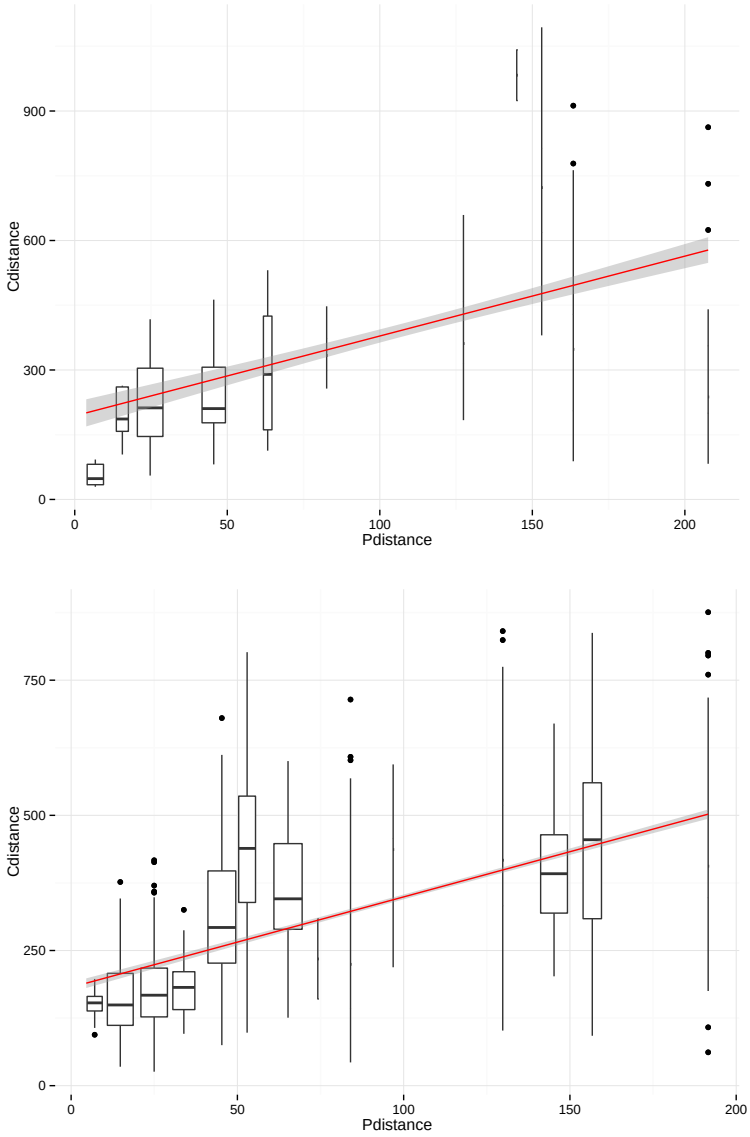

Figure 5.D.1: The species' niche centroid distances versus their phylogenetic distances for a null model simulation based on the Wayqecha (top) and San Pedro (bottom) interaction networks. The continuous red line represents the linear regression of the centroid distance versus the phylogenetic distance. In both networks, the slope is significant and positive: under the null model, the consumption propensities of closely related species are more similar than those of distantlt related species.

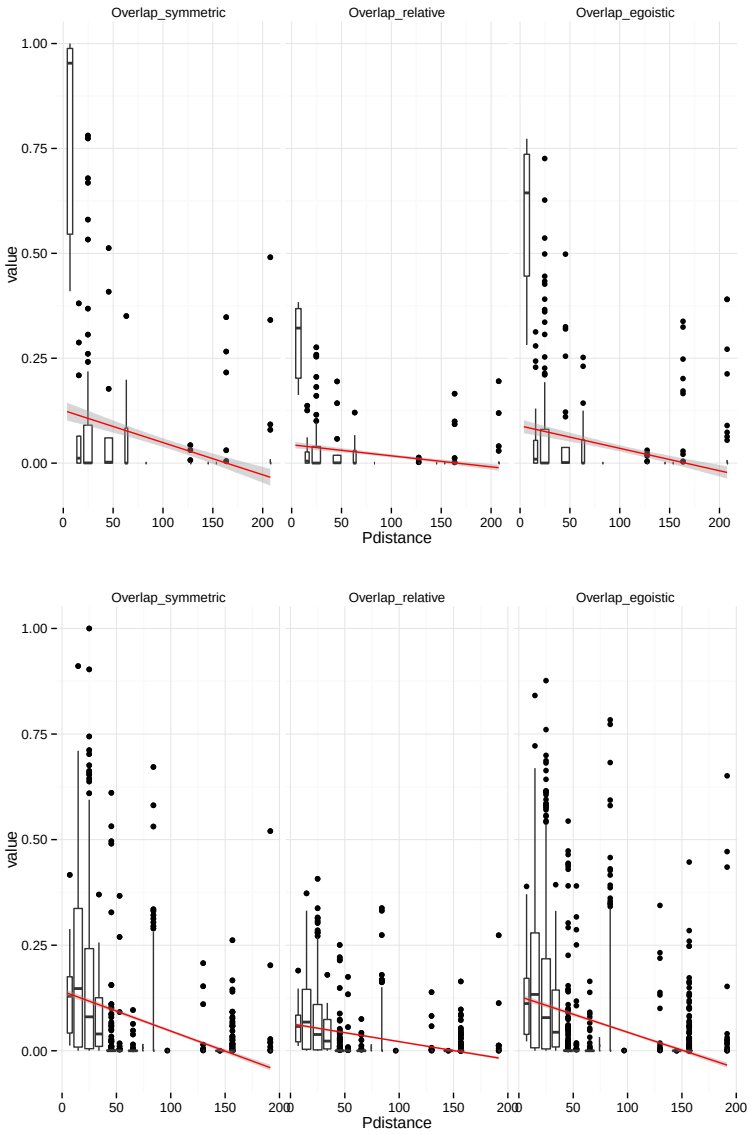

Figure 5.D.2: The species' niche overlaps versus their phylogenetic distances for a null model simulation based on the Wayqecha (top) and San Pedro (bottom) interaction networks. From left to right: the symmetric, relative and egoistic overlaps. The continuous red line in each facet represents the linear regression of the niche overlap versus the phylogenetic distance. In all cases, the slope is significant and negative: under the null model, the foraging niches of closely related species overlap more than those of far related species.

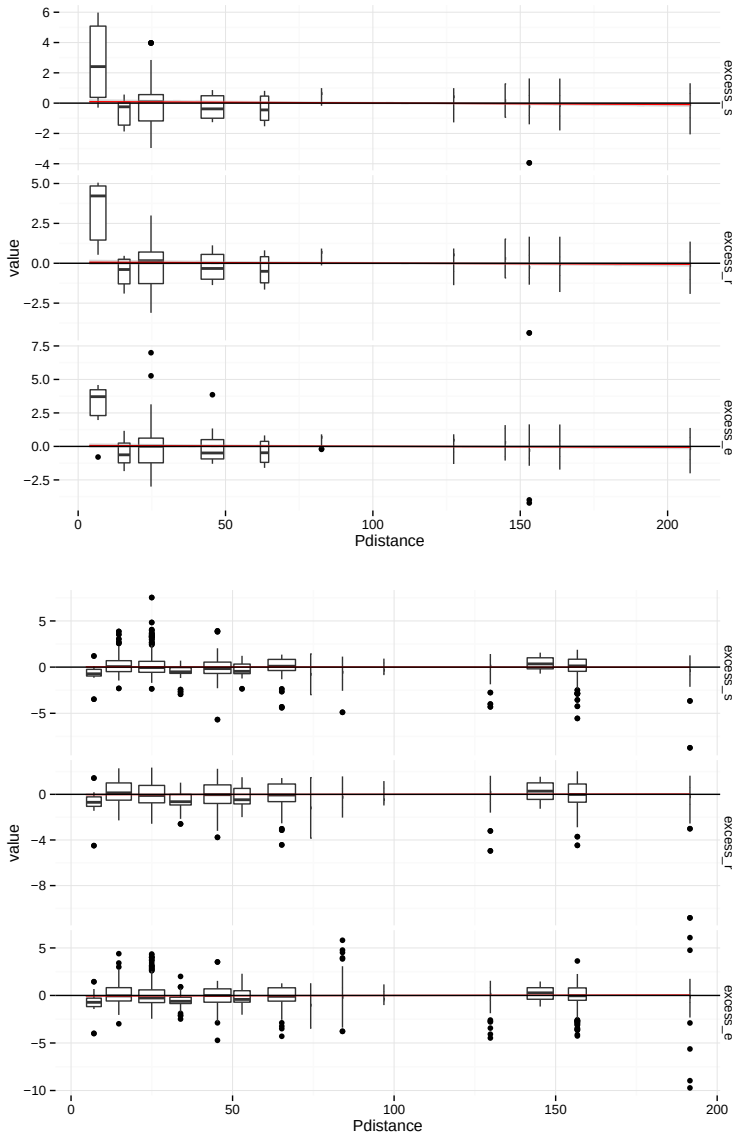

Figure 5.D.3: The species' overlap excess versus their phylogenetic distances for a null model simulation based on the Wayqecha (top) and San Pedro (bottom) interaction networks. From left to right: the excesses for the symmetric, relative and egoistic overlaps. The red continuous line in each facet is the linear regression of the overlap excess versus the phylogenetic distance. In all cases, the slope is not significant and negative: under the null model, the overlap excesses are not predicted by the species' phylogenetic distances.

and the phylogenetic distance were not significant on more than 90% of the simulations and the sign of the regression slope was not consistent across the simulations associated with a significant regression.

Chapter 6

Global centrality in population networks

Synopsis: The status of a population network in landscape genetics is commonly assessed via node measures or network statistics. Here, we use insights from the theory of finite-state Markov chains to measure the contribution of single patches to the overall effective connectedness of a population network and to test the sensitivity of the network to different perturbations, such as the removal of a patch. In particular, we introduce a novel node measure based on the average of random walk hitting times, capturing local and structural network properties. We test this analytical approach on simulated geographic networks, and explore the relationship between this measure and other common centrality measures. Finally, we see how detailed modelling of the corridor structure of a population network and of the dynamic properties of its individuals are pivotal in identifying central patches.

Notes: A version of this chapter is in preparation for submission as: GVDR, Mike Steel (School of Mathematics and Statistics, University of Canterbury) and Arne Ø. Mooers (Department of Biological Sciences, Simon Fraser University), "Assessing network connectivity through random walks".

I only went out for a walk and finally concluded to stay out till sundown, for going out, I found, was really going in.

John of the Mountains
John Muir

6.1 Introduction

Graph theory has been used in many fields to characterize local and system-wide processes in complex interconnected systems (reviewed in [Newman, 2009; Estrada, 2011]). An instance is given by *population graphs*—networks in which nodes represent discrete populations and edges represent dispersal corridors or measured genetic connectivity [Dyer and Nason, 2004]. Node measures such as betweenness and centrality, and network measures such as node degree and path-length distributions, have all been presented as useful metrics for querying such graphs [Garroway et al., 2008]. Here, we provide a further extension of network theory into ecology. In particular, we propose that if the edges linking subpopulations can be parametrized as the probability of movement by individuals (and their genes) between these subpopulations, we can use insights from the study of finite-state Markov chains to measure the overall "connectedness" of the resulting network, and to test the sensitivity of the network under perturbation. Both these may be of special interest to conservation biologists tasked with considering the effects of different management regimes, e.g., for endangered species on a patchy landscape undergoing anthropogenic modification [Osborne et al., 2000].

6.2 Population networks as Markov chains

To ground our description, without loss of generality, we consider nodes to be "patches" and edges to be "corridors", and describe the movement among nodes as being that of "individuals". A "population network" is a strongly connected directed graph $G = (V, E)$ in which each node $v_i \in V$ is a patch and the binary structure of the graph is given by the connection of the network: a link $e_{ij} = (v_i, v_j)$ is in E if and only if there is a corridor from the

patch v_i to the patch v_j. We let $N = |V|$ and $S = |E|$ denote the number of nodes and links in the graph G.

Let w denote the "weight" of each corridor. The weights w_{ij} will depend on the usability of the corridors. We will suppose that each patch v_i has an associated leaving probability $l_i \in (0, 1)$, which is the probability that an individual currently residing at v_i leaves in the next time step. Hence, the probability of remaining in the patch is $(1 - l_i) \in (0, 1)$. Moreover, we will assume that each corridor e_{ij} has an associated using cost $c_{ij} > 0$. We define the weights w_{ij} of the extant links e_{ij}:

$$w_{ij} := w(e_{ij}) := l_i \left(\frac{c_{ij}}{\sum_{j \neq i} c_{ij}} \right)^{-1} , \tag{6.1}$$

where the term between brackets is the inverse of the normalized cost. The weights of the loops e_{ii}, which express the probability of staying in the same node, are given by:

$$w_{ii} := w(e_{ii}) := 1 - l_i \qquad . \tag{6.2}$$

In general, the weights are not symmetric: $w_{ij} \neq w_{ji}$.

If $w \in \mathbb{R}_+^S$ denotes these weights on the edges, then we will let A_{Gw} denote the adjacency matrix of the weighted graph $G = (V, E, w)$ and a_{ij} denotes its entries, or, more concisely, A if the graph and the weights are made clear by the context. The entries of matrix A_{Gw} are defined as:

$$a_{ij} = \begin{cases} w_{ij}, & \text{if } e_{ij} \in E; \\ 0, & \text{if } e_{ij} \notin E \ . \end{cases} \tag{6.3}$$

The rows of A_{Gw} sum to 1 by construction. The matrix is symmetric if and only if the underlying graph G and the weights w are symmetric (i.e., $w_{ij} = w_{ji}$). In general, however, we will not assume symmetry.

The matrix A_{Gw} is stochastic and it defines a finite-state discrete-time irreducible Markov chain process $\mathcal{M}_{Gw}$, where the states of the chain are the patches of the population network and the transition probabilities between states are defined by the weights w. Conversely, we can regard A_{Gw} as the matrix of transition probabilities of the process $\mathcal{M}_{Gw}$: the probability of going from state i to state j is equal to a_{ij}.

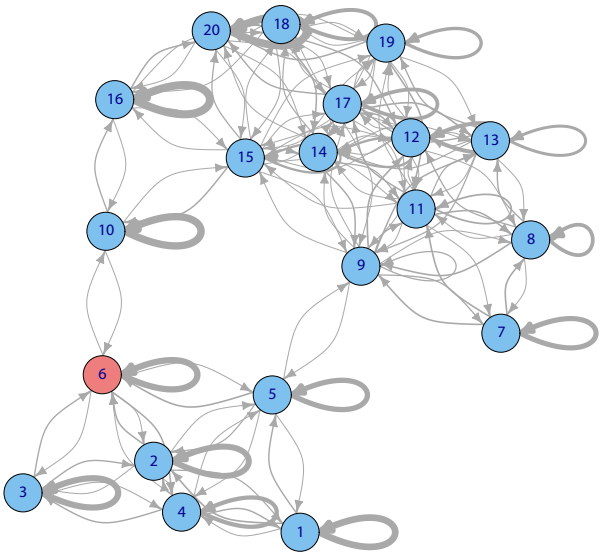

Figure 6.1: A simple example of a population network. Edge widths are proportional to transition probabilities.

6.2.1 Random walks on population networks

Let $G = (V, E, w)$ be the directed weighted graph describing the landscape network of interest and let A_{Gw} be the adjacency matrix of G. For each patch v_i, we can define a modified graph $G^{\to i}$ ("G to i"), which is obtained by removing all the links leaving v_i from G, except for the loop e_{ii}, which has its weight re-set to 1. We denote the new set of weights $w^{\to i}$. Hence, the patch v_i becomes the only absorbing state of the Markov chain $\mathcal{M}_{G^{\to i},w^{\to i}}$ defined by $G^{\to i}$: once an individual following a random walk in $G^{\to i}$ reaches the absorbing patch v_i, it stops there.

For each patch v_i, we can write the adjacency matrix of $G^{\to i}$ as:

$$A_{G^{\to i},w^{\to i}} = \left[\begin{array}{c|c} A_{-i} & A_i^{\downarrow} \\ \hline \vec{0} & 1 \end{array}\right] \tag{6.4}$$

where A_{-i} is obtained from A_{Gw} by deleting the ith row and column, $A_i^{\downarrow}$ is

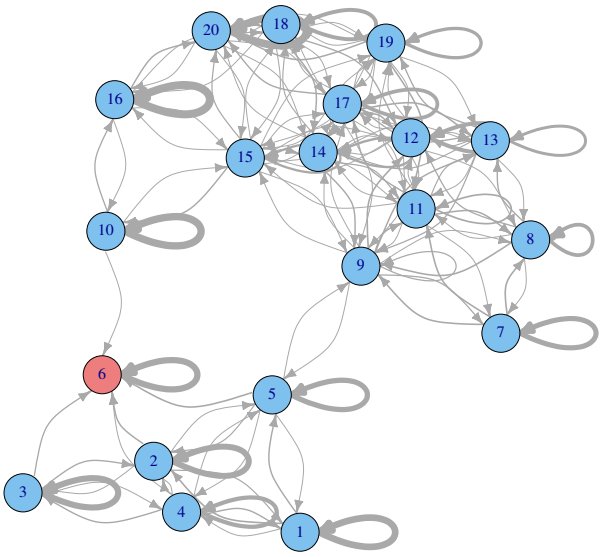

Figure 6.2: The modified population network with Patch 6 as the only absorbing patch, $G^{\to 6}$, from our simple example of population network. Edge widths are proportional to transition probabilities.

the column vector of transition probabilities from the patches $j \neq i$ to i, $\vec{0}$ is a row vector of zeros and 1 is the scalar unit.

Absorbing times A classic result from Markov chain theory allows us to compute the expected time to absorption of a random walk starting from a defined transient (non-absorbing) state [Kemeny and Snell, 1960; Grinstead and Snell, 1998]. Let P be the $N \times N$ transition probability matrix of a Markov chain $\mathcal{M}_P$ with a single absorbing state j and let Q be the minor obtained from P by deleting its jth row and column, (i.e., Q is a matrix of transition probabilities between the transient states). The expected time (in terms of the number of steps) that a random walk starting in a transient patch i spends in any another transient patch k before reaching the absorbing

state (and hence stopping) is given by the ij-th entry of the matrix:

$$\mathbf{H} = (I_{N-1} - Q)^{-1} = I_{N-1} + \sum_{n=1}^{\infty} Q^n \,, \tag{6.5}$$

where I_{N-1} is the $(N-1) \times (N-1)$ identity matrix, $^{-1}$ denotes the inverse matrix and ^{n} denotes the nth power of a matrix. The inverse of $(I_{N-1} - Q)$ exists [Kemeny and Snell, 1960, Theorem 3.2.1].

Therefore, the expected time an individual takes in following a random walk starting from a transient state i before reaching the absorpting state j is the ith row of the column vector:

$$\mathbf{t} = \mathbf{H} \cdot 1^{\downarrow}_{N-1} \tag{6.6}$$

where $1^{\downarrow}_{N-1}$ is a column vector of ones, $1^{\downarrow}_{N-1} = \{1\}^{N-1}$.

The expected hitting time from patch v_i to patch v_j, denoted as $\mathbf{T}_{ij}$, is defined as the expected time (in terms of the number of steps) an individual starting in patch v_i takes to reach the patch v_j for the first time following a random walk according to the corridor weights w.

The expected hitting time from any transient patch v_i to the any other transient patch v_j in the original Markov chain $\mathcal{M}_{Gw}$ can be computed using Eqn.(6.6). In fact, it is sufficient to notice that $\mathbf{T}_{ij}$ in G is equivalent to the expected time to absorption of a random walk in the absorbing Markov chain $\mathcal{M}_{G_j,w_j}$ starting from v_i:

$$\mathbf{T}_{ij} = \left[(I_{N-1} - A_{-j})^{-1} \cdot 1^{\downarrow}_{N-1} \right]_i \,. \tag{6.7}$$

We define the hitting matrix $\mathbf{T}$ as the $N \times N$ matrix which ij-th entries are given by Eqn.(6.7) for $i \neq j$ and are set to 0 for $i = j$. The inverse of $(I_{N-1} - A_{-j})$ exists for every $v_j \in V$, as the graph is strongly connected, and thus $\mathbf{T}$ exists.

The times $\mathbf{T}_{ij}$ express the degree of connectedness between two patches in an ecological network.

The matrix $\mathbf{T}$ determines two node quantities that were originally introduced by Noh and Rieger [2004] and are useful for establishing the centrality

of patches in population network. Specifically, from the columns of $\mathbf{T}$, we can compute the average hitting time from a random patch in the population network to a focus patch v_i (named *random walk closeness centrality* [Noh and Rieger, 2004]); from the rows of $\mathbf{T}$, we can compute the average hitting time from a focus patch v_i to a random patch in the population network. We will refer to the former as *in-walk centrality* and the second as *out-walk centrality.*

6.2.2 Hitting time centrality

We are interested in the contribution of each patch to the population network's connectedness (i.e., the ease with which an individual travels between patches in the network). In the following, we will make this concept more rigorous.

Using the notation of the previous section, let $\mathbf{T}$ be the matrix of expected hitting times for a population network G. We define the reduced network $G^{r(k)}$ obtained removing the patch v_k from G and rescaled the weights so that the rows of the adjacency matrix of $G^{r(k)}$ sum to one, that is:

$$w_{ij}^{r(k)} = w_{ij} + \frac{w_{ik}}{\text{out}(v_i) - 1} \qquad \text{for each} \quad ij \neq k \tag{6.8}$$

where $w_{ij}^{r(k)}$ is the weight of the corridor between patches v_i and v_j in the k-reduced network $G^{r(k)}$, w_{ij} is the weight of the corridor between patches v_i and v_j in G and $\text{out}(v_i)$ is the out-degree of v_i in G (counting the loop). The denominator $\text{out}(v_i) - 1$ is strictly greater than zero as the graph is strongly connected and every patch has a loop—and so $\text{out}(v_i) \geq 2$. For definition, the adjacency matrix $A_{G^{r(k)}w^{r(k)}}$ of $G^{r(k)}$ is stochastic an hence defines an irreducible Markov chain $\mathcal{M}_{G^{r(k)}w^{r(k)}}$.

We use $\mathbf{T}^{d(k)}$ ($\mathbf{T}$ *deleted* k) to denote the matrix of hitting times obtained by deleting the kth row and column from $\mathbf{T}$ and use $\mathbf{T}^{r(k)}$ ($\mathbf{T}$ *reduced* k) to denote the matrix of hitting times computed on the reduced network $G^{r(k)}$.

We define $T(v_i)$ and call this the *raw hitting time centrality* of the patch v_i, which is the quantity:

$$T(v_i) = \sum_{kl} \mathbf{T}_{kl}^{d(i)} - \mathbf{T}_{kl}^{r(i)} \tag{6.9}$$

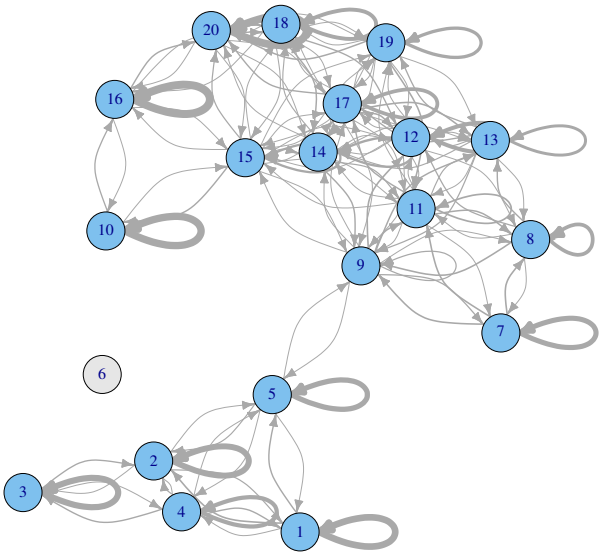

Figure 6.3: The 6-reduced population network, $G^{r(6)}$ from our simple example of a population network. We left the label of the patch six to show where it was. Edge widths are proportional to transition probabilities.

where the summation goes over every entry of $\mathbf{T}^{d(i)}$ and $\mathbf{T}^{r(i)}$. Corridors going to or coming from the patch i do not appear in any of the matrices, as they were deleted in the former case and they do not exists in the underlying reduced population network in the latter case. Under strict similarity, the *normalized* version of this measure is given by

$$T_n(v_i) = \frac{T(v_i)}{\max_{v_j} |T(v_j)|} \tag{6.10}$$

which is constrained to lie in $[-1, 1]$. Notice that the sign of the centrality reflects the fact that if one removes a patch, the expected hitting time can either increase (the measure is negative) or decrease (the measure is positive).

Notice that, in general, the reduced network $G^{r(i)}$ may no longer be connected. Let v_k and v_l be two patches residing in disconnected components of $G^{r(i)}$. In this case, the expected hitting time from v_k to v_l is infinite—a random walk starting in v_k will never reach v_l. Hence, we define $\mathbf{T}^{r(k)}_{ij} = \infty$ and, accordingly, the centrality of v_i is infinite, $T(v_i) = \infty$.

6.2.3 Discounted hitting time centrality

Katz [1953] introduced a centrality measure based on the concept of *discounted* walks. Here, walks of length m are weighted by a factor α^m, with $\alpha \in [0, 1]$, so that short walks have a higher weight than longer walks. In the framework we introduced, this is translated as:

$$\mathbf{T}_{ij,\alpha} = \left[(I_{N-1} - \alpha \cdot A_{-j})^{-1} \cdot 1^{\downarrow}_{N-1} \right]_i \tag{6.11}$$

Therefore, we define the discounted hitting time centrality of a patch v_i as:

$$T(v_i, \alpha) = \sum_{kl} \mathbf{T}^{d(i)}_{kl,\alpha} - \mathbf{T}^{r(i)}_{kl,\alpha} \tag{6.12}$$

and its corresponding normalized version as:

$$T_n(v_i, \alpha) = \frac{T(v_i, \alpha)}{\max_{v_j} |T(v_j, \alpha)|}\,, \tag{6.13}$$

which is constrained to lie in $[-1, 1]$.

6.2.4 Variance centrality

The hitting time centrality can be extended to consider the contribution of patches to the higher moments of the hitting time distribution [Hunter, 2008; Stewart, 2009]. The variance of the hitting times can be of interest in assessing the effect of removing a patch from a population network. As for the expected hitting times, we will compute the variance of the hitting times in $\mathcal{M}_{Gw}$ via the variance of the number of steps before absorption in a modified absorbing Markov chain $\mathcal{M}_{G_k w_k}$.

For each patch $v_k \in V$, we let $\mathbf{H}_k$ denote the first moment of the fundamental matrix of A_{-k} ($\mathbf{H}_k = (I_{N-1} - A_{-k})^{-1}$). Moreover, we let $\mathbf{T}_{\cdot,k}$ denote the column vector of the expected number of steps before a random walk enters the absorbing patch v_k in $\mathcal{M}_{G_k w_k}$. If we have already computed $\mathbf{T}$, then $\mathbf{T}_{\cdot k}$ is obtained from the kth column of $\mathbf{T}$, deleting the kth row. Now, the variance of the number of steps an individual following a random walk in $\mathcal{M}_{G_k w_k}$ starting at patch v_i takes before reaching the absorbing patch v_k is:

$$\mathbf{V}_{ik} = \left[\left(2\mathbf{H}_k - I_{N-1} \right) \mathbf{T}_{\cdot k} - \mathbf{T}^{(2)}_{\cdot k} \right]_i \tag{6.14}$$

where $\mathbf{T}^{(2)}_{\cdot k}$ is the column vector which entries are the square of the entries of $\mathbf{T}_{\cdot k}$.

Let $\mathbf{V}$ denote the matrix for which ij-th entry ($i \neq j$) is $\mathbf{V}_{ik}$ (the variance of the hitting time from v_i to v_j in $\mathcal{M}_{G^{\to i}, w^{\to i}}$) and has zero entries entries on the diagonal.

As we did for the expected hitting times matrix, we use $\mathbf{V}^{d(k)}$ ($\mathbf{V}$ *deleted* k) to denote the matrix of hitting times variance obtained by deleting the kth row and column from $\mathbf{V}$ and use $\mathbf{V}^{r(k)}$ ($\mathbf{V}$ *reduced* k) to denote the matrix of hitting times variance computed on the reduced network $G^{r(k)}$. Finally, we define $V(v_i)$ and call it the *variance centrality* of the patch v_i for the quantity:

$$V(v_i) = \sum_{kl} \mathbf{V}^{d(i)}_{kl} - \mathbf{V}^{r(i)}_{kl}\,, \tag{6.15}$$

where, as before, the summation is over all the patches except v_i and, if $G^{r(k)}$ is not connected, we set $V(v_i) = \infty$. As before, we define a *normalized*

version of this centrality as:

$$V_n(v_i) = \frac{V(v_i)}{\max_{v_j} |V(v_j)|} \tag{6.16}$$

which is again constrained to lie in $[-1, 1]$ and the sign of the centrality reflects whether the variance has increased or decreased.

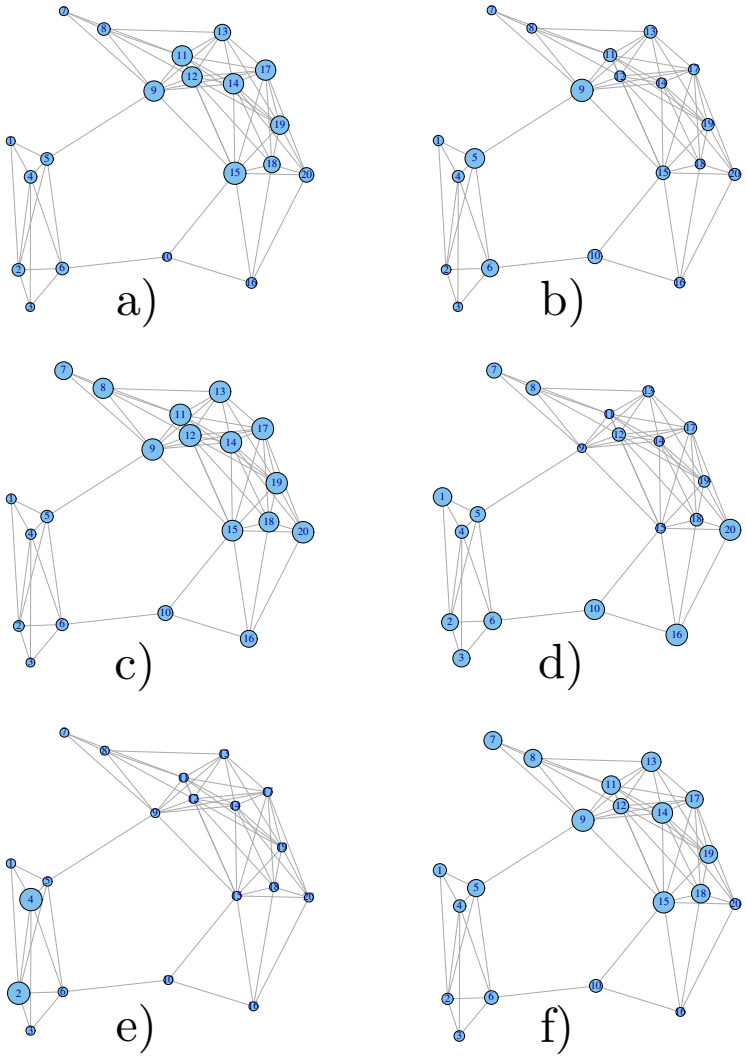

Figure 6.4: Our population network simple example drawn with nodes size proportional to a centrality measure: (a) Degree; (b) Betweenness; (c) Hitting time centrality; (d) Estrada removal centrality; (e) eigenvector centrality; (f) Closeness.

6.3 Estrada removal centrality

The "Estrada removal centrality" is based on the *subgraph centrality* originally proposed by Estrada [2000] for undirected unweighted graphs and extended to directed networks [Estrada and Rodriguez-Velazquez, 2005; Estrada, 2011].

The subgraph centrality of a node i in a undirected un-weighted graph G is the weighted sum of all closed walks starting and ending in that patch [Estrada, 2011, Sec. 7.2.3], where the weight of a walk of length l is $\frac{1}{l!}$. If A is the adjacency matrix of G, the subgraph centrality is given by:

$$EE(i) = \left[\sum_{l=0}^{\infty} \frac{A^l}{l!}\right]_{ii} = \left[\mathrm{e}^A\right]_{ii} , \tag{6.17}$$

where A^l is the l th power of A and e^A is the matrix exponential of A. We can generalize this measure, correcting the path weights by a multiplicative scalar β^l, given as:

$$EE(i,\beta) = \left[\sum_{l=0}^{\infty} \frac{\beta^l A^l}{l!}\right]_{ii} = \left[\mathrm{e}^{\beta A}\right]_{ii} \tag{6.18}$$

Here, β is a scalar interpreted in statistical-mechanical terms as an inverse temperature [Estrada and Hatano, 2007]: when β is less than one, long paths receive a heavier penalization; when β is more than one, the penalization is lighter.

An extension of the subgraph centrality to weighted undirected graphs has been proposed by Crofts and Higham [2009], where they suggest normalizing the edge weights because of the risk of "poor weight calibration" (see also [Higham et al., 2007] for more on this issue).

Now, although the calibration problem for the corridors' costs still exists, we take advantage of how the weights are already normalized and extend the subgraph centrality to weighted directed population networks. Moreover, as for the hitting times expectations and variances, we are interested in the contribution of patches to the whole network's connectedness.

Hence, as for the other two measures we introduced, we consider the difference between the Estrada centrality in the original network and in the networks obtained by sequentially removing each patch. The *Estrada removal centrality* of a patch v_i in the population network $G = (V, E, w)$ is

what we call the difference between the average of the subgraph centralities computed by deleting the ith row and column from G and the average of the subgraph centralities computed on the reduced network G_i:

$$ED(v_i) = \langle EE^{d(v_i)} \rangle - \langle EE^{r(v_i)} \rangle \,, \tag{6.19}$$

where:

$$\langle EE^{r(v_i)} \rangle = \sum_{j \neq i} \frac{EE_{G_i w_i}(v_j)}{N-1} \,, \tag{6.20}$$

and:

$$\langle EE^{d(v_i)} \rangle = \sum_{j \neq i} \frac{EE_{Gw}(v_j)}{N-1} \,. \tag{6.21}$$

6.4 Computational studies

6.4.1 Network simulation

We simulated artificial population networks by sampling simple directed random graphs from a truncated Random Geometric Graphs model [Penrose, 2003], which we now describe.

We set the number of patches in the graph, N, and the connectance radius, r. We draw N points in the unit square $[0,1] \times [0,1]$. Whenever two patches are at a distance r or less, they determine the existence in the network of a pair of symmetric links. In this case, we used a Euclidean distance but any other alternative is possible. We retained doubly connected networks only (connected networks for which removing a single patch would not disconnected the network).

For each patch v_i, we drew the probability of staying in v_i uniformly at random from the unit interval. The probability of leaving v_i is the complementary probability. We set the initial cost of each extant corridor to the Euclidean distance (in the unit square) between its two endpoints. Let a_{ij} denote the inverse of the cost of the corridor from patch v_i to patch v_j times a random noise of mean one and variance σ, or zero if the result is negative. Again, we discarded networks that failed to be doubly connected. Finally, we normalize all the outgoing probabilities so to obtain a stochastic matrix. Notice that σ determines the asymmetry of the population network corridor probabilities.

We simulated population networks spanning 20 to 2000 patches with

a radius of 0.1 to 0.5. These synthetic networks were meant to model geographic networks where the topological structure is defined by the geographic distance between patches, and the corridor costs depend on ecological, environmental and geographic reason.

We used the simulated population network to test for correlations among the proposed hitting time and variance centralities and a set of other common centrality measures: namely degree, closeness, betweenness [Freeman, 1979; Newman, 2001; Barrat et al., 2004; Opsahl et al., 2010] and eigenvector centrality [Noh and Rieger, 2004; Borgatti, 2005].

6.4.2 Large networks

For large population networks, computing the hitting time centrality for all the patches becomes demanding, although the number of operations required is polynomial on the number of patches. Our parallel implementation in Julia [Bezanson et al., 2014] was able to handle networks of up to 2000 nodes in few minutes; however, for larger networks, alternative computing approaches may be needed.

One candidate is the generalized inverse of the Laplacian matrix, by [Boley et al., 2011]: if M is the Moore-Penrose inverse of the asymmetric Laplacian and if m_{ab} denotes the ath row–bth column entry of M, then the hitting time matrix can be computed as:

$$\mathbf{T}_{ij} = m_{jj} - m_{ij} + \sum_{l}(m_{il} - m_{li})\pi_l \tag{6.22}$$

where π_l is the stationary probability of the node l. If Π denotes the matrix in which the diagonal entries are the stationary probabilities π_l and the off-diagonal entries are zero, the asymmetric Laplacian of a strongly connected directed weighted graph with the adjacency matrix Adj is defined as $\Pi(I - Adj)$.

This method is equivalent to the previous direct method, but is computationally more convenient. However, in the article, we choose to present the hitting time and variance centralities based on the direct computation method, as we think it helps to elicit the meaning of those centralities. Boley *et al.* interpreted the diagonal entries m_{ii} in M as an index of the centrality of the node v_i in the network, approximating, up to a scale factor of

N^2, the difference between the average hitting time computed on all the possible paths and the average hitting time computed on the paths passing through the node v_i. The caveats presented in Section (6.5) also hold for this centrality index,.

6.4.3 Results

An exploratory analysis showed that the hitting time centrality was correlated with degree, betweenneess, closeness and eigenvector centrality (see Fig. 6.1 for an example of a population network with 100 patches and radius of 0.2). Similarly, we found a strong linear correlation between the variance centrality and the hitting time centrality (see Fig. 6.2).

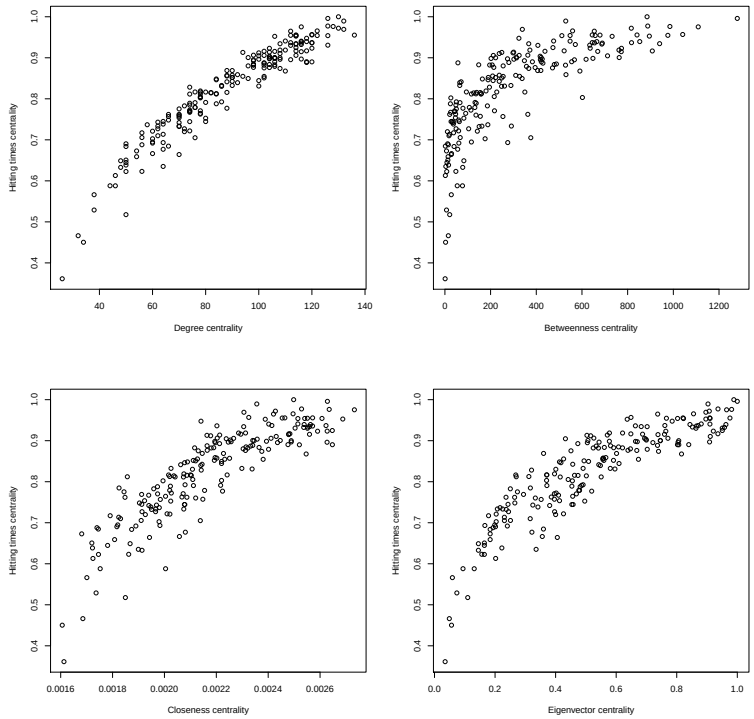

Figure 6.1: Correlation between the opposite of the normalized hitting time centrality and (a) Degree, (b) Betweenness, (c) Closeness, (d) and Eigenvector centrality in a network with 200 patches, a connection radius of 0.3 and an intensity noise of 0.05.

The correlation between the classic centralities and the hitting time centrality is not linear, and both the correlation coefficient and the goodness

of fit depend on the population network size, connectance and asymmetric noise intensity. The fit between the centralities improves as the network becomes denser and larger.

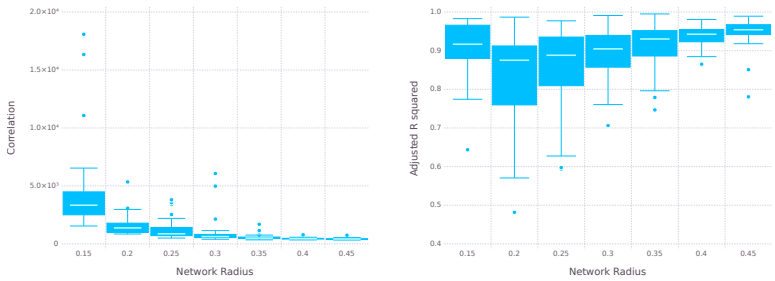

Figure 6.2: Correlation coefficient and adjusted R^2 of the linear model with hitting time centrality as the predictive variable and variance centrality as the independent variable in a network with 200 patches and varying radii. The results are presented over 42 randomizations.

The sign of the coefficient of correlation between the hitting time centrality and all the other centrality measures is positive. Interestingly yet not totally unexpectedly, the removal of "central" patches—in terms of one of the classic centrality measures—reduces the expected hitting time between the remaining patches and also its variance.

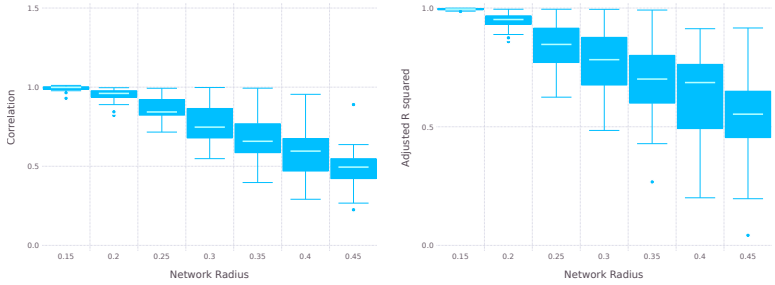

Figure 6.3: Correlation coefficient and adjusted R^2 of the linear model with the hitting time centrality as predictive variable and discounted hitting time centrality (with $\alpha = 0.5$) as the independent variable in a network with 200 patches and varying radius. Results are presented over 42 randomizations.

Moreover, as we would expect, we detected a strong linear correlation between the expected hitting time centrality and its discounted version, which was again stronger (both in correlation and in adjusted R^2 terms) in sparsely connected networks (see Fig. 6.3). Moreover, in this case, as we allow the asymmetric noise to increase, the goodness of fit of the two

centralities decreases. Hence, discounting longer paths makes a difference in the centrality ranking of patches—in particular for small or sparse graphs where the cost of corridors is sufficiently asymmetric.

6.5 Discussion

We have introduced two patch centrality measures for population networks, namely the hitting time centrality $T(v_i)$ (the overall effect of removing a patch from a network on the expected random walks' hitting times) and the variance centrality $V(v_i)$ (the overall effect of removing a patch on the variance of random walks' hitting times). The two measures can be computed from the adjacency matrix of the graph, via the introduction of a set of ancillary matrices. These latter matrices can be obtained by modifying the random walk defined on the original adjacency matrix so that each patch sequentially plays the role of being the only absorbing states in a random walk. The hitting time and variance centralities have a natural interpretation in terms of the effect on the random walks of individuals (species, genes, ...) random walks in the population network. Specific questions about the perturbation of sets of corridors or patches can be efficiently investigated in terms of the effects on expected hitting times and their variance. Hence, these novel measures may result in valuable tools for the evaluation of conservation policies affecting population networks. This, in turn, may also help in ranking patches according to their value in terms of population network connectedness.

Lost in a walk It is important to describe the scenario in which the hitting time centrality and the variance centrality fail to shed light on the structure of a network. On one hand, patches with a high degree tend to have lower expected hitting times than low-degree patches; on the other hand, patches connected by many short paths have lower hitting times than patches that are poorly connected or far apart.

It would seem natural, for some scenarios, to define the cost of an edge as the geographical distance between patches (i.e., as the Euclidean distance given by the coordinates of the patches). Therefore, it is easy to define complete graphs where all the pairs of nodes are connected by an edge of positive weight. However, we should note that many standard measures of

network connectivity, patch distance and patch centrality have less meaning when the connectivity of the graph is too high, as illustrated by von Luxburg et al. [2010]. Hence, node degrees are good estimators for the hitting time and the *commuting time* (i.e., $\mathbf{T}_{ij} + \mathbf{T}_{ji}$). Indeed, in this cases the average time for reaching patch v_j from patch v_i does not depend on the structure of the graph but just on the local properties of the nodes.

Hence, it is necessary to prepare the data for the analysis so as not to include too many links: considering a population network as a complete graph with the corridor costs given as a function of only the geographical distance between patches may lead to unrealistic patch rankings, such as rewarding patches with a high degree and overlooking the network structure. A deeper knowledge about the structure of a population network can be achieved by considering more detailed models of the corridors cost—including climatic informations, conservation status of the corridors and of the patches they lead to, geomorphological data and so on. It is preferable to not include corridors that directly link distant patches whenever those corridors do not actually exists.

Conclusions Our results showed that the hitting times measures elicit local and global structures that are not fully captured by other centrality measures. Moreover, both measures have an appealing natural explanation in terms of individual movement statistics.

It is interesting to notice the sign of the correlation between the various measures. In particular, degree, closeness, betweenness, hitting time and variance centralities are all positively correlated. In other words, removing a patch that is central in the degree, closeness or betweenness sense from a population network means a larger effect on the average hitting time: the network's average hitting time will be significantly greater after the removal of a central patch than after the removal of a peripheral patch. Moreover, the same holds for the variance of the hitting times: the removal of a patch with high degree, closeness or betweenness produces a larger effect.

Chapter 7

Conclusions

In this thesis, we provided analytical tools for studying the relationship between ecological and evolutionary processes beyond the scenarios currently considered in the literature. In particular, our analyses include unipartite ecological networks (i.e., food webs where species are not neatly separable in discrete trophic levels). In **Chapter 3**, we found a clear evolutionary trace in the structure of food webs. The evolutionary signal is present both when we consider the species' diet dissimilarities and when we consider the species' representation in the food web functional space. In fact, the species' trophic roles show a significant phylogenetic signal that is stronger for the low-dimensional backbone of the food webs than for the food webs' fine wiring. The insights we gained by modelling food webs as random dot product graphs support the notion that the species' niches can be accurately described in an inherently low-dimensional space, even when the species are part of a complex network of interactions. This result was obtained by moving from a rigidly binary food web modelling to a stochastic model and by adopting an abstract definition of the species' functional traits and foraging niches.

In the Appendix of **Chapter 3** we began to introduce an evolutionary model where the evolution of traits depends explicitly on the species' interactions. Whether this or similar models can help us to explain the trait distributions we observe empirically—in particular the distribution of traits that determine the structure of interaction networks—will be an object for future work.

The food webs' RDPG embedding discussed in **Chapter 3** offers additional ecological information. Indeed, in **Chapter 4** we have shown that the

position of the species in the food web's functional space and the pairwise distance structure that the species' positions induce can be used to estimate the species' importance (i.e., its *strain*), ecological uniqueness (i.e., its *mean distance*) and the contribution to the functional diversity of the food web. We assessed these measures for four large food webs (including both marine and land food webs) for each species as a predator (consumer), as a prey (resource) and as both a predator and a prey (consumer and resource). For the food webs we analysed, we detected a strong correlation between a species' importance, uniqueness and diversity: important species tend to be unique and to contribute greatly to the total functional diversity of the food web. Moreover, the ranking of the species based on their importance, uniqueness or diversity which we computed by considering only the interactions' presence or absence was consistent with the rankings which we obtained by considering the (simulated) relative strength of the interactions. In other words, the species having higher importance, uniqueness and diversity in the topological food webs are, with high frequency, the species with higher importance, uniqueness and diversity in the weighted networks. Finally, we showed that the importance, uniqueness and diversity of the species is not uniformly distributed among the tips of the food webs' phylogenies but is disproportionally higher in some clades.

Indeed, we could identify clades of species with both high evolutionary distinctiveness and high ecological uniqueness. However, the relationship between these two definition of "originality" appears to be complex, as it is shown by the lack of linear correlation between evolutionary ecological originality. We may ask what are the mechanism that determine the emergence of a clade originality, and under which condition (both ecological and evolutionary) the two will correlate. Moreover, we showed that the measures of ecological originality we introduce are robust to the specification of interaction strengths. Further research is needed to ascertain the generality of this results to a wider class of strength distributions.

In **Chapters 3** and **4** we saw that the species' evolutionary history has a deep impact on their ecological roles. Next, in **Chapter 5**, we investigated how these ecological roles have evolved. Again, we did so by moving from a graph representation to a metric space representation of food webs (in this case, bird-plant networks). We found a strong negative correlation between a pair of birds' niche overlap and their phylogenetic distance. Similarly,

the foraging niche centroids are distributed as we would expect under a multidimensional Brownian motion model of evolution. In other words, closely related bird species have more similar consumption propensities and their niches overlap more than distantly related birds. We provided evidence that the diversification between closely related species is produced mainly by a modification of the birds' consumption propensities (which is likely to be caused by ecological mechanisms); the redefinition of the niche boundaries becomes predominant for distantly related bird species. The observed niche trajectory suggests that the diversification may not be just the product of neutral drifting, but rather be accentuated by the competition for shared resources between frugivorous birds.

Further eco-evolutionary hypotheses can be considered in order to explain the observed trend of diversification. We can formulate more specific hypotheses by acknowledging the species natural history and their geographic origin, and by considering explicitly the competition effects on the birds' evolutionary trajectories.

In **Chapters 3**, **4** we stressed the notion that the importance of a species in a network should be assessed as a *global* property instead of a *local* property. The same rationale motivates our analysis of geographic population networks in **Chapter 6**. The corridor structures among geographic patches are crucial to understand evolutionary processes where spatial factors are relevant (e.g., the dynamics of genes' flows, adaptive diversification, ...). When a patch becomes unavailable, the event affects the connectivity of the whole network in a way that is difficult to predict simply by local properties.

Across this thesis, we provided evidence for the importance of the relationship between ecology and evolution. At least for some important traits determining the way species interact, this relationship appears symmetric: ecological processes occurring on food webs (such as competition and predation) influence the evolutionary trajectory of species traits; the evolutionary history of the species shape the deep structure of food webs. In contrast with the classic coevolutionary scenario ("diagonal" networks such as host-parasite or grass-herbivour systems), the evolution of the species in a food web is driven by diffuse and complex interactions. Therefore, we need to consider species from a global (whole network) point of view and to adopt novel representation of ecosystems, beyond rigid graph models.

Bibliography

Abascal-Monroy, I. M., Zetina-Rejón, M. J., Escobar-Toledo, F., López-Ibarra, G. A., Sosa-López, A., and Tripp-Valdez, A. (2015). Functional and structural food web comparison of terminos lagoon, mexico in three periods (1980, 1998, and 2011). *Estuaries and Coasts*, in press: doi: 10.1007/s12237–015–0054–0.

Abbe, E. and Sandon, C. (2015). Recovering communities in the general stochastic block model without knowing the parameters. *ArXiv*, preprint:1506.03729.

Abrams, P. A. (2000). The evolution of predator-prey interactions: Theory and evidence. *Annual Review of Ecology and Systematics*, 31:79–105.

Adams, D. C. (2014). A generalized k statistic for estimating phylogenetic signal from shape and other high-dimentional multivariate data. *Systematic Biology*, 63(5):685–697.

Agrawal, A. A., Hastings, A. P., Johnson, M. T., Maron, J. L., and Salminen, J.-P. (2012). Insect herbivores drive real-time ecological and evolutionary change in plant populations. *Science*, 338(6103):113–116.

Alatalo, R. V., Gustafsson, L., and Lundberg, A. (1986). Interspecific competition and niche changes in tits (parus spp.): evaluation of nonexperimental data. *The American Naturalist*, 127(6):819–834.

Allesina, S. (2011). Predicting trophic relations in ecological networks: a test of the allometric diet breadth model. *Journal of Theoretical Biology*, 279(1):161–168.

Allesina, S., Alonso, D., and Pascual, M. (2008). A general model for food web structure. *Science*, 320(5876):658–661.

Allesina, S., Grilli, J., Barabás, G., Tang, S., Aljadeff, J., and Maritan, A. (2015). Predicting the stability of large structured food webs. *Nature communications*, 6:7842.

Allesina, S. and Pascual, M. (2009). Food web models: a plea for groups. *Ecology letters*, 12(7):652–662.

Allesina, S. and Tang, S. (2015). The stability–complexity relationship at age 40: a random matrix perspective. *Population Ecology*, 57(1):63–75.

Allhoff, K. T., Ritterskamp, D., Rall, B. C., Drossel, B., and Guill, C. (2015). Evolutionary food web model based on body masses gives realistic networks with permanent species turnover. *Nature Scientific Reports*, 5:10955.

Andrews, H. C. and Patterson III, C. (1976). Singular value decomposition (svd) image coding. *Communications, IEEE Transactions on*, 24(4):425–432.

Arditti, J., Elliott, J., Kitching, I. J., and Wasserthal, L. T. (2012). 'good heavens what insect can suck it'–Charles Darwin, *Angraecum sesquipedale* and *Xanthopan morganii praedicta*. *Botanical Journal of the Linnean Society*, 169(3):403–432.

Banašek-Richter, C., Bersier, L.-F., Cattin, M.-F., Baltensperger, R., Gabriel, J.-P., Merz, Y., Ulanowicz, R. E., Tavares, A. F., Williams, D. D., Ruiter, P. C. d.,

Winemiller, K. O., and Naisbit, R. E. (2009). Complexity in quantitative food webs. *Ecology*, 90(6):1470–1477.

Barber, C. B., Dobkin, D. P., and Huhdanpaa, H. (1996). The quickhull algorithm for convex hulls. *ACM Transactions on Mathematical Software*, 22(4):469–483.

Barnes, C., Bethea, D., Brodeur, R., Spitz, J., Ridoux, V., Pusineri, C., Chase, B., Hunsicker, M., Juanes, F., Kellermann, A., et al. (2008). Predator and prey body sizes in marine food webs: Ecological archives e089-051. *Ecology*, 89(3):881–881.

Barrat, A., Barthelemy, M., Pastor-Satorras, R., and Vespignani, A. (2004). The architecture of complex weighted networks. *Proceedings of the National Academy of Sciences of the United States of America*, 101(11):3747–3752.

Bartoszek, K. (2013). *Stochastic models in phylogenetic comparative methods: analytical properties and parameter estimation*. PhD thesis, Göteborgs universitet. Naturvetenskapliga fakulteten.

Baskerville, E. B., Dobson, A. P., Bedford, T., Allesina, S., Anderson, T. M., and Pascual, M. (2011). Spatial guilds in the serengeti food web revealed by a bayesian group model. *PLoS computational biology*, 7(12):e1002321.

Bates, D., Mächler, M., Bolker, B., and Walker, S. (2015). Fitting linear mixed-effects models using lme4. *Journal of Statistical Software*, 67(1):1–48.

Bavelas, A. (1950). Communication patterns in task-oriented groups. *Journal of the Acoustical Society of America*, 22(6):725–730.

Beaulieu, J. M., Jhwueng, D.-C., Boettiger, C., and O'Meara, B. C. (2012). Modeling stabilizing selection: expanding the ornstein–uhlenbeck model of adaptive evolution. *Evolution*, 66(8):2369–2383.

Bellingeri, M. and Bodini, A. (2015). Food web's backbones and energy delivery in ecosystems. *Oikos*, in press: doi: 10.1111/oik.02244.

Benton, M. J. (2009). The red queen and the court jester: species diversity and the role of biotic and abiotic factors through time. *Science*, 323(5915):728–732.

Berenos, C., Schmid-Hempel, P., and Mathias Wegner, K. (2009). Evolution of host resistance and trade-offs between virulence and transmission potential in an obligately killing parasite. *Journal of Evolutionary Biology*, 22(10):2049–2056.

Bersier, L.-F. and Kehrli, P. (2008). The signature of phylogenetic constraints on food-web structure. *Ecological Complexity*, 5(2):132–139.

Bezanson, J., Edelman, A., Karpinski, S., and Shah, V. B. (2014). Julia: A fresh approach to numerical computation. *arXiv*, preprint:1411.1607.

Billingsley, P. (2008). *Probability and measure*. John Wiley & Sons.

Blomberg, S. P., Garland, T., and Ives, A. R. (2003). Testing for phylogenetic signal in comparative data: behavioral traits are more labile. *Evolution*, 57(4):717–745.

Böhning-Gaese, K. and Oberrath, R. (1999). Phylogenetic effects on morphological, life-history, behavioural and ecological traits of birds. *Evolutionary Ecology Research*, 1(3):347–364.

Boley, D., Ranjan, G., and Zhang, Z.-L. (2011). Commute times for a directed graph using an asymmetric laplacian. *Linear Algebra and its Applications*, 435(2):224–242.

Bonacich, P. and Lloyd, P. (2001). Eigenvector-like measures of centrality for asymmetric relations. *Social Networks*, 23(3):191–201.

Borg, I. and Groenen, P. J. F. (1997). *Modern Multidimensional Scaling: Theory and Applications*, volume 2 of *Statistics in Social Science and Public Policy*. Springer-Verlag, New York.

Borgatti, S. P. (2005). Centrality and network flow. *Social networks*, 27(1):55–71.

Bosq, D. and Nguyen, H. T. (2013). *A course in stochastic processes: stochastic models and statistical inference*, volume 34. Springer Science & Business Media.

Brandes, U. (2001). A faster algorithm for betweenness centrality*. *Journal of Mathematical Sociology*, 25(2):163–177.

Brännström, Å., Johansson, J., Loeuille, N., Kristensen, N., Troost, T. A., Lambers, R. H. R., and Dieckmann, U. (2012). Modelling the ecology and evolution of communities: a review of past achievements, current efforts, and future promises. *Evolutionary Ecology Research*, 14(5):601–625.

Brockhurst, M. A., Morgan, A. D., Fenton, A., and Buckling, A. (2007). Experimental coevolution with bacteria and phage: the pseudomonas fluorescens—ϕ2 model system. *Infection, Genetics and Evolution*, 7(4):547–552.

Butler, M. A. and King, A. A. (2004). Phylogenetic comparative analysis: a modeling approach for adaptive evolution. *The American Naturalist*, 164(6):683–695.

Cadotte, M. W., Dinnage, R., and Tilman, D. (2012). Phylogenetic diversity promotes ecosystem stability. *Ecology*, 93(sp8):S223–S233.

Caldarelli, G., Higgs, P. G., and McKane, A. J. (1998). Modelling coevolution in multispecies communities. *Journal of Theoretical Biology*, 193(2):345–358.

Calder, W. A. (1984). *Size, function, and life history*. Courier Corporation.

Canard, E. F., Mouquet, N., Mouillot, D., Stanko, M., Miklisova, D., and Gravel, D. (2014). Empirical evaluation of neutral interactions in host-parasite networks. *The American Naturalist*, 183(4):468–479.

Capitán, J. A., Arenas, A., and Guimerà, R. (2013). Degree of intervality of food webs: From body-size data to models. *Journal of Theoretical Biology*, 334:35–44.

Cattell, R. B. (1966). The scree test for the number of factors. *Multivariate behavioral research*, 1(2):245–276.

Cavalli-Sforza, L. L. and Edwards, A. W. F. (1967). Phylogenetic analysis. models and estimation procedures. *American journal of human genetics*, 19(3 Pt 1):233–257.

Chase, J. M. and Leibold, M. A. (2003). *Ecological niches: linking classical and contemporary approaches*. University of Chicago Press.

Chatterjee, S. et al. (2014). Matrix estimation by universal singular value thresholding. *The Annals of Statistics*, 43(1):177–214.

Chesson, P. (2000). Mechanisms of maintenance of species diversity. *Annual Review of Ecology and Systematics*, 31(1):343–366.

Clarke, M., Thomas, G. H., and Freckleton, R. P. (2015). Trait evolution in adaptive radiations: modelling and measuring interspecific competition on phylogenies. *bioRxiv*, preprint: doi: 10.1101/033647.

Clavel, J., Escarguel, G., and Merceron, G. (2015). mvmorph: an r package for fitting multivariate evolutionary models to morphometric data. *Methods in Ecology and Evolution*, 6(11):1311–1319.

Closs, G. P. and Lake, P. S. (1994). Spatial and temporal variation in the structure of an intermittent-stream food web. *Ecological Monographs*, 64(1):2–21.

Cody, M. L. (1974). *Competition and the structure of bird communities*, volume 7 of *Monographs in Population Biology*. Princeton University Press.

Connell, J. H. (1961). The influence of interspecific competition and other factors on the distribution of the barnacle *Chthamalus stellatus*. *Ecology*, 42(4):710–723.

Coulson, T., Rohani, P., and Pascual, M. (2004). Skeletons, noise and population growth: the end of an old debate? *Trends in Ecology & Evolution*, 19(7):359–364.

Crawford, J. W., Redlinski, I., Steiner, C. F., and Cáceres, C. E. (2015). Life-history evolution in a daphnia ambigua population during community assembly. *Journal of Plankton Research*, 37(2):409–416.

Crofts, J. J. and Higham, D. J. (2009). A weighted communicability measure applied to complex brain networks. *Journal of the Royal Society Interface*, 6(33):411–414.

Darwin, C. (1859). *On the Origin of Species by Means of Natural Selection: or the Preservation of Favored Races in the Struggle for Life*. John Murray, London.

Darwin, C. (1888). *The various contrivances by which orchids are fertilised by insects*. John Murrary, London.

Darwin, C. (1889). *The structure and distribution of coral reefs*. Smith, Elder & Co., London.

Darwin, C. (1892). *The formation of vegetable mould, through the action of worms, with observations on their habits*. John Murray, London.

Dawah, H. A., Hawkins, B. A., and Claridge, M. F. (1995). Structure of the parasitoid communities of grass-feeding chalcid wasps. *Journal of animal ecology*, 64:708–720.

de Visser, S. N., Freymann, B. P., and Olff, H. (2011). The serengeti food web: empirical quantification and analysis of topological changes under increasing human impact. *Journal of Animal Ecology*, 80(2):484–494.

Débarre, F., Nuismer, S., and Doebeli, M. (2014). Multidimensional (co) evolutionary stability. *The American Naturalist*, 184(2):158–171.

Dehling, D. M., Fritz, S. A., Töpfer, T., Päckert, M., Estler, P., Böhning-Gaese, K., and Schleuning, M. (2014a). Functional and phylogenetic diversity and assemblage structure of frugivorous birds along an elevational gradient in the tropical andes. *Ecography*, 37(11):1047–1055.

Dehling, D. M., Jordano, P., Schaefer, H. M., Boehning-Gaese, K., and Schleuning, M. (2016). Morphology predicts species' functional roles and their degree of specialisation in plant-frugivore interactions. *Proceedings of the Royal Society B: Biological Sciences.*, in press.

Dehling, D. M., Töpfer, T., Schaefer, H. M., Jordano, P., Böhning-Gaese, K., and Schleuning, M. (2014b). Functional relationships beyond species richness patterns: trait matching in plant–bird mutualisms across scales. *Global Ecology and Biogeography*, 23(10):1085–1093.

Dodsworth, S., Chase, M. W., Kelly, L. J., Leitch, I. J., Macas, J., Novák, P., Piednoël, M., Weiss-Schneeweiss, H., and Leitch, A. R. (2015). Genomic repeat abundances contain phylogenetic signal. *Systematic Biology*, 64(1):112–126.

Doebeli, M. (2011). *Adaptive Diversification (MPB-48)*. Princeton University Press.

Doebeli, M. and Ispolatov, I. (2010). Complexity and diversity. *Science*, 328(5977):494–497.

Doebeli, M. and Ispolatov, I. (2014). Chaos and unpredictability in evolution. *Evolution*, 68(5):1365–1373.

Doi, H., Vander Zanden, M. J., and Hillebrand, H. (2012). Shorter food chain length in ancient lakes: Evidence from a global synthesis. *PLoS ONE*, 7(6):e37856.

Doob, J. L. (1942). The brownian movement and stochastic equations. *Annals of Mathematics*, 43(2):351–369.

Drossel, B., Higgs, P. G., and McKane, A. J. (2001). The influence of predator–prey population dynamics on the long-term evolution of food web structure. *Journal of Theoretical Biology*, 208(1):91–107.

Drossel, B. and McKane, A. J. (2003). Modelling food webs. In Bornholdt, S. and Schuster, H. G., editors, *Handbook of Graphs and Networks: From the Genome to the Internet*, pages 218–247. Wiley-VCH Verlag GmbH & Co. KGaA.

Drossel, B., McKane, A. J., and Quince, C. (2004). The impact of nonlinear functional responses on the long-term evolution of food web structure. *Journal of Theoretical Biology*, 229(4):539–548.

Drury, J., Clavel, J., Manceau, M., and Morlon, H. (2015). Estimating the effect of competition on trait evolution using maximum likelihood inference. *bioRxiv*, preprint: doi: 10.1101/023473.

Dryden, I. L. and Mardia, K. V. (1998). *Statistical shape analysis*, volume 4. Wiley Chichester.

Dunne, J. A., Williams, R. J., Martinez, N. D., Wood, R. A., and Erwin, D. H. (2008). Compilation and network analyses of cambrian food webs. *PLoS biology*, 6(4):e102.

Dyer, R. J. and Nason, J. D. (2004). Population graphs: the graph theoretic shape of genetic structure. *Molecular Ecology*, 13(7):1713–1727.

Ehrlich, P. R. and Raven, P. H. (1964). Butterflies and plants: a study in coevolution. *Evolution*, 18(4):586–608.

Eklöf, A., Helmus, M. R., Moore, M., and Allesina, S. (2012). Relevance of evolutionary history for food web structure. *Proceedings of the Royal Society B: Biological Sciences*, 279(1733):1588–1596.

Eklöf, A., Jacob, U., Kopp, J., Bosch, J., Castro-Urgal, R., Chacoff, N. P., Dalsgaard, B., Sassi, C., Galetti, M., Guimarães, P. R., et al. (2013). The dimensionality of ecological networks. *Ecology letters*, 16(5):577–583.

Eldredge, N. (2003). The sloshing bucket: How the physical realm controls evolution. In Schuster, P. and Crutchfield, J. P., editors, *Evolutionary dynamics: Exploring the interplay of selection, accident, neutrality, and function*, page 3. Oxford University Press, Oxford, New York.

Ellis, C. N., Traverse, C. C., Mayo-Smith, L., Buskirk, S. W., and Cooper, V. S. (2015). Character displacement and the evolution of niche complementarity in a model biofilm community. *Evolution*, 69(2):283–293.

Elton, C. S. (1927). *Animal ecology*. Macmillan Co., New York.

Erdös, P. and Rényi, A. (1960). On the evolution of random graphs. *Publ. Math. Inst. Hung. Acad. Sci*, 5:17–61.

Estrada, E. (2000). Characterization of 3d molecular structure. *Chemical Physics Letters*, 319(5):713–718.

Estrada, E. (2007). Characterization of topological keystone species: local, global and "meso-scale" centralities in food webs. *Ecological Complexity*, 4(1):48–57.

Estrada, E. (2011). *The structure of complex networks: theory and applications*. Oxford University Press.

Estrada, E. and Hatano, N. (2007). Statistical-mechanical approach to subgraph centrality in complex networks. *Chemical Physics Letters*, 439(1):247–251.

Estrada, E. and Rodriguez-Velazquez, J. A. (2005). Subgraph centrality in complex networks. *Physical Review E*, 71(5):056103.

Faith, D. P. (1992). Conservation evaluation and phylogenetic diversity. *Biological Conservation*, 61(1):1–10.

Faye, L., Matthey-Doret, R., and Mooers, A. (2015). Valuing species on the cheap. *Animal Conservation*, 18(4):313–314.

Felsenstein, J. (1985). Phylogenies and the comparative method. *The American Naturalist*, 125(1):1–15.

Fisher, C. K. and Mehta, P. (2014). The transition between the niche and neutral regimes in ecology. *Proceedings of the National Academy of Sciences*, 111(36):13111–13116.

Fleming, T. H. (1979). Do tropical frugivores compete for food? *American Zoologist*, 19(4):1157–1172.

Fontana, S., Petchey, O. L., and Pomati, F. (2015). Individual-level trait diversity concepts and indices to comprehensively describe community change in multidimensional trait space. *Functional Ecology*, in press: doi: 10.1111/1365–2435.12551.

Fortuna, M. A., Krishna, A., and Bascompte, J. (2013). Habitat loss and the disassembly of mutalistic networks. *Oikos*, 122(6):938–942.

Fortuna, M. A., Stouffer, D. B., Olesen, J. M., Jordano, P., Mouillot, D., Krasnov, B. R., Poulin, R., and Bascompte, J. (2010). Nestedness versus modularity in ecological networks: two sides of the same coin? *Journal of Animal Ecology*, 79(4):811–817.

Freckleton, R. P. and Harvey, P. H. (2006). Detecting non-brownian trait evolution in adaptive radiations. *PLoS biology*, 4(11):e373.

Freeman, L. C. (1979). Centrality in social networks conceptual clarification. *Social networks*, 1(3):215–239.

Friedman, J., Hastie, T., and Tibshirani, R. (2001). *The elements of statistical learning*, volume 1. Springer series in statistics Springer, Berlin.

Fussmann, G., Loreau, M., and Abrams, P. (2007). Eco-evolutionary dynamics of communities and ecosystems. *Functional Ecology*, 21(3):465–477.

Futuyma, D. J. and Agrawal, A. A. (2009). Macroevolution and the biological diversity of plants and herbivores. *Proceedings of the National Academy of Sciences*, 106(43):18054–18061.

Futuyma, D. J. and Moreno, G. (1988). The evolution of ecological specialization. *Annual Review of Ecology and Systematics*, 19:207–233.

Futuyma, D. J. and Slatkin, M. (1983). *Coevolution*. Sinauer Associates Incorporated, Sunderland, Massachusetts.

Garamszegi, L. Z., editor (2014). *Modern Phylogenetic Comparative Methods and Their Application in Evolutionary Biology*. Springer.

Garamszegi, L. Z. and Mundry, R. (2014). Multimodel-inference in comparative analyses. In *Modern Phylogenetic Comparative Methods and Their Application in Evolutionary Biology*, pages 305–331. Springer.

Garland, T., Dickerman, A. W., Janis, C. M., and Jones, J. A. (1993). Phylogenetic analysis of covariance by computer simulation. *Systematic Biology*, 42(3):265–292.

Garroway, C. J., Bowman, J., Carr, D., and Wilson, P. J. (2008). Applications of graph theory to landscape genetics. *Evolutionary Applications*, 1(4):620–630.

Gascuel, O. and Steel, M., editors (2007). *Reconstructing evolution. New mathematical and computational advances*. Oxford University Press.

Gause, G. F. (1934). *The Struggle for Existence*. The Williams & Wilkins Company, Baltimore.

Gavish, M. and Donoho, D. L. (2014). The optimal hard threshold for singular values is $\frac{4}{\sqrt{3}}$. *Information Theory, IEEE Transactions on*, 60(8):5040–5053.

Gavrilets, S. and Losos, J. B. (2009). Adaptive radiation: contrasting theory with data. *Science*, 323(5915):732–737.

Gerhold, P., Cahill, J. F., Winter, M., Bartish, I. V., and Prinzing, A. (2015). Phylogenetic patterns are not proxies of community assembly mechanisms (they are far better). *Functional Ecology*, 29(5):600–614.

Grady, D., Thiemann, C., and Brockmann, D. (2012). Robust classification of salient links in complex networks. *Nature communications*, 3(864).

Grant, P. R. and Grant, B. R. (2011). *How and why species multiply: the radiation of Darwin's finches*. Princeton University Press.

Gravel, D., Poisot, T., Albouy, C., Velez, L., and Mouillot, D. (2013). Inferring food web structure from predator–prey body size relationships. *Methods in Ecology and Evolution*, 4(11):1083–1090.

Grinstead, C. M. and Snell, J. L. (1998). *Introduction to probability*. American Mathematical Soc.

Habel, K., Grasman, R., Stahel, A., Stahel, A., and Sterratt, D. C. (2014). *geometry: Mesh generation and surface tesselation*. version 0.3-5.

Hackett, S. J., Kimball, R. T., Reddy, S., Bowie, R. C., Braun, E. L., Braun, M. J., Chojnowski, J. L., Cox, W. A., Han, K.-L., Harshman, J., et al. (2008). A phylogenomic study of birds reveals their evolutionary history. *Science*, 320(5884):1763–1768.

Hafner, M. S. and Page, R. D. (1995). Molecular phylogenies and host-parasite cospeciation: gophers and lice as a model system. *Philosophical Transactions of the Royal Society B: Biological Sciences*, 349(1327):77–83.

Hall, P. and Barbour, A. D. (1984). Reversing the berry-esséen inequality. *Proceedings of the American Mathematical Society*, 90(1):107–110.

Hand, B. K., Lowe, W. H., Kovach, R. P., Muhlfeld, C. C., and Luikart, G. (2015). Landscape community genomics: understanding eco-evolutionary processes in complex environments. *Trends in Ecology & Evolution*, 30(3):161–168.

Hansen, T. F. (1997). Stabilizing selection and the comparative analysis of adaptation. *Evolution*, 51(5):1341–1351.

Hansen, T. F., Pienaar, J., and Orzack, S. H. (2008). A comparative method for studying adaptation to a randomly evolving environment. *Evolution*, 62(8):1965–1977.

Harmon, L. J., Losos, J. B., Jonathan Davies, T., Gillespie, R. G., Gittleman, J. L., Bryan Jennings, W., Kozak, K. H., McPeek, M. A., Moreno-Roark, F., Near, T. J., et al. (2010). Early bursts of body size and shape evolution are rare in comparative data. *Evolution*, 64(8):2385–2396.

Harper-Smith, S., Berlow, E. L., Knapp, R. A., Williams, R. J., and Martinez, N. D. (2005). Communicating ecology through food webs: visualizing and quantifying the effects of stocking alpine lakes with trout. In de Ruiter, P., Wolters, V., Moore, J. C., and Melville-Smith, K., editors, *Dynamic Food Webs: Multispecies Assemblages, Ecosystem Development, and Environmental Change*, Theoretical Ecology Series, pages 407–423. Academic Press.

Hartmann, K. and Steel, M. (2007). Phylogenetic diversity: from combinatorics to ecology. In Gascuel, O. and Steel, M., editors, *Reconstructing evolution: new mathematical and computational approaches*, pages 171–196. Oxford University Press.

Higham, D. J., Kalna, G., and Kibble, M. (2007). Spectral clustering and its use in bioinformatics. *Journal of computational and applied mathematics*, 204(1):25–37.

Hillebrand, H. and Matthiessen, B. (2009). Biodiversity in a complex world: consolidation and progress in functional biodiversity research. *Ecology Letters*, 12(12):1405–1419.

Holland, P. W., Laskey, K. B., and Leinhardt, S. (1983). Stochastic blockmodels: First steps. *Social networks*, 5(2):109–137.

Holling, C. S. (1973). Resilience and stability of ecological systems. *Annual review of ecology and systematics*, 4:1–23.

Holt, R. D. (1987). On the relation between niche overlap and competition: the effect of incommensurable niche dimensions. *Oikos*, 48(1):110–114.

Huelsenbeck, J. P., Rannala, B., and Masly, J. P. (2000). Accommodating phylogenetic uncertainty in evolutionary studies. *Science*, 288(5475):2349–2350.

Hunter, J. J. (2008). Variances of first passage times in a markov chain with applications to mixing times. *Linear Algebra and its Applications*, 429(5–6):1135 – 1162.

Hurvich, C. M. and Tsai, C.-L. (1989). Regression and time series model selection in small samples. *Biometrika*, 76(2):297–307.

Huson, D. H., Rupp, R., and Scornavacca, C. (2010). *Phylogenetic networks*. Cambridge University Press.

Hutchinson, G. E. (1957). Concluding remarks. *Cold Spring Harbor Symposia on Quantitative Biology*, 22:415–427.

Hutchinson, G. E. (1965). *The ecological theater and the evolutionary play*. Yale University Press.

Ingram, T., Harmon, L. J., and Shurin, J. B. (2009). Niche evolution, trophic structure, and species turnover in model food webs. *The American Naturalist*, 174(1):56–67.

Isaac, N. J., Turvey, S. T., Collen, B., Waterman, C., and Baillie, J. E. (2007). Mammals on the edge: conservation priorities based on threat and phylogeny. *PLoS One*, 2(3):e296.

Ispolatov, I., Madhok, V., and Doebeli, M. (2016). Individual-based models for adaptive diversification in high-dimensional phenotype spaces. *Journal of Theoretical Biology*, 390:97–105.

Itô, H. C. and Ikegami, T. (2006). Food-web formation with recursive evolutionary branching. *Journal of Theoretical Biology*, 238(1):1–10.

Itô, H. C., Shimada, M., and Ikegami, T. (2009). Coevolutionary dynamics of adaptive radiation for food-web development. *Population ecology*, 51(1):65–81.

Itô, K. (1944). Stochastic integral. *Proceedings of the Imperial Academy*, 20(8):519–524.

Ives, A. R. and Godfray, H. C. J. (2006). Phylogenetic analysis of trophic associations. *The American Naturalist*, 168(1):E1–E14.

Ives, A. R., Midford, P. E., and Garland, T. (2007). Within-species variation and measurement error in phylogenetic comparative methods. *Systematic Biology*, 56(2):252–270.

Jacob, U., Thierry, A., Brose, U., Arntz, W. E., Berg, S., Brey, T., Fetzer, I., Jonsson, T., Mintenbeck, K., Mollmann, C., et al. (2011). The role of body size in complex food webs: A cold case. *Advances In Ecological Research*, 45:181–223.

James, A., Plank, M. J., Rossberg, A. G., Beecham, J., Emmerson, M., and Pitchford, J. W. (2015). Constructing random matrices to represent real ecosystems. *The American Naturalist*, 185(5):680–692.

Jennings, S., Greenstreet, S., Hill, L., Piet, G., Pinnegar, J., and Warr, K. (2002). Long-term trends in the trophic structure of the north sea fish community: evidence from stable-isotope analysis, size-spectra and community metrics. *Marine Biology*, 141(6):1085–1097.

Jetz, W., Thomas, G. H., Joy, J. B., Hartmann, K., and Mooers, A. Ø. (2012). The global diversity of birds in space and time. *Nature*, 491(7424):444–448.

Jetz, W., Thomas, G. H., Joy, J. B., Redding, D. W., Hartmann, K., and Mooers, A. Ø. (2014). Global distribution and conservation of evolutionary distinctness in birds. *Current Biology*, 24(9):919–930.

Jhwueng, D.-C. and Maroulas, V. (2014). Phylogenetic ornstein–uhlenbeck regression curves. *Statistics & Probability Letters*, 89:110–117.

Joly, S., Heenan, P. B., and Lockhart, P. J. (2013). Species radiation by niche shifts in new zealand's rockcresses (pachycladon, brassicaceae). *Systematic Biology*, 63(2):syt104.

Jonsson, T., Cohen, J. E., and Carpenter, S. R. (2005). Food webs, body size, and species abundance in ecological community description. *Advances in ecological research*, 36:1–84.

Jordán, F. (2009). Keystone species and food webs. *Philosophical Transactions of the Royal Society B: Biological Sciences*, 364(1524):1733–1741.

Jordán, F., Liu, W., and Davis, A. J. (2006). Topological keystone species: measures of positional importance in food webs. *Oikos*, 112(3):535–546.

Jordán, F., Liu, W., and Mike, Á. (2009). Trophic field overlap: a new approach to quantify keystone species. *Ecological Modelling*, 220(21):2899–2907.

Kaliontzopoulou, A. and Adams, D. C. (2016). Phylogenies, the comparative method, and the conflation of tempo and mode. *Systematic Biology*, 65(1):1–15.

Kamilar, J. M. and Cooper, N. (2013). Phylogenetic signal in primate behaviour, ecology and life history. *Philosophical Transactions of the Royal Society of London B: Biological Sciences*, 368(1618): doi: 10.1098/rstb.2012.0341.

Karatzas, I. and Shreve, S. (2012). *Brownian motion and stochastic calculus*, volume 113. Springer Science & Business Media.

Katz, L. (1953). A new status index derived from sociometric analysis. *Psychometrika*, 18(1):39–43.

Kawakita, A., Takimura, A., Terachi, T., Sota, T., and Kato, M. (2004). Cospeciation analysis of an obligate pollination mutualism: Haveglochidion trees (euphorbiaceae) and pollinating epicephala moths (gracillariidae) diversified in parallel? *Evolution*, 58(10):2201–2214.

Kemeny, J. G. and Snell, J. L. (1960). *Finite markov chains*, volume 356. van Nostrand Princeton, NJ.

Klein, D. J. and Randić, M. (1993). Resistance distance. *Journal of Mathematical Chemistry*, 12(1):81–95.

Lafferty, K. D., DeLeo, G., Briggs, C. J., Dobson, A. P., Gross, T., and Kuris, A. M. (2015). A general consumer-resource population model. *Science*, 349(6250):854–857.

Lai, S.-M., Liu, W.-C., and Jordán, F. (2012). On the centrality and uniqueness of species from the network perspective. *Biology letters*, 8(4):570–573.

Lara, C., Pérez, B., Castillo-Guevara, C., and Serrano-Meneses, M. A. (2015). Niche partitioning among three tree-climbing bird species in subtropical mountain forest sites with different human disturbance. *Zoological Studies*, 54(1):1–7.

Ledger, M., Edwards, F., and Woodward, G. (unpublished). unpublished, see Petchey et al. [2008a].

Lei, J., Rinaldo, A., et al. (2014). Consistency of spectral clustering in stochastic block models. *The Annals of Statistics*, 43(1):215–237.

Letten, A. D. and Cornwell, W. K. (2015). Trees, branches and (square) roots: why evolutionary relatedness is not linearly related to functional distance. *Methods in Ecology and Evolution*, 6(4):439–444.

Lewontin, R. C. (2001). *The triple helix: Gene, organism, and environment*. Harvard University Press.

Li, S. (2011). Concise formulas for the area and volume of a hyperspherical cap. *Asian Journal of Mathematics and Statistics*, 4(1):66–70.

Lieberman, B. S. (2012). Adaptive radiations in the context of macroevolutionary theory: a paleontological perspective. *Evolutionary Biology*, 39(2):181–191.

Livi, C. M., Jordán, F., Lecca, P., and Okey, T. A. (2011). Identifying key species in ecosystems with stochastic sensitivity analysis. *Ecological Modelling*, 222(14):2542–2551.

Loeuille, N. and Loreau, M. (2009). Emergence of complex food web structure in community evolution models. In Verhoef, H. A. and Morin, P. J., editors, *Community Ecology: Processes, Models, and Applications*, pages 163–178. Oxford University Press, Oxford.

Losos, J. B. (2008). Phylogenetic niche conservatism, phylogenetic signal and the relationship between phylogenetic relatedness and ecological similarity among species. *Ecology letters*, 11(10):995–1003.

Luczkovich, J. J., Borgatti, S. P., Johnson, J. C., and Everett, M. G. (2003). Defining and measuring trophic role similarity in food webs using regular equivalence. *Journal of Theoretical Biology*, 220(3):303–321.

Lyzinski, V., Sussman, D., Tang, M., Athreya, A., and Priebe, C. E. (2013). Perfect clustering for stochastic blockmodel graphs via adjacency spectral embedding. *arXiv*, preprint:1310.0532.

MacArthur, R. H. (1972). *Geographical ecology: patterns in the distribution of species*. Princeton University Press.

Mace, G. M., Gittleman, J. L., and Purvis, A. (2003). Preserving the tree of life. *Science*, 300(5626):1707–1709.

Maire, E., Grenouillet, G., Brosse, S., and Villéger, S. (2015). How many dimensions are needed to accurately assess functional diversity? a pragmatic approach for assessing the quality of functional spaces. *Global Ecology and Biogeography*, 24(6):728–740.

Maret, T. J. and Collins, J. P. (1997). Ecological origin of morphological diversity: a study of alternative trophic phenotypes in larval salamanders. *Evolution*, 5(13):898–905.

Matias, C. and Robin, S. (2014). Modeling heterogeneity in random graphs: a selective review. *arXiv*, preprint:1402.4296.

May, R. M. (1971). Stability in multispecies community models. *Mathematical Biosciences*, 12(1):59–79.

May, R. M. (1972). Will a large complex system be stable? *Nature*, 238:413–414.

May, R. M. (2006). Network structure and the biology of populations. *Trends in Ecology & Evolution*, 21(7):394–399.

May, R. M. (2009). Food-web assembly and collapse: mathematical models and implications for conservation. *Philosophical Transactions of the Royal Society B: Biological Sciences*, 364(1524):1643–1646.

Melián, C. J., Vilas, C., Baldó, F., González-Ortegón, E., Drake, P., and Williams, R. J. (2011). Eco-evolutionary dynamics of individual-based food webs. *Advances in Ecological Research*, 45:225–268.

Memmott, J., Martinez, N., and Cohen, J. (2000). Predators, parasitoids and pathogens: species richness, trophic generality and body sizes in a natural food web. *Journal of Animal Ecology*, 69(1):1–15.

Mills, S. L., Soulé, M. E., and Doak, D. F. (1993). The keystone-species concept in ecology and conservation. *BioScience*, 43(4):219–224.

Miranda, M. and Parrini, F. (2015). Congruence between species phylogenetic and trophic distinctiveness. *Biodiversity and Conservation*, 24(2):355–369.

Mörters, P. and Peres, Y. (2010). *Brownian motion*, volume 30. Cambridge University Press.

Mullon, C., Fréon, P., Cury, P., Shannon, L., and Roy, C. (2009). A minimal model of the variability of marine ecosystems. *Fish and Fisheries*, 10(2):115–131.

Münkemüller, T., Boucher, F. C., Thuiller, W., and Lavergne, S. (2015). Phylogenetic niche conservatism–common pitfalls and ways forward. *Functional Ecology*, 29(5):627–639.

Naisbit, R. E., Kehrli, P., Rohr, R. P., and Bersier, L.-F. (2011). Phylogenetic signal in predator-prey body-size relationships. *Ecology*, 92(12):2183–2189.

Naisbit, R. E., Rohr, R. P., Rossberg, A. G., Kehrli, P., and Bersier, L.-F. (2012). Phylogeny versus body size as determinants of food web structure. *Proceedings of the Royal Society B: Biological Sciences*, 279(1741):3291–3297.

Neubert, M. G. and Caswell, H. (1997). Alternatives to resilience for measuring the responses of ecological systems to perturbations. *Ecology*, 78(3):653–665.

Newman, M. (2009). *Networks: an introduction*. Oxford University Press.

Newman, M. E. (2001). Scientific collaboration networks. ii. shortest paths, weighted networks, and centrality. *Physical review E*, 64(1):016132.

Nickel, C. L. M. (2007). *Random dot product graphs: A model for social networks*. PhD thesis, The Johns Hopkins University.

Noh, J. D. and Rieger, H. (2004). Random walks on complex networks. *Physical review letters*, 92(11):118701.

Nosil, P. (2012). *Ecological speciation*. Oxford University Press.

Nosil, P. and Crespi, B. J. (2006). Experimental evidence that predation promotes divergence in adaptive radiation. *Proceedings of the National Academy of Sciences*, 103(24):9090–9095.

Nuismer, S. L. and Harmon, L. J. (2015). Predicting rates of interspecific interaction from phylogenetic trees. *Ecology letters*, 18(1):17–27.

Odling-Smee, F. J., Laland, K. N., and Feldman, M. W. (2003). *Niche construction: the neglected process in evolution*. Number 37 in Monographs in Population Biology. Princeton University Press.

Odling-Smee, J., Erwin, D. H., Palkovacs, E. P., Feldman, M. W., and Laland, K. N. (2013). Niche construction theory: a practical guide for ecologists. *The Quarterly review of biology*, 88(1):3–28.

O'Gorman, E. J., Yearsley, J. M., Crowe, T. P., Emmerson, M. C., Jacob, U., and Petchey, O. L. (2010). Loss of functionally unique species may gradually

undermine ecosystems. *Proceedings of the Royal Society of London B: Biological Sciences*, 278(1713): doi: 10.1098/rspb.2010.2036.

Oksanen, J., Blanchet, F. G., Kindt, R., Legendre, P., Minchin, P. R., O'Hara, R. B., Simpson, G. L., Solymos, P., Stevens, M. H. H., and Wagner, H. (2015). *vegan: Community Ecology Package*. version 2.2-1.

O'Meara, B. C. and Beaulieu, J. M. (2014). Modelling stabilizing selection: The attraction of ornstein–uhlenbeck models. In *Modern Phylogenetic Comparative Methods and Their Application in Evolutionary Biology*, pages 381–393. Springer.

Opitz, S. (1996). *Trophic interactions in Caribbean coral reefs*. The WorldFish Center Working Papers. International Center for Living Aquatic Resources, Manila, Philippines.

Opsahl, T., Agneessens, F., and Skvoretz, J. (2010). Node centrality in weighted networks: Generalizing degree and shortest paths. *Social Networks*, 32(3):245–251.

Osborne, M. J., Norman, J., Christidis, L., and Murray, N. (2000). Genetic distinctness of isolated populations of an endangered marsupial, the mountain pygmy-possum, burramys parvus. *Molecular Ecology*, 9(5):609–613.

Page, R. D. (2003). *Tangled trees: phylogeny, cospeciation, and coevolution*. University of Chicago Press.

Pagel, M. D. (1992). A method for the analysis of comparative data. *Journal of Theoretical Biology*, 156(4):431–442.

Pagel, M. D. (1999). Inferring the historical patterns of biological evolution. *Nature*, 401(6756):877–884.

Pauly, D., Christensen, V., and Walters, C. (2000). Ecopath, ecosim, and ecospace as tools for evaluating ecosystem impact of fisheries. *ICES Journal of Marine Science: Journal du Conseil*, 57(3):697–706.

Pearman, P. B., Lavergne, S., Roquet, C., Wüest, R., Zimmermann, N. E., and Thuiller, W. (2014). Phylogenetic patterns of climatic, habitat and trophic niches in a european avian assemblage. *Global ecology and biogeography*, 23(4):414–424.

Pennell, M. W., Eastman, J. M., Slater, G. J., Brown, J. W., Uyeda, J. C., FitzJohn, R. G., Alfaro, M. E., and Harmon, L. J. (2014). geiger v2. 0: an expanded suite of methods for fitting macroevolutionary models to phylogenetic trees. *Bioinformatics*, 30(15):2216–2218.

Pennell, M. W., FitzJohn, R. G., Cornwell, W. K., and Harmon, L. J. (2015). Model adequacy and the macroevolution of angiosperm functional traits. *The American Naturalist*, 186(2):E33–E50.

Penrose, M. (2003). *Random geometric graphs*, volume 5 of *Oxford Studies in Probability*. Oxford University Press Oxford.

Petchey, O. L., Beckerman, A. P., Riede, J. O., and Warren, P. H. (2008a). Size, foraging, and food web structure. *Proceedings of the National Academy of Sciences*, 105(11):4191–4196.

Petchey, O. L., Eklöf, A., Borrvall, C., and Ebenman, B. (2008b). Trophically unique species are vulnerable to cascading extinction. *The American Naturalist*, 171(5):568–579.

Petchey, O. L. and Gaston, K. J. (2006). Functional diversity: back to basics and looking forward. *Ecology letters*, 9(6):741–758.

Pianka, E. R. (1981). Competition and niche theory. In May, R. M., editor, *Theoretical Ecology: Principle and Applications*, pages 167–196. Blackwell Publishing Ltd.

Poisot, T. (2015). When is co-phylogeny evidence of coevolution? In Morand, S., Krasnov, B. R., and Littlewood, D. T., editors, *Parasite Diversity and Diversification: Evolutionary Ecology Meets Phylogenetics*, pages 420–433. Cambridge University Press.

Poisot, T., Stouffer, D. B., and Gravel, D. (2015). Beyond species: why ecological interaction networks vary through space and time. *Oikos*, 124(3):243–251.

Post, D. M. and Palkovacs, E. P. (2009). Eco-evolutionary feedbacks in community and ecosystem ecology: interactions between the ecological theatre and the evolutionary play. *Philosophical Transactions of the Royal Society B: Biological Sciences*, 364(1523):1629–1640.

Proulx, S. R., Promislow, D. E., and Phillips, P. C. (2005). Network thinking in ecology and evolution. *Trends in Ecology & Evolution*, 20(6):345–353.

R Core Team (2013). *R: A Language and Environment for Statistical Computing*. R Foundation for Statistical Computing, Vienna, Austria. http://www.R-project.org/.

Rangel, T. F., Colwell, R. K., Graves, G. R., Fučíková, K., Rahbek, C., and Diniz-Filho, J. A. F. (2015). Phylogenetic uncertainty revisited: Implications for ecological analyses. *Evolution*, 69(5):1301–1312.

Real, R. and Vargas, J. M. (1996). The probabilistic basis of jaccard's index of similarity. *Systematic Biology*, 45(3):380–385.

Redding, D. W. and Mooers, A. Ø. (2006). Incorporating evolutionary measures into conservation prioritization. *Conservation Biology*, 20(6):1670–1678.

Refrégier, G., Le Gac, M., Jabbour, F., Widmer, A., Shykoff, J. A., Yockteng, R., Hood, M. E., and Giraud, T. (2008). Cophylogeny of the anther smut fungi and their caryophyllaceous hosts: prevalence of host shifts and importance of delimiting parasite species for inferring cospeciation. *BMC Evolutionary Biology*, 8(1):100.

Reuman, D. C., Mulder, C., Banašek-Richter, C., Blandenier, M.-F. C., Breure, A. M., Den Hollander, H., Kneitel, J. M., Raffaelli, D., Woodward, G., and Cohen, J. E. (2009). Allometry of body size and abundance in 166 food webs. *Advances in Ecological Research*, 41:1–44.

Revell, L. J. (2012). phytools: An r package for phylogenetic comparative biology (and other things). *Methods in Ecology and Evolution*, 3:217–223.

Revell, L. J., Harmon, L. J., and Collar, D. C. (2008). Phylogenetic signal, evolutionary process, and rate. *Systematic Biology*, 57(4):591–601.

Rohe, K., Chatterjee, S., and Yu, B. (2011). Spectral clustering and the high-dimensional stochastic blockmodel. *The Annals of Statistics*, 39(4):1878–1915.

Rohr, R. P. and Bascompte, J. (2014). Components of phylogenetic signal in antagonistic and mutualistic networks. *The American Naturalist*, 184(5):556–564.

Rohr, R. P., Saavedra, S., and Bascompte, J. (2014). On the structural stability of mutualistic systems. *Science*, 345(6195):1253497 – 1–9.

Rohr, R. P., Scherer, H., Kehrli, P., Mazza, C., and Bersier, L.-F. (2010). Modeling food webs: exploring unexplained structure using latent traits. *The American Naturalist*, 176(2):170–177.

Roopnarine, P. D. (2010). Networks, extinction, and palecommunity food webs. In Alroy, J. and Hunt, G., editors, *Quantitative methods in paleobiology*, volume 16 of *The Paleontological Society Papers*, page 143–161. Paleontological Society.

Roopnarine, P. D. (2012). Red queen for a day: models of symmetry and selection in paleoecology. *Evolutionary Ecology*, 26(1):1–10.

Rosindell, J., Hubbell, S. P., He, F., Harmon, L. J., and Etienne, R. S. (2012). The case for ecological neutral theory. *Trends in Ecology & Evolution*, 27(4):203–208.

Rossberg, A. G. (2013). *Food webs and biodiversity: foundations, models, data*. John Wiley & Sons.

Rossberg, A. G., Brännström, Å., and Dieckmann, U. (2010). How trophic interaction strength depends on traits. *Theoretical Ecology*, 3(1):13–24.

Rossberg, A. G., Matsuda, H., Amemiya, T., and Itoh, K. (2006). Food webs: experts consuming families of experts. *Journal of Theoretical Biology*, 241(3):552–563.

Saavedra, S., Rohr, R. P., Fortuna, M., Selva, N., and Bascompte, J. (2015). Seasonal species interactions minimize the impact of species turnover on the likelihood of community persistence. *Ecology*, in press: doi: 10.1890/15–1013.1.

Sale, P. F. (1974). Overlap in resource use, and interspecific competition. *Oecologia*, 17(3):245–256.

Schaffer, W. M. (1981). Ecological abstraction: The consequences of reduced dimensionality in ecological models. *Ecological Monographs*, 51(4):384–401.

Schmidt-Nielsen, K. (1984). *Scaling: why is animal size so important?* Cambridge University Press.

Semple, C. and Steel, M. (2003). *Phylogenetics*. Oxford University Press.

Silvertown, J., Dodd, M., and Gowing, D. (2001). Phylogeny and the niche structure of meadow plant communities. *Journal of Ecology*, 89(3):428–435.

Silvestro, D., Kostikova, A., Litsios, G., Pearman, P. B., and Salamin, N. (2015). Measurement errors should always be incorporated in phylogenetic comparative analysis. *Methods in Ecology and Evolution*, 6(3):340–346.

Smith, F. A. and Lyons, S. K. (2013). *Animal body size: linking pattern and process across space, time, and taxonomic group*. University of Chicago Press.

Solé, R. V. and Bascompte, J. (2006). *Self–Organization in Complex Ecosystems*, volume 42 of *Monographs in Population Biology*. Princeton University Press.

Stephenson, K. and Zelen, M. (1989). Rethinking centrality: Methods and examples. *Social Networks*, 11(1):1–37.

Stewart, W. J. (2009). *Probability, Markov chains, queues, and simulation: the mathematical basis of performance modeling*. Princeton University Press.

Stouffer, D. B. (2010). Scaling from individuals to networks in food webs. *Functional Ecology*, 24(1):44–51.

Stouffer, D. B., Camacho, J., Guimera, R., Ng, C. A., and Nunes Amaral, L. A. (2005). Quantitative patterns in the structure of model and empirical food webs. *Ecology*, 86(5):1301–1311.

Stouffer, D. B., Rezende, E. L., and Amaral, L. A. N. (2011). The role of body mass in diet contiguity and food-web structure. *Journal of Animal Ecology*, 80(3):632–639.

Stouffer, D. B., Sales-Pardo, M., Sirer, M. I., and Bascompte, J. (2012). Evolutionary conservation of species' roles in food webs. *Science*, 335(6075):1489–1492.

Stuart, Y. E. and Losos, J. B. (2013). Ecological character displacement: glass half full or half empty? *Trends in Ecology & Evolution*, 28(7):402–408.

Sussman, D. L., Tang, M., and Priebe, C. E. (2014). Consistent latent position estimation and vertex classification for random dot product graphs. *Pattern Analysis and Machine Intelligence, IEEE Transactions on*, 36(1):48–57.

Takahashi, D., Brännström, Å., Mazzucco, R., Yamauchi, A., and Dieckmann, U. (2013). Abrupt community transitions and cyclic evolutionary dynamics in complex food webs. *Journal of Theoretical Biology*, 337:181–189.

Tang, M., Sussman, D. L., Priebe, C. E., et al. (2013). Universally consistent vertex classification for latent positions graphs. *The Annals of Statistics*, 41(3):1406–1430.

Thomas, G. H. and Freckleton, R. P. (2012). Motmot: models of trait macroevolution on trees. *Methods in Ecology and Evolution*, 3(1):145–151.

Thompson, J. N. (1994). *The Coevolutionary Process*. The University of Chicago Press.

Thompson, J. N. (2005). *The geographic mosaic of coevolution*. The University of Chicago Press.

Thompson, J. N. (2013). *Relentless evolution*. The University of Chicago Press.

Uyeda, J. C., Caetano, D. S., and Pennell, M. W. (2015). Comparative analysis of principal components can be misleading. *Systematic Biology*, 64(4):677–689.

Vallina, S. M. and Le Quéré, C. (2011). Stability of complex food webs: Resilience, resistance and the average interaction strength. *Journal of Theoretical Biology*, 272(1):160–173.

Vermeij, G. J. (1987). *Evolution and escalation: an ecological history of life*. Princeton University Press.

Villéger, S., Mason, N. W., and Mouillot, D. (2008). New multidimensional functional diversity indices for a multifaceted framework in functional ecology. *Ecology*, 89(8):2290–2301.

Voje, K. L., Holen, Ø. H., Liow, L. H., and Stenseth, N. C. (2015). The role of biotic forces in driving macroevolution: beyond the red queen. *Proceedings of the Royal Society of London B: Biological Sciences*, 282(1808):20150186.

von Luxburg, U., Radl, A., and Hein, M. (2010). Hitting and commute times in large graphs are often misleading. *arXiv*, preprint:1003.1266.

Walker, B., Stotz, D. F., Pequeno, T., and Fitzpatrick, J. W. (2006). Birds of the manu biosphere reserve. *Fieldiana Zoology*, 110:23–49.

Wang, Y. J. and Wong, G. Y. (1987). Stochastic blockmodels for directed graphs. *Journal of the American Statistical Association*, 82(397):8–19.

Wasserman, S. (1994). *Social network analysis: Methods and applications*, volume 8. Cambridge University Press.

Wax, N., editor (1954). *Selected Papers on Noise and Stochastic Processes*. Dover Publications, New York.

Wennekes, P. L., Rosindell, J., and Etienne, R. S. (2012). The neutral—niche debate: a philosophical perspective. *Acta biotheoretica*, 60(3):257–271.

Wiener, N. (1923). Differential-space. *Journal of Mathematics and Physics*, 2(1):131–174.

Wiens, J. J., Ackerly, D. D., Allen, A. P., Anacker, B. L., Buckley, L. B., Cornell, H. V., Damschen, E. I., Jonathan Davies, T., Grytnes, J.-A., Harrison, S. P., et al. (2010). Niche conservatism as an emerging principle in ecology and conservation biology. *Ecology letters*, 13(10):1310–1324.

Wilkinson, G. N. and Rogers, C. E. (1973). Symbolic description of factorial models for analysis of variance. *Journal of the Royal Statistical Society. Series C (Applied Statistics)*, 22(3):392–399.

Williams, R. J., Anandanadesan, A., and Purves, D. (2010). The probabilistic niche model reveals the niche structure and role of body size in a complex food web. *PloS one*, 5(8):e12092.

Williams, R. J. and Martinez, N. D. (2000). Simple rules yield complex food webs. *Nature*, 404(6774):180–183.

Williams, R. J. and Martinez, N. D. (2008). Success and its limits among structural models of complex food webs. *Journal of Animal Ecology*, 77(3):512–519.

Willis, E. O. (1966). Interspecific competition and the foraging behavior of plain-brown woodcreepers. *Ecology*, 47(4):667–672.

Winemiller, K. O., Fitzgerald, D. B., Bower, L. M., and Pianka, E. R. (2015). Functional traits, convergent evolution, and periodic tables of niches. *Ecology Letters*, 18(8):737–751.

Winter, M., Devictor, V., and Schweiger, O. (2013). Phylogenetic diversity and nature conservation: where are we? *Trends in Ecology & Evolution*, 28(4):199–204.

Woodward, G., Ebenman, B., Emmerson, M., Montoya, J. M., Olesen, J. M., Valido, A., and Warren, P. H. (2005a). Body size in ecological networks. *Trends in Ecology & Evolution*, 20(7):402–409.

Woodward, G. and Hildrew, A. G. (2001). Invasion of a stream food web by a new top predator. *Journal of Animal Ecology*, 70(2):273–288.

Woodward, G., Speirs, D. C., and Hildrew, A. G. (2005b). Quantification and resolution of a complex, size-structured food web. *Advances in ecological research*, 36:85–135.

Xu, J., Massoulié, L., and Lelarge, M. (2014). Edge label inference in generalized stochastic block models: from spectral theory to impossibility results. *arXiv*, preprint:1406.6897.

Yeakel, J. D., Pires, M. M., Rudolf, L., Dominy, N. J., Koch, P. L., Guimarães, P. R., and Gross, T. (2014). Collapse of an ecological network in ancient egypt. *Proceedings of the National Academy of Sciences*, 111(40):14472–14477.

Yodzis, P. and Winemiller, K. O. (1999). In search of operational trophospecies in a tropical aquatic food web. *Oikos*, 87(2):327–340.

Young, S. J. and Scheinerman, E. R. (2008). Directed random dot product graphs. *Internet Mathematics*, 5(1-2):91–111.

Zhu, M. and Ghodsi, A. (2006). Automatic dimensionality selection from the scree plot via the use of profile likelihood. *Computational Statistics & Data Analysis*, 51(2):918–930.

Zook, A. E., Eklöf, A., Jacob, U., and Allesina, S. (2011). Food webs: Ordering species according to body size yields high degree of intervality. *Journal of Theoretical Biology*, 271(1):106–113.

Gingest du über eine Ebene, hättest den guten Willen zu gehen und machtest doch Rückschritte, dann wäre es eine verzweifelte Sache; da du aber einen steilen Abhang hinaufkletterst, so steil etwa, wie du selbst von unten gesehen bist, können die Rückschritte auch nur durch die Bodenbeschaffenheit verursacht sein, und du mußt nicht verzweifeln.[1]

Die Zürauer Aphorismen
Aphorismus 14
Franz Kafka

[1] If you were walking across a plain, felt every desire to walk, and yet found yourself going backward, it would be a cause for despair; but as you are in fact scaling a steep precipice, as sheer in front of you as you are from the ground, then your backward movement can be caused only by the terrain, and you would be wrong to despair.
Translation by Hofmann, M. (2006). *The Zurau Aphorisms.* Schocken.